

AD-A146 719

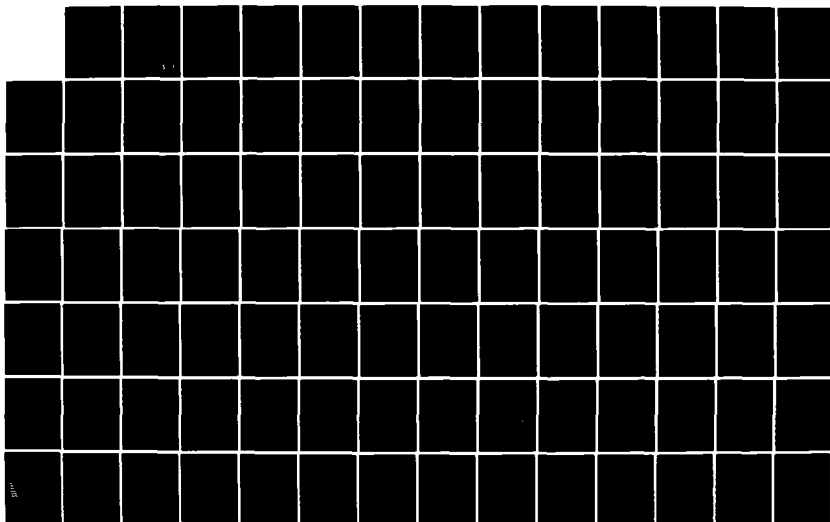
THE EFFECT OF BOW SHAPE ON DECK WETNESS IN HEAD SEAS
(U) NAVAL ACADEMY ANNAPOLIS MD DIV OF ENGINEERING AND
WEAPONS A R LLOYD APR 84 USNA-EM-17-84

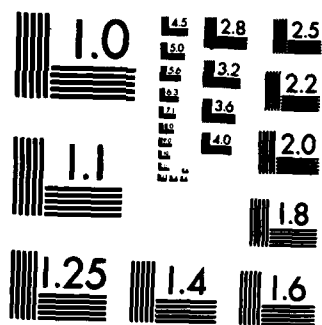
1/2

UNCLASSIFIED

F/G 13/10

NL





(20)

AD-A146 719

DTIC FILE COPY

Report EW-17-84

THE EFFECT OF BOW SHAPE
ON
DECK WETNESS IN HEAD SEAS

DR. A R J M LLOYD*

April 1984

UNITED STATES NAVAL ACADEMY
DIVISION OF
ENGINEERING AND WEAPONS
ANNAPOLIS, MARYLAND

This document has been approved
for public release and sale; its
distribution is unlimited.

DTIC
ELECTE
OCT 1 3 1984
S E D

84 10 04 009

United States Naval Academy
Annapolis, Maryland 21402

Division of Engineering and Weapons

Report EW-17-84

THE EFFECT OF BOW SHAPE
ON
DECK WETNESS IN HEAD SEAS

DR. A R J M LLOYD*

April 1984

*A R J M LLOYD
PhD BSc FRINA
Principal Scientific Officer
Admiralty Marine Technology Establishment
Haslar, Gosport, Hampshire, UK

Naval Sea Systems Command
NAVSEA Visiting Research Professor

1982-1983

Naval Systems Engineering Department
Division of Engineering and Weapons
United States Naval Academy
Annapolis, Maryland 21401 USA

Approved for public release;
distribution unlimited

Accession For	
NTIS GRA&I	<input checked="" type="checkbox"/>
DTIC TAB	<input type="checkbox"/>
Unannounced	<input type="checkbox"/>
Justification	
By _____	
Distribution/	
Availability Codes	
Dist	Avail and/or Special
A1	



The Effect of Bow Shape
on
Deck Wetness in Head Seas

by

A R J M LLOYD
PhD BSc FRINA
Principal Scientific Officer
Admiralty Marine Technology Establishment
Haslar, Gosport, Hampshire, UK

NAVSEA Visiting Research Professor

1982-83

Naval Systems Engineering Department
Division of Engineering and Weapons
United States Naval Academy
Annapolis Maryland 21401 USA

Accession For	
NTIS GRA&I	<input checked="checked" type="checkbox"/>
DTIC TAB	<input type="checkbox"/>
Unannounced	<input type="checkbox"/>
Justification	
By	
Distribution/	
Availability Codes	
Dist	Avail and/or Special
A-1	

April 1984

Summary

Experiments to examine the deck wetness process and to determine the effect of above water bow form on deck wetness in head seas were conducted in the 380 ft Towing Tank of the United States Naval Academy. A systematic series of bow forms, in which flare and overhang were varied, was tested on a model of the FFG7 frigate at one speed in irregular head waves corresponding to commonly occurring conditions in the North Atlantic in winter.

It was found that above water bow form had remarkably little effect on relative motions or deck wetness and the greatest incidence of deck wetness occurred with one of the extremely flared forms.

A new method of calculating the probability of deck wetness is proposed and verified. The calculation explains why the bows tested all had a similar performance and suggests that this is about the best that could be achieved at the chosen freeboard. Application of the calculation to a wider range of bow designs shows that a similar, near optimum, performance should be achieved providing the flare and overhang are given certain minimum values. Excessive flare and overhang will not ensure improved performance.

Contents

- Figure 1. FFG7 Body Plan.
- Figure 2. FFG7 Bow Form Series.
- Figure 3. Notation.
- Figure 4. USNA Bow Forms.
- Figure 5. 35 Degrees and 45 Degrees Bow Body Plans.
- Figure 6. Variation of Local Flare Angle.
- Figure 7. USNA Knuckle Bows.
- Figure 8. 35 Degrees Flare and 35 Degrees/45 Degrees K Knuckle Body Plans.
- Figure 9. Relative Bow Motion Capacitance Strips.
- Figure 10. Calibration of Relative Motion Capacitance Strips.
- Figure 11. Impact Pressure Array.
- Figure 12. Significant Wave Height by Modal Wave Period from Reference 30.
- Figure 13. Wave Spectrum WG First Attempt.
- Figure 14. Wave Spectrum WG Second Attempt.
- Figure 15. Wave Spectrum WG Third Attempt.
- Figure 16. Typical Relative Motion Signal.
- Figure 17. Typical Corrected Relative Motion Signal.
- Figure 18. Calm Water Bow Wave Profiles.
- Figure 19. Probability Distribution of Wake Peaks and Troughs.
- Figure 20. Probability Distribution of Wave Peaks and Troughs.
- Figure 21. Mean Relative Motion in Waves.
- Figure 22. Mean Value of Relative Motion in Various Wave Spectra 40 Degrees Bow.
- Figure 23. Bow Wave Profile.
- Figure 24. Rms Relative Motions.
- Figure 25. Rms Relative Motion in Various Wave Spectra 40 Degrees Bow.

Contents

- Figure 26. Rms Relative Motions.
- Figure 27. Probability Distributions of Relative Bow Motion 35 Degrees Bow.
- Figure 28a. Probability Distributions of Relative Bow Motion Knuckle Bow.
- Figure 28b. Probability Distributions of Relative Bow Motion Knuckle Bow.
- Figure 29a. Probability of Exceeding Freeboard.
- Figure 29b. Probability of Exceeding Freeboard.
- Figure 29c. Probability of Exceeding Freeboard.
- Figure 30. Probability of Relative Motion Exceeding Freeboard.
- Figure 31. Relative Motion Peaks Per Hour.
- Figure 32a. Freeboard Exceedances Per Hour.
- Figure 32b. Freeboard Exceedances Per Hour.
- Figure 33. Bow Performance.
- Figure 34. Rms Relative Motion Comparison with Theory.
- Figure 35. Predicted Rms Relative Motions.
- Figure 36. Required Swell Up Factor.
- Figure 37. Critical Absolute Vertical Water Velocity.
- Figure 38. Probabilities Associated with Deck Wetness Bow 30.
- Figure 39. Probability of Deck Wetness.
- Figure 40. Estimated Probability of Deck Wetness.
- Figure 41. Predicted and Measured Probability of Deck Wetness.
- Figure 42. Predicted and Measured Deck Wetness Frequency.
- Figure 43. Local Flare Angle Nominal Flare Angle 40 Degrees.
- Figure 44. Critical Velocity.
- Figure 45. Computed Wetness Probabilities for 40 Degrees Flare and Various Overhangs.

Contents

Figure 46. Predicted Bow Performance.

Figure A1.1 Design Method for Section Shape at Station 2.

Figure A1.2 Design Method for Stem Profile.

Figure A1.3 Design Method for Waterlines.

Distribution.

THE EFFECT OF BOW SHAPE ON DECK WETNESS IN HEAD SEAS

By A R J M Lloyd

1. OBJECTIVES

The work described in this report was intended to examine the deck wetness process in detail and to determine the effect of above water bow form on deck wetness in irregular head seas.

2. INTRODUCTION

Deck Wetness has long been recognised as one of the factors which determine the seakindliness of a ship. In extreme conditions the frequent shipping of water may lead to the capsize of the vessel: in more moderate conditions the loss of the vessel is unlikely but frequent deck wetness may still cause damage to exposed fittings and deck cargo and make the upper deck untenable for the crew. In a warship this may seriously degrade the ship's operational effectiveness by limiting the crew's ability to man and reload weapons and to complete tasks such as replenishment at sea.

The frequency and severity of deck wetness can, of course, be reduced by avoiding high speeds and head seas : but the resulting limitations on mobility can also be regarded as a reduction in operational effectiveness. In short, the wet warship is likely to be a much less successful weapons platform than the dry ship.

The current interest in operational effectiveness and warship mobility has led to studies aimed at developing criteria for acceptable deck wetness frequency and severity. The author proposed a wetness frequency criterion of one wetting every 100 seconds or 36 wettings per hour in Reference 1 but this was subsequently adjusted to one wetting every 40 seconds or 90 wettings per hour in Reference 2. These proposals were based on the reported behaviour of ships at sea and individual captain's judgements of acceptable wetness frequency.

For ship design purposes it is necessary to predict the deck wetness frequency during the design stage and to compare the results with the criteria available. If the predicted deck wetness were more severe than the extant criteria suggest is acceptable the design would be modified (increased freeboard, modifications to bow shape) until the criteria were met.

At the time of writing a broad general framework for the calculation seems to have been generally agreed (see, for example, Reference 3) but specific details are still a matter of debate.

The usual practice is to employ strip theory to calculate the notional rms relative motion at the bow (ie the relative motion derived from calculations of the absolute motion and the undisturbed wave alongside the bow) in suitable irregular seaways. Some kind of correction for "swell up" is then made to allow for the fact that

the presence of the ship's hull amplifies the notional relative motion. Bales (Reference 3) suggested the addition of two empirically derived contributions : the swell up which would be caused by the hull oscillating in calm water and the distortion of the incident wave caused by the presence of the (restrained) ship's hull. Tasaki's work (Reference 4) was cited for information on the former and Van Sluijs (Reference 5) was suggested for the latter.

Further data on the effect of hull oscillations in calm water including theoretical predictions have since been published in Reference 6.

In contrast, Blok and Huisman, in Reference 7, defined a "swell up coefficient" (SUC) as the true relative motion/notional relative motion and found, from experiments, that the SUC had values of the order of 1.5 near the bow where deck wetness occurs most frequently. The SUC was found to be essentially independent of frequency and a function only of speed, hull station and the local change in the ship's draught. Thus, for example, they were able to show that the swell up coefficient obtained by running a model at deep draught in calm water was essentially the same as that obtained when the model's local draught varied by the same amount due to ship motions in waves.

They went on to suggest that the swell up could therefore be calculated using simple bow wave prediction techniques at a range of draughts (for example Reference 8) although no results of this technique were given.

Whatever technique is used for estimating swell up the Rayleigh formula is invoked to calculate the probability of the relative motion exceeding the effective freeboard. The effective freeboard is the geometric freeboard (measured from the calm water surface at zero speed) with corrections for sinkage, trim and the bow wave profile. In general the effective freeboard is less than the geometric freeboard, particularly at high speed. The effects of sinkage and trim are usually small (at the bow) and the reduction in freeboard due to the bow wave can be calculated using Shearer's method (Reference 8).

This technique is used to calculate the probability of deck submergence at a number of forward stations to find the highest probability of deck wetness : this probability can be converted to a frequency if the average period of the relative motion is known.

This method is embodied in the AMTE(H) PAT Suite of seakeeping computer programs (Reference 9) and, no doubt, in other similar prediction methods.

It should be noted that these predictions are not strictly predictions of deck wetness but rather predictions of freeboard exceedance. Practical experience at sea demonstrates that it is quite possible with a flared bow for the local sea surface to rise above the level of the deck without any water being shipped inboard and the predictions may therefore be pessimistic. Indeed none of

the techniques described above (with the exception of the swell up calculation suggested in Reference 7) takes any account of above water form.

These techniques therefore provide a somewhat doubtful method of calculating the required freeboard and the practising Naval Architect must resort to intuition, experience or, at best, experiment to determine appropriate above water bow form. In these circumstances it is hardly surprising that the merits of flare, knuckle and other above water features have been topics of seemingly perennial debate among naval architects and sailors for many years.

The Victorian predilection for ramming as a naval tactic encouraged bow designs which were widely believed to promote deck wetness (see for example page 107 of Reference 10 and Reference 11). These "ram" bows soon went out of fashion and the arguments then centred around the desirability of flare and the rake of the stem. Probably the earliest systematic model experiments to investigate the effects of flare were made in 1887. These are briefly mentioned in Sir Archibald Denny's discussion of Reference 12 but no details or results are given.

Kent (Reference 12) reported the results of experiments on three models : two of these had the same underwater hull form but different above water bow forms. The models were towed in regular head waves and observations of ship motions and deck wetness were made.

Kent found that the flared form was superior to the unflared form (as regards deck wetness) only in short steep waves : in all other conditions the performance was the same.

This view was supported by MacDonald and Telfer in Reference 13. However some of the discussion to both papers suggested that this opinion was not wholly in accord with the experience of practical seafarers although even in this community there were differences of opinion.

Edward and Todd reported the results of some comparative experiments on three different models of steam drifters in Reference 14. These tests are of historic interest as they are apparently the first in which an objective measurement of deck wetness was attempted : the water shipped by each model was collected and weighed but the results reported are only qualitative.

The models were tested at 9 knots in both regular and irregular head waves : the model with low freeboard quickly sank in the regular wave tests. The other two models had the same freeboard but different hull forms both above and below the waterline. The model with the greatest flare again proved superior with regard to the quantity of water shipped in both tests.

Kent (Reference 15) (and Macgregor in a discussion of Kent's paper) suggested that improved deck wetness characteristics should be

achieved by adopting a raked stem. This was attributed to a more favourable location of the bow wave crest ("bow breaker") and the larger effective forward waterplane area.

Allan reported the results of model tests on four different drifters in Reference 16. All the models had different underwater hull forms as well as different freeboards and above water bow shapes including knuckles. It is difficult to draw objective conclusions on the effects of bow shape on deck wetness from this work but Allan's opinion was that the heavily flared form was superior in a head sea. Two of the designs were built at full scale: the form with high freeboard, low flare and a knuckle was found to be "wet forward" whereas the alternative design with low freeboard, no knuckle and high flare was found to be dry.

In contrast to this hardening body of opinion concerning the merits of flare and stem rake Saunders sounds a note of caution in References 17 and 18: "... the idea that a widely flaring bow prevents spray from reaching the deck and upper works may be a disappointing delusion ..." and "... there appears to be no hydrodynamic superiority for the bow profile which is moderately or sharply raked above the designed waterline ...". For superior deck wetness characteristics Saunders recommends for above water bow form: "The highest practicable freeboard" and "Forebody sections of the V type embodying small or moderate flare and the greatest practicable uniformity of section slope in the region where the bow meets the water surface when pitching".

Newton reported a definitive series of model experiments on deck wetness in Reference 19. A destroyer model was fitted with five different above water bow forms and tested in regular head waves. The forms included variations of freeboard, flare and knuckle and wetness was visually assessed as "dry", "wet" or "very wet". The freeboard variations were obtained by simply adding a vertical bulwark to the basic bow form so that a knuckle was inevitably included in the resulting bow design.

It was stated that the modified bows with additional flare and a knuckle behave as if they had increased freeboard. The extent of this effective increment in freeboard was determined by finding the "freeboard" necessary to bring the results for the modified bows into line with the results for the basic bows. On the basis of this rather slim and subjective evidence, Newton proposed a tentative formula relating the geometric parameters of the knuckle to the effective (additional) freeboard.

In contrast to these results Abkowitz (Reference 20) found the effects of flare only marginal and Tasaki found that a model fitted with a flared bow shipped most water in regular waves in Reference 4.

Swaan and Vossers tested a range of models based on the series 60 form in Reference 21. The tests were done in regular bow and head waves and it was found that the model with extreme flare experienced greater relative bow motion (at least in bow waves), and might

therefore be more susceptible to deck wetness, even if the flare was effective at throwing the resulting "piled up water" to each side.

Van Sluijs and Gie tested a model of a "compact" frigate in regular and irregular head waves in Reference 22. The model was tested with a conventional bow and a heavily flared bow with a knuckle. It was found that the rigid body motions (pitch and heave) were unaffected by the above water bow form but the flared form gave a reduction in relative motion, especially in high waves. It should be noted however that the recorded relative motions were, in this case, greater than the height of the knuckle: it is not clear whether the reduction in relative motion was "real" or simply caused by the knuckle shedding water away from the model's side.

A programme of experiments aimed at investigating the effect of bow shape on deck wetness has been pursued for some years at AMTE(H). Relevant publications are listed as References 23-28 and this work is summarised in Reference 29. These experiments employed a model of a frigate with a number of interchangeable bow sections. The bows were systematic variations about a parent form and included variations of freeboard, flare, stem overhang and stem sharpness. The model was tested in irregular head waves at a number of speeds. Rigid body and relative bow motions were measured and deck wetness was quantified by recording the impacts experienced by a vertical surface mounted on the fore's'cle. A catch tank was also used in some experiments. Some of the results were inconclusive and it was suggested that this might have been because the run times (up to about 30 minutes at full scale) were insufficient to allow stable statistics of deck wetness frequency and severity to be obtained. However it was clear that additional freeboard was beneficial in reducing wetness and the results also showed that a small overhang was undesirable: Contrary to expectations excessive flare appeared to give increased wetness frequency.

The notional relative bow motion was derived by subtracting the incident wave from the absolute bow motion time history. The rms values of this notional relative motion, pitch and heave were found to be essentially unaffected by changes in bow form. The actual relative motion, measured directly by a stem mounted probe, was, in most cases, also independent of bow form; but it was found that a high overhang seemed to reduce the relative motion and a large flare seemed to increase the relative motion. Both of these results supported the trends found for deck wetness.

Table 1 shows a summary of the effects of bow form according to the references cited. Clearly there are wide variations of opinion, particularly on the merits of flare.

3. DECK WETNESS EXPERIMENTS AT UNITED STATES NAVAL ACADEMY

The experiments described in this report were designed to provide information on the deck wetness "process". Essentially the philosophy behind the experiments was based on lessons learned from the AMTE(H) experiments described in References 23-29 but with

certain additional specific objectives. These were:

- a. To examine deck wetness in a number of typical North Atlantic sea spectra.
- b. To measure relative motions at a number of closely spaced stations near the forward perpendicular where deck submergence was expected to be most frequent.
- c. To derive the mean value of the relative motions in waves for comparison with the calm water bow wave.
- d. To test the validity of the Rayleigh formula for predicting the frequency of occurrence of deck submergence (give the measured rms relative motion).
- e. To obtain information on swell up by comparing the actual relative motion with the notional relative motion (obtained by subtracting the incident wave from the absolute motion time history).
- f. To measure the frequency and severity of deck wetness using suitable pressure sensitive instrumentation mounted in a vertical plane on the fo'c'sle.
- g. To relate the frequency of deck wetness (impacts) to the frequency of deck submergence.
- h. To obtain information on the effects of above water bow form by running experiments with a systematic series of geometrically related bow forms.
- i. To compare the results with theoretical predictions and to derive new methods of including above water bow geometry in predictions of deck wetness.

4. MODEL

The experiments were conducted using an unappended wooden model of the FFG7 frigate. The model was built to $1/36$ scale in sugar pine in the Naval Academy Division of Engineering and Weapons Workshops. Dimensions are given in Table 2 and a body plan is shown in Figure 1. Note that the standard US system of station numbering is used in the body plan and throughout this report. Station 0 is the Forward Perpendicular and station 20 is the Aft Perpendicular.

The model was supplied with a total of seven alternative bows also constructed of sugar pine. These bows were designed to fare smoothly into the rest of the hull along the design waterline and at station 5 as shown in Figure 2. All bows had a constant geometric freeboard equivalent to .06L (7.46 metres at full scale).

Bows 1-6 formed a family of shapes in which flare δ_2 (at station 2) and overhang x_0 were varied in a consistent manner (see Figures 2 and 3 for notation). In particular it should be noted that the overhang was always related to the flare by

$$\frac{x_o}{L} = .002 \delta_2 \quad (\delta_2 \text{ in degrees})$$

In this way large flare was always associated with large overhang or stem rake. Table 3 gives the flare and overhang of each bow. Full details of the bow design method are given in Appendix 1 but a brief description is also given here.

The bows were designed using polynomials to represent the waterlines, the section shape at station 2 and the stem profile above the design water line. Each polynomial was defined by suitable boundary conditions to ensure a smooth mating with the rest of the hull surface and to achieve the desired flare angle at station 2 at the deck. The actual water lines were generated using a specially written computer program BMILL1 on the Naval Academy Time Sharing (NATS) Honeywell computer system and subsequently also implemented on the AMTE(H) Prime Computer. The program was arranged to generate body plans for inspection on a Tektronix 4051 graphic display unit. Other facilities included the ability to display three dimensional views on the Evans and Sutherland picture system and full size body plans on the Xynetics flat bed plotter in the CADIG Computing Centre; but the most important feature was the ability to transfer the lines to the numerically controlled milling machine in the Division of Engineering and Weapons Workshop. This enabled the major part of the manufacture of each bow to be done automatically leaving only the final finishing and fitting to be done by hand. Figure 4 shows the body plans of these six bows. Note that these plans use a 60 station system instead of the more usual 20 station convention. Section shapes were therefore defined at two additional stations between each pair of conventional stations.

Figure 5 shows a more detailed comparison between the body plans of the 35 degrees and 45 degrees bows. The common underwater lines can be seen.

Figure 6 shows the variation of local flare angle for each bow. As expected all bows have the same flare angle of about 22 degrees at station 5 where they merge into rest of the hull and have their nominal values at station 2. Flare generally increases forward of station 2 and then decreases as the stemhead is approached.

A special version of program BMILL1 entitled BMILLK was written to design a family of knuckle bows. The knuckle was at a constant height of .0375L (4.66 m at full scale) above the design waterline. In each case the bow was defined in terms of a flare angle at the knuckle and a "phantom" flare angle at the deck (See Figure 3). The phantom flare angle chosen was 35 degrees so that the deck plan and the stem profile were identical to those of the 35 degrees bow. The section shape at station 2 between the design waterline and the knuckle was represented by a polynomial in the usual way : above the knuckle the section at Station 2 was represented by a straight line joining the knuckle to the previously defined deck edge. Figure 7 shows the resulting family of knuckle bows : the bow with a knuckle flare angle of 45 degrees was selected for manufacture and testing and was designated Bow 35/45 K. Figure 8 shows a more

detailed comparison of this bow with the 35 degrees bow. The common underwater hull form and identical deck width can be seen.

The bows and the hull were finished with moss green enamel paint rubbed down to a semi matt finish using wet and dry sandpaper.

Before each experiment the model was ballasted to the desired displacement and trim (see Table 2) and the longitudinal radius of gyration K_{yy} adjusted to $0.25L$ using the bifilar suspension test method. It was found impossible to achieve this radius of gyration with the two heaviest bows (50 degrees and 55 degrees flare) and the model was tested with a radius of gyration of $0.27L$ in these cases (See Table 3).

5. MODEL INSTRUMENTATION

5.1. Relative Bow Motion

The model was fitted with capacitance strips to measure relative motion at the bow as shown in Figure 9. These strips were made up from successive layers of 50 mm waterproof adhesive ("scotch") tape, 13 mm aluminium foil and 50 mm Teflon adhesive tape. The aluminium foil acted as one plate of the capacitor while the Teflon tape functioned as the dielectric. The water provided the other "plate" of the capacitor, contact being maintained by bare aluminium foil return strips on the hull surface. The capacitance of the strips formed in this way was essentially directly proportional to the length of strip submerged and was monitored by suitable circuits.

Strips were fixed to the model at the stem and at stations $\frac{1}{3}$, 1, 2 and 3, as shown in Figure 9. Since the strips were essentially straight it was impossible to follow the curved stem profile exactly and the stem strip was therefore applied at a tangent to the stem profile at the stem head. In all cases the raked stem strip was applied to the starboard side of the model and the vertical station strips were applied to the port side. In some of the later experiments the strip at station 3 was not fitted and a second raked strip fitted on the starboard side instead. This strip was mounted parallel to the stem strip and intersected the deck edge at station -0.46 (ie forward of the forward perpendicular).

Although the capacitance strips were found to give a basically linear response (Capacitance directly proportional to length of strip immersed) the curvature of the hull surface to which they were attached introduced a non linear aspect to their calibration. Each capacitance strip was therefore calibrated individually by mounting it on a wooden template cut to the section shape at the appropriate station. The template and strip were immersed to various depths to calibrate the strip as shown in Figure 10. The resulting non linear calibration curve was stored for subsequent use on the Hydromechanics Laboratory Computer. In some later experiments at the Academy a watertight box was built around the length of hull in question and the strips were calibrated by filling the box with water to various measured depths.

5.2. Wetness Impacts

Deck Wetness was monitored using the array of pressure sensitive cells illustrated in Figure 11. These cells were formed by spot facings in an aluminium plate. The face of the plate was covered with a layer of thin surgical rubber glued in place to form a diaphragm over each cell. A pressure tapping at the back of each cell enabled it to be connected via plastic tubing to one of twelve 3.5 KN/m^2 (0.5 psi) pressure transducers mounted on the carriage. In some later experiments only four transducers were used. The array was mounted on the model at station 5 (at the after end of each bow) and positioned on the port side. Symmetry was maintained by a dummy array on the starboard side.

Calibration was achieved by lowering the array to successive depths in a tank of water.

5.3. Ship Motions and Incident Waves

Absolute bow motion at station 2 and heave were monitored using string and potentiometer systems. The incident wave time history was recorded alongside station 2 about 1 metre to starboard using the standard Hydromechanics Laboratory Sonic probe. Bow vertical acceleration was recorded using a $\pm 1g$ accelerometer mounted inside each bow at station 2 (station 3 for the 55 degrees bow).

6. EXPERIMENT FACILITY

The experiments were conducted in the 380 feet (115 m) towing tank in the Hydromechanics Laboratory of the US Naval Academy. The low speed carriage was used to tow the model. All data channels were digitised at 51.2 Hz and transmitted "ashore" using the carriage's standard laser system.

The Hydromechanics Laboratory PDP 11 computer was used to acquire the data and data processing was completed between runs using specially written analysis programs (see Section 7 and Appendix 2).

Irregular waves were generated using the laboratory's MATS wavemaker system.

7. EXPERIMENTS

7.1. Wave Spectra

Preliminary experiments to generate and store a library of suitable irregular wave time histories were conducted in February and June 1983. Some waves were regenerated for repeat experiments in January 1984. Figure 12, taken from Reference 30, was used to guide the choice of suitable significant wave heights and modal periods to represent typical conditions in the North Atlantic in winter and the Bretschneider two parameter wave spectrum formulation was used.

Table 4 lists the time histories generated. In each case (ie for

each significant wave height and period) two time histories were generated by selecting different "random" numbers to govern the phase relationships between the component sine waves making up the wave-maker drive signal. Each time history lasted 350 seconds. Allowing for the time required for the slowest moving waves to travel the length of the tank this gave a usable time history for testing purposes of 230 seconds, equivalent to 23 minutes at full scale. Thus a total of 46 minutes at full scale was available for each case considered. After the model test program had commenced and a better idea of typical (impact) wetness frequencies obtained, an extra time history WU was generated to allow additional experiments to be conducted in the chosen "basic" condition with $H_{1/3} = 5.5$ metres, $T_0 = 12.4$ seconds. Thus, for this condition, a total of 69 minutes of full scale testing could be simulated.

The technique for generating a wave time history involved running successive experiments and iterating the wavemaker transfer function using the computer's standard programs until the measured spectrum converged and coalesced with the desired spectrum. Figures 13-15 show a typical set of iterations. For the first run the wavemaker transfer function is assumed to be unity and independent of frequency and Figure 13 shows the result obtained. A much better result is obtained after one iteration (Figure 14) and a near perfect result achieved at the third attempt (Figure 15).

Curiously, it was found that the "random" number had a significant effect on the rate at which the measured spectrum converged on the desired spectrum. Those listed in Table 4 generally gave rapid convergence (in three runs) but others, eg 123456 and 757531, never achieved a satisfactory match, even after more than ten iterations.

Some of the resulting wave time histories were analysed using the Hydromechanics Laboratory computer program STA to determine significant wave heights (mean of highest third of all wave heights). Results are shown in Table 5 (designated "wave" tests) and are generally within 1 per cent of the desired value.

The encountered waves were also monitored during the model experiments and analysed to obtain rms wave elevations σ_ζ using the specially written WETANA program (See section 7.4). If the wave energy spectrum is assumed narrow banded it can be shown that the significant wave height $\bar{H}_{1/3}$ is given by

$$\bar{H}_{1/3} = 4.00 \sigma_\zeta$$

and Table 5 gives significant wave heights derived on this basis for each model experiment. In general the results are about 5 per cent higher than the nominal values. The reason for this discrepancy is not known. The very low result obtained with Bow 40 at 5.5 m/15.0 seconds can probably be attributed to the short run time of only 14 minutes in these experiments. This may not have been sufficient to allow reliable statistics to be obtained.

Also shown in Table 5 are the results obtained during some experiments which were repeated at the Academy in January 1984. These gave significant wave heights about 5 per cent less than the nominal value. The reason for this discrepancy is not known but it may be associated with a computer malfunction which made it necessary to regenerate the required wave time histories from scratch instead of using the ones generated for the original experiments.

7.2. Preliminary Experiments

The model was run for the first time with the 40 degrees bow on June 1 1983. No instrumentation was fitted since the intention was to determine suitable test conditions (to ensure reasonably severe deck wetness) and suitable locations for the relative motion capacitance strips.

The model was run in wave time history WB ($H_{1/3} = 4.5$ metres, $T_0 = 12.4$ seconds at full scale) at speeds equivalent to 20 and 22 knots. These conditions did not appear to give an adequate frequency of deck wetness and a more severe wave WG/WH/WU ($H_{1/3} = 5.5$ metres, $T_0 = 12.4$ seconds) and 22 knots was selected as the standard test condition.

7.3. Experiment Procedure

A novel and demanding experiment of this nature inevitably involves a period in which the laboratory staff, by trial and error, learn the best procedures to use. The procedure described here is the one which eventually evolved but it should be pointed out that it was not always followed exactly, particularly in the early stages of the project.

After calibrating the relative motion strips by the methods described in section 5.1 the model was fitted with the bow to be tested and the relative motion strips and supporting electronic equipment installed. The complete model was then ballasted to give the required trim and longitudinal moment of inertia before being rigged under the towing carriage. Remaining instrumentation was connected and zeroed.

A calm water run was made first to establish the running trim and the calm water bow wave and this run was repeated at the end of the experiment series. Runs in the selected wave time histories followed. In the first run data acquisition began 120 seconds after the wave maker was started. This allowed time for the slowest moving waves in the wave spectrum to travel the entire length of the tank and ensured that the model experienced the complete range of wave lengths in the run. At a model speed equivalent to 22 knots at full scale it was found that the maximum run time (governed by the length of the tank) was about 36 seconds (3.6 minutes at full

scale). After a wait of about 20 minutes (to allow the tank water to settle) the second run was started nominally 156 (ie $120 + 36$) seconds after the wavemaker start time. This ensured that the second run was made in a wave time history different from the first although both time histories were part of the same longer history having the desired wave spectrum.

This procedure was repeated with each successive run starting a nominal 36 seconds later in the wave time history. Each time history was long enough to accommodate six model runs and this gave a test programme of 18 runs for each bow in the standard wave spectrum. Each bow was therefore tested for a time nominally equivalent to 63 minutes at full scale.

Actual data acquisition start times differed slightly from the nominal start times due to operator error and hardware faults in the carriage start system. As far as possible the start times achieved during the first runs with the 35 degrees bow were repeated for all other bows so that the runs would be as nearly exactly comparable as possible.

Bow 40 was the only bow tested with the other wave spectra. Twelve runs were conducted with wave time histories WI and WJ ($H_{1/3} = 6.5$ metres, $T_o = 12.4$ seconds) and WO and WP ($H_{1/3} = 5.5$ metres, $T_o = 13.8$ seconds). Only four runs were completed with time history WQ since this was found to give hardly any deck wetness.

In all cases the carriage was started 8 seconds before the data acquisition commenced to allow time for the model to be accelerated to the test speed.

Repeat experiments with the 40 degrees bow were completed in the standard wave spectrum. Additional experiments with limited instrumentation were also conducted in this spectrum with the 30 degrees and 45 degrees bows in January 1984.

Individual runs are listed in Appendix 2.

7.4. Data Analysis

Data was acquired from all instrumentation channels as described in Section 5 and selected channels were displayed as time histories for visual inspection on the terminal monitor screen before accepting the run as a valid experiment. If the data were deemed acceptable they were saved and stored on the Hydromechanics Laboratory computer and analysed before the next run.

Analysis was completed using specially written computer programs entitled WETPITCH, CLIP, WETANA and WETANB. After all the runs for a given bow had been completed program WETANC was used to complete the analysis. These programs are described in full in Appendix 2, but a brief description of the analysis is also given here.

Program WETPITCH was first run to create time histories of pitch and

notional relative bow motion by suitable manipulation of the heave, absolute bow motion and encountered wave time histories.

The relative motion time histories included many occasions when the relative motion exceeded the freeboard and/or draught of the model. These could be readily identified by the "flat tops" to the signals as shown in Figure 16. Analysis of these signals to obtain mean and rms values and probabilities of exceedance would inevitably give misleading results and program CLIP was therefore written to restore the "missing" peaks and troughs in the records. The program was run using the measured relative motion time histories as input and created corresponding "corrected" time histories which were used in the subsequent analysis.

In order to simplify the detection of "flat tops" the program was arranged artificially to clip the peaks and troughs at specified levels (fractionally less than the freeboard and draught) and the missing peaks were replaced by suitable cubic polynomials. Figure 17 shows the result obtained for the raw data of Figure 16.

Program WETANA analysed the time histories of the corrected relative bow motions, notional relative bow motion and the encountered wave. Each signal was analysed to give the mean and rms value and a histogram of peaks and troughs. The times at which the relative motions exceeded the local freeboard were also determined and written to a temporary scratch file.

This file was subsequently listed by Program WETANB which then analysed the impact pressure time histories to calculate histograms and mean and significant pressures for each pressure transducer. The number of impacts, their pressure levels and the times at which they occurred were also determined. These times were correlated with the times when the relative motion exceeded the freeboard so that those freeboard exceedances which resulted in an impact could be identified.

Program WETANC was used to collate the results obtained from individual runs with WETANA and WETANB and produce overall results for the entire series of experiments with each bow. Results calculated included:

- a. Mean and rms motions weighted according to individual run times (mean rms values were actually calculated by weighting the variances).
- b. Probability distributions of peaks and troughs in the motions and corresponding results based on the Rayleigh formula using the measured rms motion.
- c. Total numbers of motion peaks and troughs and impacts.
- d. Mean and significant values and histograms of impact pressures.
- e. Total number of freeboard exceedances at each station and freeboard exceedances per hour.

- f. Impacts per hour.
- g. Total run time.
- h. Bow efficiency defined by

$$\eta = 1 - \frac{N_W}{N_F}$$

where N_W and N_F are the number of recorded wettings (impacts) and freeboard exceedances. Thus an efficiency of 1.0 would imply that the bow succeeded in keeping every freeboard exceedance (if there were any) off the deck; conversely a zero efficiency would mean that every freeboard exceedance resulted in a wetting.

8. RESULTS

8.1. Calm Water

Figure 18 shows the bow wave height measured in the calm water runs. The above water bow form would not be expected to have very much effect on the bow wave and the results have therefore been amalgamated to produce an average calm water bow wave for all bows. This is plotted over the experiment results for each individual bow. In most cases the individual results match the average very well and it is confirmed that the above water bow form does not appear to influence the shape of the bow wave.

Also shown in Figure 18 is the mean notional relative motion in calm water. This corresponds to the local sinkage (at station 2) and excludes the local bow wave. The local sinkage also appears to be independent of above water bow form and accounts for only a small proportion of the bow wave.

8.2. Waves

The correlation between the observed and nominal significant wave heights has already been discussed in Section 7.1. Figures 19 and 20 show the measured probability of wave peaks and troughs exceeding various levels for two wave spectra (5.5 m/12.4 seconds and 6.5/12.4 seconds). These are compared with theoretical distributions based on the Rayleigh Distribution formula using the measured rms wave elevations:

$$P(x > X) = \exp \left[\frac{-X^2}{2\sigma^2} \right]$$

The experiment results are skewed showing that high peaks are more likely and deep troughs less likely than the symmetrical Rayleigh formula would indicate. The discrepancy is even more marked for the higher significant wave height (Figure 20). This result might have been expected since it is well known that very steep waves have sharp crests and comparatively rounded troughs.

8.3. Mean Relative Motions in Waves

Figure 21 shows the mean relative motions in waves for each bow in the standard wave spectrum. Again an average result has been calculated for all bows and this is a reasonable approximation to most of the individual results. The raked relative motion strips on the starboard side of the model give rather inconsistent results : the reason for this is not known. Also shown is the mean notional relative motion at station 2. This represents the contribution of sinkage and trim (or the mean values of heave and pitch) to the mean relative motion : in all cases the contribution is almost negligible.

Figure 22 shows similar results for Bow 40 in the other wave spectra. These results are compared with the result obtained for Bow 40 in the standard wave spectrum: from the limited evidence available it would appear that the mean relative motion increases with modal period but is independent of significant wave height.

The results given in Figure 21 are plotted as a function of flare angle in Figure 23. These show that the mean relative motion is a relatively weak function of flare angle : maximum values occur at flare angles of 40 or 45 degrees. The strong dependence on flare angle of the mean relative motion at the stem can be largely attributed to the amplifying effect of the increasing rake of the relative motion capacitance strip.

Figure 23 also shows the calm water bow wave measurements taken from Figure 18. These show a similar weak dependency on flare angle (as has already been assumed) but are consistently higher than the mean relative motions in waves. This is an important result since most existing deck wetness calculation methods assume that the freeboard is reduced by the height of the calm water bow wave. It would appear that this assumption is probably pessimistic.

In contrast an opposite trend was found by O'Dea in tests on an SL7 containership in Reference 31: here the mean relative motions in waves were found to be higher than the calm water bow wave.

O'Dea attributed this to the presence of a thin sheet of water adjacent to the hull surface at the bow (Reference 32). This sheet of water apparently emanated from the rounded waterline endings above the load waterline and its height was believed to be enhanced as the bow plunged downwards into the waves. No opposite effects occurred as the bow rose out of the water and this resulted in the observed increase in the mean relative motion. It will be noted that the bows tested in the experiments described in this report all had sharp waterline endings so that this phenomenon, if it does exist, would not be expected to be present in these cases.

8.4. Rms Relative Motions in Waves

Figure 24 shows the rms relative motions measured with each bow in the standard wave spectrum. Again an average result has been calculated for all bows. Also shown are the notional relative motions

at station 2 : the true rms relative motion at this station is some 50 per cent higher and this confirms the findings of Blok and Huisman in Reference 7.

Figure 25 shows similar results for the 40 degrees bow in the other wave spectra. Increasing modal period decreases the relative motions : as expected the relative motions increase with significant wave height.

Figure 26 shows the results of Figure 24 plotted as a function of flare angle. At the stem the influence of flare is again exaggerated by the rake of the capacitance strips. Elsewhere the relative motion is almost independent of flare but there appears to be an enhanced relative motion for the 50 degree bow at station $1/3$. As if to compensate, this bow showed the lowest relative motions at stations 1 and 2.

8.5. Probability Distributions of Relative Motion

Figure 27 shows a typical result for the probability distributions of relative motions for the 35 degrees bow. Each graph shows the probability of exceeding specified peak and trough amplitudes for a particular measurement station. In each case the results are plotted about a zero mean: ie the amplitudes of the peaks and troughs are measured relative to the mean value of the relative motion time history. This mean value lies above the design waterline (see Figure 21) and the relative motion scales of Figure 27 are therefore offset from the design waterline. The actual locations of the waterline are shown and this enables the amplitudes corresponding to the local draught and freeboard to be determined in each case.

Also shown for comparison are the probability distribution curves based on the Rayleigh formula using the measured rms relative motions.

These results can be used to determine the probability of the relative motion exceeding the freeboard according to the experiment results and according to the Rayleigh formula.

The precise form of the replaced peaks in the CLIP routine will have had some effect on these probability distributions at amplitudes greater than the freeboard and draught. However this is not important in the current context because the distributions have only been used to determine probability levels at the deck edge and almost any reasonable form of extrapolation would have given virtually the same results. The form of the replaced peaks will also have had some effect on the measured rms motions but this is expected to be very small. Many of the probability distributions do have slight discontinuities at the deck edge and at the keel and this is presumably due to imperfections in the CLIP routine.

A rather more complex technique was used for the knuckle bow. It was clear from a visual inspection of the records that the relative

motions were usually truncated at the knuckle line. In other words the water was being shed from the hull surface at the knuckle, as intended. So using the CLIP routine in the usual way had virtually no effect on the relative motion signals and the resulting probabilities, denoted by circles in Figure 28, relate to water in contact with the hull surface. In most cases these results show a sharp drop in probability at the knuckle line.

It was also of interest to estimate the statistics of the relative height of the water surface on either side of the bow (ie not in contact with the hull surface above the knuckle line) and appropriate results were obtained by using the CLIP program to replace the missing peaks at the knuckle rather than at the deck. The probabilities, shown by triangles in Figure 28, relate to water not in contact with the hull above the knuckle. The latter technique was also used to derive the rms and mean relative motions and the corresponding Rayleigh probability curve shown in Figure 28.

In practice it was found that this refinement made very little difference to the mean and rms values.

In general the Rayleigh formula fitted the results fairly well for all bows but consistently good results were obtained at the stem. At station $\frac{1}{3}$ the formula consistently underestimated the probabilities at the deck level but the discrepancies were not large.

Further aft the formula consistently overestimated the probabilities of exceeding the freeboard.

These results have been used to derive the probabilities of the relative motion exceeding the freeboard shown in Figure 29. In each case curves based on the measured probabilities and the Rayleigh prediction (based on measured rms values) are shown. Unfortunately there are insufficient data to enable wholly reliable curves to be drawn and some licence and imagination has been used to produce the results shown. It should be remembered that these are very sensitive to small errors in the measured rms and mean values of the motions : with these provisos only tentative conclusions can be drawn.

In general it seems that the maximum probability of the relative motion exceeding the freeboard occurs between the forward perpendicular and station 1. Aft of this point the probability diminishes rapidly to very low levels (in some cases there were no freeboard exceedances at stations 2 and 3 in the entire experiment). Forward of the maximum the probabilities diminish significantly but then rise to a (usually lower) maximum at the stem head.

The maximum probabilities (both at the stem head and near the Forward Perpendicular) are generally quite well predicted by the Rayleigh formula but, as already mentioned, the predicted probabilities are consistently too high further aft. This is, however, of little practical importance because interest is invariably centred on the maxima.

The predicted probabilities are always too high for the 55 degrees bow. It is believed that this may be because the water simply falls away from contact with the heavily flared hull surface under the influence of gravity.

Figure 29 (c) shows results for the knuckle bow and includes the estimated probability of the water surface not in contact with the hull above the knuckle rising above the deck level. This is, of course, much more likely to occur than the true freeboard exceedance of water in contact with the hull surface.

If it is assumed that a freeboard exceedance at one of the less probable stations is always accompanied by an exceedance at the most probable station it follows that the probability of an exceedance anywhere is the same as the maximum probability. These maximum probabilities are plotted in Figure 30.

Bearing in mind the caveats mentioned above it is clear that these results are rather tentative: nevertheless it seems that the probability of the relative motion exceeding the freeboard (abaft the stem head) is independent of bow shape for moderate flare angles, but increases to a maximum at 50 degrees flare angle. The probability is reduced at 55 degrees flare angle.

The probability of immersing the stem head is apparently rather more sensitive to bow shape; but the maximum probability again occurs at 50 degrees flare angle.

The knuckle is effective at reducing the probability of immersion of the deck edge but this is apparently offset by an increase in the probability of stem head immersion.

Figure 31 shows the total number of relative motion peaks per hour for each bow in the standard wave spectrum and these have been used with the probability results to obtain the number of freeboard exceedances per hour in Figure 32. These results have been used, in turn, to derive the maximum number of freeboard exceedances and the number of immersions of the stem head per hour in Figure 33. These results broadly confirm the trends found for probability in Figure 30.

8.6. Impact Pressures

The original intention was to use the pressure sensitive array to determine impact pressure distributions and to compare the impact pressures experienced with each bow. However it was found that the pressure calibrations were rather unstable (probably due to inadequate quality control of the diaphragm material and the adhesive used to attach the diaphragms to the array block) and the results obtained were not very reliable. Consequently the analysis has concentrated on determining only the total number of impacts counted per hour of run time (at full scale).

For the purposes of the analysis an impact was accepted as such if:

- a. It resulted in a pressure pulse of at least 10 KN/sq m at ship scale (equivalent to 5.8 lb/sq ft at model scale).

b. It was recorded on at least two pressure transducers.

This technique eliminated the spurious impacts caused by electronic noise in the transducer system. Since an impact was counted as such only if it exceeded a given threshold level it is clear that the changes in the pressure calibrations must have had some effect on the recorded number of impacts. However, most of the visually obvious impacts were well over the threshold level (even allowing for calibration changes) and there was always a good correlation between visual observations and the number of impacts recorded in each run.

Figure 33 and Table 6 show the results obtained and these may be readily compared with the number of freeboard and stem head exceedances per hour.

The impact pressure frequency results are rather scattered and this is probably attributable to the unstable pressure calibrations. Within the likely accuracy of the experiment it appears that bow flare angle has little or no effect on deck wetness frequency with the exception of the high result obtained for the 50 degrees bow. This result is supported by the unusually high number of freeboard and stem head exceedances recorded for this bow as well as by visual impressions obtained during the experiments.

It is immediately obvious that most of the freeboard exceedances do not result in an impact and it is clear that all the bows are quite effective at keeping water off the deck. The knuckle bow may be marginally the most effective bow in that it has the smallest number of impacts per hour.

8.7. Bow Efficiency

The bow efficiency parameter defined in section 7.4 might be expected to quantify the visual impression of bow effectiveness as perceived by the ship's crew in that it is equivalent to the proportion of freeboard exceedances which do not result in an impact or deck wetting. Figure 33 shows the results obtained from the experiments: for moderate flare angles the bow efficiency is fairly constant at about 0.85 but this is reduced as the flare angle increases above 45 degrees. In other words a greater proportion of freeboard exceedances result in deck wetness at these large flare angles and these bows would therefore be judged to be relatively ineffective.

Clearly the bow efficiency parameter is not a reliable guide to the true performance of the bow : the 55 degrees bow had a relatively small number of impacts and was therefore really quite effective, but it also had an unusually small number of freeboard exceedances and thus would appear, in the absence of a comparison with other bows, to be ineffective.

The knuckle bow's efficiency, calculated for true freeboard exceedances in contact with the bow, is also rather low. This, however, would not correspond with a crewman's visual impression of

the bow's performance since he would inevitably judge it in relation to the height of the water on either side of the bow (not in contact with the hull surface above the knuckle). An efficiency based on this estimation is also shown and this is much the same as for the moderately flared bows.

9. THEORETICAL PREDICTIONS

9.1. Calm Water Bow Wave and Mean Relative Motions in Waves

Shearer's theory (Reference 8) has been used to predict the calm water bow wave for the model at a full scale speed of 22 knots. The results are compared with the mean values obtained for all bows in Figure 18. Close to the stem the prediction is too low but good results are obtained at stations 2 and 3.

The same prediction is compared with the mean relative motion in waves (averaged for all bows) in Figure 21. This is often assumed to be the same as the calm water bow wave in studies of deck wetness but it has already been shown that it is actually rather lower. Perhaps fortuitously, Shearer's theory gives a reasonable prediction which is probably adequate for practical purposes.

9.2. Relative Motions in Waves

Figure 34 shows the rms relative motions (averaged for all bows) compared with theoretical predictions using the suite of strip theory computer programs described in Reference 9. The curve marked "no swell up" is the result computed by simple vector addition of the local absolute vertical motion and the undisturbed incident wave. It lies, as expected, considerably below the experiment results for actual relative bow motion because these include the effects of swell up. This calculated result should be compared with the notional relative motion result obtained in the experiment at Station 2. The calculated result is about 15 per cent too high.

Also shown in Figure 34 is the actual relative motion computed with the swell up assessed by the method suggested by Blok and Huisman in Reference 7. The method employs Shearer's theory (Reference 8) to calculate the rate of change of bow wave height with ship draught; Blok and Huisman's experimental work suggested that this would enable the swell up coefficient to be calculated from

$$SUC = 1 + \frac{dh}{dT}$$

where \bar{h} is the height of the bow wave or the mean relative motions in waves and T is the ship draught. The true relative motion should then be given by

$$S = S_{NOT} \cdot (SUC)$$

where S_{NOT} is the notional relative motion. Blok and Huisman's

experiments showed that the swell up coefficient defined in this way for approximately the same Froude Number lay in the range 1.1 - 1.5 and this conclusion is broadly confirmed by the experiment results shown here. However the values calculated by the method they suggest are generally too small. Evidently Shearer's theory, while apparently adequate for bow wave prediction at a typical draught, is not sufficiently reliable to predict the rate of change of bow wave height with draught.

9.3. Swell Up Factor

Accurate prediction of the relative motions is obviously a prerequisite for the prediction of deck wetness. It seems, at present, that the discrepancies found in the prediction of notional relative motion and the lack of any reliable method of predicting swell up preclude the attainment of this goal. In order to avoid this problem and allow concentration on the deck wetness process it was decided to:

- a. Decrease the calculated notional relative motion by 15 per cent everywhere to compensate for the discrepancy noted above.
- b. Use a swell up derived by comparing measured relative motions with corrected notional motions.

It was found convenient to define the swell up in terms of an apparent amplification of the incident wave rather than the direct amplification of the relative motion used by Blok and Huisman. To emphasise the distinction the swell up factor is defined by

$$SUF = \frac{\zeta}{\zeta_{NOT}}$$

where ζ is the actual incident wave amplitude adjacent to the hull surface and ζ_{NOT} is the "notional" wave amplitude which would be measured far away from the ship. Thus a swell up factor of 1.0 corresponds to an undistorted incident wave (ie no swell up; notional relative motion = actual relative motion); a value of 2.0 gives a moderate swell up with the local wave amplitude doubled and so on. For the purposes of this work it was assumed that the swell up factor was independent of frequency.

The PAT suite of seakeeping computer programs (Reference 9) was specially modified at AMTE(H) to allow computation of relative motions with arbitrary swell up factors and the results are shown in Figure 35. (Note that these results have been factored to align the predicted rms notional relative motion ($SUF = 1.0$) at station 2 with the result measured in the experiments).

Figure 35 has been used to derive swell up factors for each bow and each station by comparing predicted and measured relative motions. For example the measured rms relative motion at station 1 on Bow 30 was 4.0 metres and this value is predicted with a swell up

factor of 3.0.

The resulting required swell up factors are shown in Figure 36. In each case the individual results are compared with the mean for all bows. All the results have a similar character rising from about 2.0 at station 3 to about 3.5 at station $\frac{1}{3}$. A notable exception is Bow 50 which has a much higher swell up at station $\frac{1}{3}$.

9.4. Prediction of Deck Wetness

It is clear from the results shown in Figure 33 that freeboard exceedances do not necessarily result in deck wetness. Simple considerations of the deck wetness process (see Appendix 3) lead to the conclusion that the resulting sheet of water thrown up by the bow will only come inboard if its vertical velocity (relative to the earth) is less than a certain critical velocity. Appendix 3 shows that the critical velocity is

$$\dot{\zeta}_{\text{CRIT}} = \frac{g \sin \alpha \cos \alpha}{\omega \tan \delta}$$

where α is the slope of the deck edge in plan view $\left(\frac{-dy}{dx} \right)$.

There are thus two conditions to be simultaneously satisfied if a wetting is to occur:

- a. The relative motion must exceed the freeboard at some station.

and

- b. The absolute vertical velocity of the water surface at the same station must be less than the critical velocity.

If the Rayleigh probability formula is assumed to apply the probability of the relative motion exceeding the freeboard is

$$P_F = \exp \left[- \frac{(F - \bar{S})^2}{2 \sigma_s^2} \right]$$

where F is the local (geometric) freeboard,

\bar{S} is the mean value of the relative motion in waves,

and σ_s is the rms relative motion.

The probability of the absolute vertical water velocity not exceeding the critical velocity is difficult to evaluate at the instant when the spray sheet leaves the deck edge. As an approximation we assume that it is given by the associated probability of the peak velocity:

$$P_{\zeta_{CRIT}} = 1 - \exp \left[\frac{-\zeta_{CRIT}^2}{2\sigma_{\zeta}^2} \right]$$

where σ_{ζ} is the rms absolute vertical water velocity immediately adjacent to the hull surface.

Both σ_s and σ_{ζ} include swell up effects.

If these two events are assumed to be independent the joint probability of them both occurring is

$$P_{WET} = P_F \cdot P_{\zeta_{CRIT}}$$

(see Reference 33).

Since the bows tested in the experiments described in this report were all defined analytically it was possible to calculate exact values of the critical velocity at each station and these are plotted in Figure 37. As expected, the heavily flared bows have low critical velocities.

So, for a given probability of freeboard exceedance, these bows would be expected to have a reduced probability of deck wetness.

A simple computer program entitled PWET was written for the AMTE(H) PRIME computer to calculate the probability of deck wetness according to the above formulae. The program calculated probabilities as a function of bow form, hull station and swell up factor. In the first instance the program was used with calculated rms motions (corrected as shown in Figure 35) and the measured mean value of the relative motions in waves for each bow (Figure 21). Figure 38 shows a typical set of results for Bow 30. As expected, the probability of the relative motions exceeding the freeboard increases with swell up factor. Conversely the probability of the vertical velocity of the water not exceeding the critical velocity decreases with swell up factor (because the water velocity increases).

Figure 39 shows the resulting product, the probability of wetness, as a function of swell up factor for each bow.

The points plotted on these diagrams relate to the required swell up factors determined in Figure 36. It will be seen that these results therefore essentially relate to the motion values measured.

in the experiments. It was impossible to determine a swell up factor for the stem head : however since the stem head is almost always out of the water and forward of the rest of the hull it seems certain that swell up effects must be small. In the event a swell up factor of 1.0 has been assumed.

The locus of the plotted points in Figure 39 therefore represents the predicted probability, based on the measured motions, of a freeboard exceedance which would result in a wetting. The results are plotted in a more conventional form in Figure 40.

It can be seen that the peak probability station apparently moves forward as the flare angle increases until it reaches the stem head at Bow 40. For higher flare angles the probability is therefore governed not so much by the flare as by the location of the stem head. Figure 41 shows the estimated peak probability obtained from Figure 40 plotted as a function of flare angle. The results are compared with the measured probabilities of deck wetness. These have been obtained by dividing the measured number of impacts per hour by the number of relative motion peaks per hour interpolated at the appropriate (most frequent wetness) station from Figures 31 and 32.

The predicted level of wetness probability agrees reasonably well with the experiment results. However the experiment results tend to show that the wetness probability increases slightly with flare angle while the opposite trend is found for the predictions. Nevertheless it is emphasised that the general level of the predictions is about right and this represents a considerable advance on the simple calculations of the probability of freeboard exceedance which have previously been the norm.

These predictions have been essentially based on experiment measurements of relative motions and effective freeboard in order to demonstrate an understanding of the wetness process without the complicating issue of the accuracy of the motion predictions. A practising naval architect would not usually have access to accurate relative motion data during a design study and would have to rely on straightforward motion computations. This situation has been simulated by calculating the wetness probability using the calculated notional relative motions (uncorrected for the 15 per cent discrepancy discussed earlier) with an assumed constant swell up factor of 3.0 for the FP and stations abaft the FP. A swell up factor of 1.0 was assumed for the stem head and Shearer's method was used to estimate the mean relative motions in waves. The results are shown as dotted curves in Figure 40 and derived peak probabilities are given in Figure 41.

These are rather higher than the results obtained with the measured motions. It is clear from Figure 39 that the choice of swell up factor does not influence the calculated probability very much and Figure 21 shows that Shearer's method is adequate for predicting the mean relative motion. So the change in the probability level must be largely attributed to the 15 per cent discrepancy between the predicted and measured relative motions.

Finally Figure 42 shows the same results plotted in the form of number of deck wettings per hour.

10. THE OPTIMUM BOW

The techniques described in the previous sections have been used to calculate the probability of deck wetness for a wider range of bow shapes than were tested in the experiments. In particular the overhang was varied independently of flare angle and a total of 36 bow designs were investigated. Flare angles from 10 degrees to 60 degrees in steps of 10 degrees and overhangs $\left(\frac{x_o}{L}\right)$ from .02 to .12 in steps of .02 were used.

For the purposes of this study the calculated relative motions and a mean relative motion (effective freeboard reduction) given by Shearer's method were used. The swell up factor was assumed to be 1.0 at the stem head and 3.0 at and abaft the Forward Perpendicular.

In the event it was found that the bow designs with a nominal flare angle of 10 degrees gave negative flare angles (tumblehome) near the stem and the critical velocity approach was considered inapplicable. These bows were therefore eliminated from the study.

As an example Figure 43 shows the variation of local flare angle for the 40 degrees bow with various overhangs and Figure 44 shows the corresponding critical velocities. As expected the flare angle abaft station 2 is almost independent of overhang (indeed it is always exactly 40 degrees at station 2) but forward of this point it increases with overhang. This leads to a large reduction in the critical velocity so that these large overhang bows might, on this basis alone, be expected to be comparatively dry.

Figure 45 shows the probability of wetness computed for these bows on the basis already described : these results are again for a ship speed of 22 knots in the "standard" wave condition.

For small overhangs the relative motion at the stem head is small and this gives a low probability of wetness even though the critical velocity is very high. Further aft the probability of exceeding the freeboard is higher because of the swell up and the maximum probability of wetness generally occurs close to the Forward Perpendicular. As the overhang is increased the relative motions and the probability of wetness increase at the stem head. This is accompanied by a reduction in the probability of wetness further aft because of the more favourable critical velocity. The net result is to move the maximum probability station forward until wetness is governed by the behaviour at the stem head.

Figure 46 shows the calculated wetness probability for the bows considered in this study. Wetness apparently decreases with both flare and overhang but excessive values will not be expected to guarantee a particularly dry ship.

Also shown in Figure 46 are the corresponding predictions and measured results for the bows tested in the experiments. These all lie close to the troughs of the curves and this explains why so little variation in performance was found.

The beneficial effect of overhang has been confirmed in experiments described in References 23 and 29.

In view of the assumptions required and the relative simplicity of the theory it would be stretching credibility to use the results of Figure 46 to determine in optimum bow design with any degree of precision. Nevertheless it is clear that a wide range of bow forms would be expected to give the near optimum results obtained in the experiments.

For design guidance it would appear that a minimum nominal flare angle (at station 2) of about 30 degrees and a minimum overhang of about .06 times the ship length are needed. Exceeding these values will not be expected to improve performance very much. It is stressed that these recommendations strictly apply only to the FFG7 design for which these calculations have been made; but similar results would be expected for other conventional frigates and destroyers in similar sea states.

11. CONCLUSIONS

This report has described a comprehensive series of experiments to determine the effect of above water bow form on deck wetness in irregular head seas. A systematic series of six bows defined by a nominal flare angle and an associated stem overhang were tested on a model of the FFG7 frigate in the 380 ft (115 m) towing tank at the US Naval Academy. An additional bow incorporating a knuckle was also tested. All bows had the same freeboard.

The bows were tested at a single speed corresponding to 22 knots at full scale in a Bretschneider sea spectrum with a significant wave height of 5.5 metres and a modal period of 12.4 seconds. This represents a commonly occurring condition in the North Atlantic in winter. Each bow was run for a time equivalent to at least one hour at full scale. A limited number of tests were also conducted in other sea spectra.

The experiments measured relative bow motion at several stations close to the stem and deck wettings were counted by monitoring impacts on a pressure sensitive array on the fo'c's'le.

It was found that the above water bow form had remarkably little effect on the relative motions or the frequency of deck wetness. The four moderately flared bows (30 degrees, 35 degrees, 40 degrees and 45 degrees flare angles) all showed essentially identical characteristics. Only the two most extreme designs exhibited any significant departure from this norm. The 50 degrees bow had the highest number of freeboard exceedances and the highest number of recorded impacts. This appears to be associated with an unusually large relative motion at station $\frac{1}{3}$ coupled with an unexpectedly high probability of exceeding the freeboard.

The most extreme bow (55 degrees flare) had a much reduced frequency of freeboard exceedance but this did not result in a significant reduction in deck wetness.

The knuckle bow gave a small reduction in the frequency of deck wetness.

A simple theoretical analysis has been developed to allow the probability of deck wetness to be computed as a function of bow form. Calculations on this basis confirm that the bows tested in the experiments would all be expected to have a similar performance and suggest that this is about the best that can be achieved.

Extending the calculations to cover a wider range of bow designs suggests that a broadly similar, near optimum, performance would be expected at a given freeboard from any bow with a flare angle greater than about 30 degrees and an overhang greater than about 0.06 times the ship length. Excessive flare and overhang will not ensure a better performance.

It is recommended that the theory is further verified by testing two additional bows having apparently unfavourable features. Suitable choices would be

20 degrees Flare .08 overhang

40 degrees Flare .03 overhang

These bows would be expected to have two or three times the wetness frequency experienced in the present experiments.

12. ACKNOWLEDGEMENTS

The major part of the work described in this report was completed during the author's tenure as NAVSEA visiting Research professor at the United States Naval Academy. Financial support from the US Naval Sea Systems Command is gratefully acknowledged.

A demanding experiment programme of this nature cannot possibly be accomplished without a great deal of willing support and co-operation from a large number of people. The author would like to record his appreciation of the efforts of the following individuals

Paco Rodriguez who advised and assisted with the computer aided design work.

Tom Price who made the models.

and the staff of the Hydromechanics Laboratory under the able leadership of Professor Bruce Johnson and John Hill

Joe Salsich who organised the project, prepared the models and ran the experiments.

John Zseleczky who unveiled the mysteries of the Hydro-mechanics Laboratory Computer, contributed a great deal of essential expertise to the development of the Software and ran the experiments.

Don Bunker who designed and built the pressure array, prepared the models and ran the experiments.

Steve Enzinger who took photographs and ran the experiments.

Norm Tyson who prepared the instrumentation and could, by his mere presence, ensure that faults in the carriage drive system would magically disappear.

REFERENCES

1. A R J M Lloyd and R N Andrew. Criteria for Ship Speed in Rough Weather. 18 ATTC August 1977.
2. R N Andrew and A R J M Lloyd. Full Scale Comparative Measurements of the Behaviour of Two Frigates in Severe Head Seas. TRINA Vol 123 1981.
3. N K Bales. Minimum Freeboard Requirements for Dry Foredecks: A Design Procedure. SNAME STAR Symposium. April 1979.
4. R Tasaki. On Shipping Water in Head Waves. Journal of the Society of Naval Architects of Japan Vol 107 July 1960.
5. M F Van Sluijs. Ship Relative Motions and Related Phenomena. Symposium on the Dynamics of Marine Vehicles and Structures in Waves. London 1974.
6. J F O'Dea and H D Jones. Absolute and Relative Motion. Measurements on a model of a High Speed Containership. 20 ATTC Hoboken 1983.
7. J J Blok and J Huisman. Relative Motions and Swell Up for a Frigate Bow. RINA Spring meetings 1983.
8. J R Shearer. A Preliminary Investigation of the Discrepancies between the Calculated and Measured Wavemaking of Hull Forms. Trans. NECIES Vol 67. 1950-51.
9. P R Loader. The User Guide for the PAT-82 Ship Motion Program Suite. AMTE(H) TM 81025. December 1981.
10. W Hovgaard. General Design of Warships E F Spon Ltd. London and New York. 1920.
11. W Hovgaard. Trials on Three Danish Torpedo Boats. Engineering. July 26 and August 2 ; 1889.
12. J L Kent. Experiments on Mercantile Ship Models in Waves. TINA Vol 64. 1922.
13. K MacDonald and E V Telfer. Seakindliness and Ship Design. NECIES Vol LIV. 1937-38.
14. J Edward and F M Todd. Steam Drifters: Tank and Sea Test. TIESS Vol 82. 1939.
15. J L Kent. The Design of Seakindly Ships. NECIES. Vol 66 1949;50.
16. J F Allan. Research on Design of Drifters. TINA Vol 93. 1951.

17. H E Saunders. The Influence and Behaviour of the Above Water Body. Chapter 26 Hydrodynamics in Ship Design. Volume I. SNAME 1957.
18. H E Saunders. The Design of Ships to Insure Good Performance in Waves. Chapter 20 Hydrodynamics in Ship Design. Volume III SNAME 1957.
19. R N Newton. Wetness Related to Freeboard and Flare. TRINA. Volume 102. 1960.
20. M A Abkowitz. Seakeeping Considerations in Design and Research. SNAME New England Section 1957.
21. W A Swaan and G Vossers. The effect of Forebody Section Shape on Ship Behaviour in Waves. TRINA Volume 103 1961.
22. M F Van Sluijs and T S Gie. Behaviour and Performance of Compact Frigates in Head Seas ISP Volume 19. No 210 February 1972.
23. A R J M Lloyd and D Sharpe. Effect of Bow Shape on Deck Wetness. AMTE(H) TM 78008. February 1978.
24. S Sivaprakasam. Deck Wetness Experiments. MSc Thesis Department of Mechanical Engineering University College London. 1980.
25. A M Tucker. Deck Wetness Experiments. MSc Thesis. Department of Mechanical Engineering University College London. 1981.
26. A R J M Lloyd and M A Hammond. The Effect of Bow Shape on Ship Motions and Deck Wetness. AMTE(H) Report R82012 July 1982.
27. R W Greenwood. Deck Wetness. MSc Thesis. Department of Mechanical Engineering University College London. 1982.
28. H J Armstrong. The Effect of Full Length Hull Flare on Ship Motions and Deck Wetness. MSc Thesis. Department of Mechanical Engineering University College London. 1983.
29. A R J M Lloyd. Deck Wetness Experiments. 20 ATTC. Hoboken. 1983.
30. S L Bales, W T Lee and J M Voelker. Standardised Wave and Wind Environments for NATO Operational Areas. DTNSRDC Report SPD-0919-01. July 1981.
31. J F O'Dea. Relative Motion and Deck Wetness Investigation of the SL-7 Containership. DTNSRDC Report SPD-1081-01. April 1983.
32. J F O'Dea. Private Communication. 1984.

33. M K Ochi and W E Bolton . Statistics for Prediction of Ship Performance in a Seaway. International Shipbuilding Progress. Volume 20 No 222.

Table 1

Literature Survey on Effects of Above Water Bow Form on Deck Wetness

Author	Reference	Freeboard	Flare	Overhang or Rake	Knuckle
Hovgaard	10, 11			+	
Kent	12, 13		+	+	
McDonald and Telfer	13		+		
Edward and Todd	14	+	+		
Allan	16		+		
Saunders	17, 18	+	-	-	
Newton	19	+	+		+
Abkowitz	20		+		
Tasaki	4		-		
Swaan and Vossers	21		-		
Van Sluijs and Gie	22		+		+
Lloyd et al	23, 26 29	+	-	+	

+ : Beneficial effects

- : Detrimental effects

Table 2

FFG7 HULL PARTICULARS

	Model	Ship
Length	3.45 m	124.4 m
Beam	0.392 m	14.1 m
Draught	0.130 m	4.66 m
Trim	Level	Level
LCG Aft Midships	.015 m	.55 m
Ship Mass	78.4 kg (Fresh Water)	3750 tonnes (Salt Water)

Table 3

BOW FORM PARTICULARS

Bow No	δ_2	$\frac{X_o}{L}$	$\frac{K_{YY}}{L}$
1	30 degrees	.06	.25
2	35 degrees	.07	.25
3	40 degrees	.08	.25
4	45 degrees	.09	.25
5	50 degrees	.10	.27
6	55 degrees	.11	.27
7	35 degrees ($\delta_K = 45$ degrees)	.07	.25

WAVE CONDITIONS FOR MODEL TESTS

Table 4

	Ship Scale			Model Scale				"Random" Number
	H _{1/3} m	T ₀ Sec	Probability Of Occurrence Per Cent	H _{1/3} m	T ₀ Sec	f ₀ Desired Hz	f ₀ Achieved Hz	
WB WC	4.5	12.4	3.8	0.125	2.07	0.484	0.480	267387 245760
WG WH WU	5.5	12.4	3.9	0.153	2.07	0.484	0.480	267387 245760 757573
WI WJ	6.5	12.4	1.9	0.181	2.07	0.484	0.480	267387 245760
WS* WT*	7.5	12.4	0.4	0.280	2.07	0.484	0.480	267387 245760
WO WP	5.5	13.8	1.7	0.153	2.30	0.435	0.440	267387 245760
WQ WR*	5.5	15.0	1.4	0.153	2.50	0.400	0.400	267387 245760

Frame Length 25 Seconds Highest Harmonic 32
 No of Points 512 Usable Time 230 Seconds
 No of Frames 14
 Lowest Harmonic 8
 * Not used in Experiments

Table 5

ACHIEVED SIGNIFICANT WAVE HEIGHTS

Nominal Spectrum		Test	Measured Significant Wave Height	Measured/ Nominal Significant Wave Height
Significant Wave Height	Modal Period			
Metres	Seconds		Metres	
5.5	12.4	Wave	5.5	1.00
		Bow 30	5.84	1.06
		Bow 35	5.80	1.05
		Bow 40	5.85	1.06
		Bow 40 repeat	5.88	1.07
		Bow 45	5.80	1.05
		Bow 50	5.97	1.09
		Bow 55	5.76	1.05
		Knuckle Bow	5.73	1.04
		Bow 30 (Jan 1984)	5.15	0.94
		Bow 45 (Jan 1984)	5.32	0.97
5.5	13.8	Wave	-	
		Bow 40	5.64	1.03
5.5	15.0	Wave	-	
		Bow 40	5.05	0.92
6.5	12.4	Wave	6.55	1.01
		Bow 40	6.52	1.00

NB: Significant wave heights for "wave" tests were obtained directly (average of highest third) using the Hydrolab computer STA program.

Significant wave heights for bow tests were obtained by multiplying rms elevations by 4.0.

Table 6

IMPACT PRESSURE RESULTS

Bow	Impacts Per Hour	Relative Motion Peaks/Hour	Probability Of Impact
30	49.7	630	.079
	41.0		.065
35	55.4	615	.090
40	46.5	664	.070
	67.2	710	.095
45	62.6	648	.097
	50.0		.077
50	82.8	644	.129
55	51.8	643	.081
Knuckle	46.1	664	.069

Appendix 1

BOW DESIGN METHOD

1. Introduction

The bows were all designed to fare smoothly into the FFG7 hull form at station 5 and at the chosen waterline (draught = 0.0375L or 4.66 m, level trim). All bows had a freeboard of .06L (7.46m) and no shear.

The bows were generated using a system of polynomial curves to represent waterlines, section shape at station 2 and the stem profile. This method resulted in a family of bows defined only by a single parameter, the flare angle at station 2. Details of the design method follow.

2. Co-ordinate System

The origin of co-ordinates is at the intersection of the stem and the forward perpendicular. x_s is positive forward, z is positive down and y is positive to starboard.

3. Flare Angle and Overhang

Flare angle is defined at station 2 as shown in Figure A1.1. Overhang is arbitrarily defined as

$$\frac{x_o}{L} = 0.002 \delta_2 \text{ (degrees)} \quad (1)$$

(See Figure A1.2)

Thus large flare angles are associated with large overhangs.

4. Section Shape at Station 2

Above the load waterline the section shape is defined by

$$\frac{y_2}{L} = b_0 + b_1 \frac{z}{L} + b_2 \left(\frac{z}{L} \right)^2 \quad (2)$$

as shown in Figure A1.1.

Boundary conditions are:

- a. Offset at load waterline

$$\frac{y_2}{L} = .01655 \text{ at } z = 0 \text{ (from FFG7 body plan)}$$

b. Slope at load waterline:

$$\frac{dy_2}{dz} = - .2734 \text{ at } z = 0 \text{ (from FFG7 body plan)}$$

c. Slope at deck:

$$\frac{dy_2}{dz} = - \tan \delta_2 \text{ at } \frac{z}{L} = - \frac{F}{L} = - .06$$

$$\text{Hence } b_0 = .01655 \quad (3)$$

$$b_1 = -.2734 \quad (4)$$

$$b_2 = \frac{\tan \delta_2 + b_1}{.12} \quad (5)$$

Thus the section shape at station 2 is completely defined by the single parameter δ_2 . Hence, if δ_2 is known, the offset y_2 at any waterline can be determined.

5. Stem Profile

Above the load waterline the stem profile is defined by

$$\frac{x_s}{L} = C_0 + C_1 \frac{z}{L} + C_2 \left(\frac{z}{L} \right)^2 \quad (6)$$

as shown in Figure A1.2.

Boundary Conditions are:

a. Overhang at origin of co-ordinates

$$\frac{x_s}{L} = 0 \text{ at } z = 0$$

b. Slope at origin of co-ordinates

$$\frac{dx_s}{dz} = - .8333 \text{ at } z = 0$$

c. Overhang at stem head

$$\frac{x_s}{L} = \frac{x_0}{L} \text{ at } \frac{z}{L} = - \frac{F}{L} = .06$$

$$\text{Hence } C_0 = 0 \quad (7)$$

$$C_1 = - .8333 \quad (8)$$

$$C_2 = \frac{\left(\frac{x_0}{L} - 0.05 \right)}{0.0036} \quad (9)$$

If the flare angle is defined $\frac{x_0}{L}$ can be determined from equation 1. Hence the stem shape can be determined if δ_2 is known.

6. Waterlines

Above the load waterline the waterlines are given by

$$\frac{y}{L} = a_0 + a_1 \left(\frac{x}{L} \right) + a_2 \left(\frac{x}{L} \right)^2 + a_3 \left(\frac{x}{L} \right)^3 \quad (10)$$

as shown in Figure A1.3.

(The coefficients $a_0 - a_3$ are different for each waterline).

Boundary conditions are:

- a. Overhang at stem:

$$\frac{y}{L} = 0 \text{ at } \frac{x}{L} = \frac{x_s}{L}$$

- b. Offset at station 5:

$$\frac{y}{L} = \frac{y_5}{L} \text{ at } \frac{x}{L} = -0.25 \text{ (From FFG7 Body Plan)}$$

- c. Slope at station 5:

$$\frac{dy}{dx} = \left(\frac{dy}{dx} \right) \text{ at } \frac{x}{L} = -0.25 \text{ (From FFG7 Body Plan)}$$

- d. Offset at Station 2:

$$\frac{y}{L} = \frac{y_2}{L} \text{ at } \frac{x}{L} = -0.1 \text{ (From quadratic already defined at Station 2)}$$

Hence

$$a_3 = \frac{\left[\left[(A-B) \frac{x_s}{L} + 0.25A - 0.1B \right] \left(\frac{dy}{dx} \right)_5 + \frac{Ay_5}{L} - \frac{By_2}{L} \right]}{\left[\left[\left(\frac{x_s}{L} \right)^3 - 0.1875 \frac{x_s}{L} \right] (B-A) + 0.03125A - 0.01775B \right]} \quad (11)$$

$$a_2 = \frac{\left(\frac{x_s}{L} + 0.1\right) \left(\frac{dy}{dx}\right)_5 + \frac{y_2}{L} - a_3 \left[\left(\frac{x_s}{L}\right)^3 + 0.1875 \frac{x_s}{L} + 0.01775\right]}{A} \quad (12)$$

$$a_1 = \left(\frac{dy}{dx}\right)_5 + 0.5 a_2 - 0.1875 a_3 \quad (13)$$

$$a_0 = -a_1 \left(\frac{x_s}{L}\right) - a_2 \left(\frac{x_s}{L}\right)^2 - a_3 \left(\frac{x_s}{L}\right)^3 \quad (14)$$

$$\text{where } A = -\left(\frac{x_s}{L}\right)^2 - 0.5 \left(\frac{x_s}{L}\right) - 0.04 \quad (15)$$

$$B = -\left(\frac{x_s}{L}\right)^2 - 0.5 \left(\frac{x_s}{L}\right) - 0.0625 \quad (16)$$

Thus if the flare angle δ_2 is defined:

- i. $\frac{y_2}{L}$ can be determined from equation 2.
- ii. $\frac{x_0}{L}$ can be determined from equation 1.
- iii. $\frac{x_s}{L}$ can be determined from equation 6.
- iv. $\frac{y_5}{L}$ and $\left(\frac{dy}{dx}\right)_5$ are known already and the waterline value of $\frac{y}{L}$ can be determined from equation 10.

7. Bow Form Family

The equations described above form the basis of a NATS Computer program (subsequently implemented at AMTE(H)) entitled BMILL1 which was used to define the family of bows which were used in the experiment. Flare angles chosen for testing were 30 degrees, 35 degrees, 40 degrees, 45 degrees, 50 degrees and 55 degrees.

8. Knuckle Bows

The equations described above were adapted to generate a family of knuckle bows along similar lines. The knuckle bows were defined by a knuckle flare angle and a "phantom" flare angle. The phantom flare angle was used to define the stem profile and the deck shape as for the ordinary bows: thus a knuckle bow with, say, a

30 degrees phantom flare angle would have the same stem profile and deck as an ordinary bow with a 30 degrees flare angle.

The knuckle was arbitrarily defined as parallel to the load waterline and keel at $0.0375L$ above the load waterline. The knuckle flare angle δ_K was defined at the knuckle at station 2.

Equation 2 was used, with appropriately modified boundary conditions, to define the section shape at station 2 between the load waterline and the knuckle.

Above the knuckle the section at station 2 was defined by a straight line between the knuckle and the edge of the deck.

In this way the stem profile and section at station 2 could be defined by specifying the phantom and knuckle flare angles : hence the waterlines could be generated in the same way as for the ordinary bows.

The above treatment gives a knuckle which merges into the rest of the hull form at the stem and at station 5 and a deck plan and stem profile identical to one member of the family of ordinary bows.

A modified version of program BMILL1 entitled BMILLK was used to generate a family of knuckle bows using a phantom flare angle of 35 degrees. A single knuckle bow with a knuckle flare angle of 45 degrees was selected for testing from this family.

9. Bow Manufacture

The bows were made of wood on the CADIG numerically controlled milling machine using ordinates generated by the programs BMILL1 and BMILLK. These ordinates are stored in files entitled BSM and BSTEM. The ordinates were defined at 32 waterlines where waterline 13 corresponded to the load waterline. Thus milling was performed only from waterlines 13 to 32. Waterlines were 11.28 mm (0.444 inches) apart. Station spacing was $\frac{1}{60}$ of the waterline length corresponding to 57.6 mm (2.267 inches).

Appendix 2

DATA ANALYSIS

1. Experiment Runs

A total of 224 experiments were conducted. These are listed in Tables A2.1 (experiments in waves) and Table A2.2 (experiments in calm water). Each run in waves was commenced at a given delay time after the wavemaker had been started. The first run was started after a delay of 120 seconds to allow time for the slowest moving waves to reach the end of the tank. Each tank run took about 36 seconds. Subsequent runs were therefore started nominally at multiples of 36 seconds delay after the 120 seconds initial delay. Actual delays used varied slightly due to operator error and hardware faults and are listed in Table A2.1.

2. Raw Data Files

Each experiment produced a total of 21 raw data time history files. Each file consisted of a (nominal) 36 second record digitised at 51.2 Hz. File names used were:

RBM1.AL	Relative motion at stem
RBM2.AL	Relative motion at station $\frac{1}{3}$
RBM3.AL	Relative motion at station 1
RBM4.AL	Relative motion at station 2
RBM5.AL	Relative motion at station 3. Relative motion parallel to the stem at station - 0.46 at the deck in some experiments with Bow 40
HEVE.AL	Heave
ABM.AL	Absolute bow motion at station 2.
ENCW.AL	Encountered wave elevation alongside station 2
BOAC.AL	Bow Acceleration at station 2. Station 3 for Bow 55.
P0.AL	Impact pressure 0
P11.AL	Impact pressure 11

Files having the same name but relating to different delay times, bows or wave time histories were distinguished by the PDP 11 system of version numbers. Thus the first file named RBM1 would be stored as version 1 under the complete name: RBM1.AL;1, the second as RBM1.AL;2 and so on. Version numbers for each run are listed in Tables A2.1 and A2.2. Note that these numbers are octal.

3. Program WETPITCH

The first step in the analysis was to run program WETPITCH. This program read the data files HEVE and ABM and calculated corresponding time histories for pitch (file name PTCH.AL) and notional relative bow motion at station 2. (file name NRBM.AL).

Pitch was defined as:

$$\theta = \frac{a-z}{x} \cdot \frac{180}{\pi} \text{ degrees (positive bow up)}$$

where a is the absolute bow motion at station 2 (positive up)

z is the heave at the CG (positive up)

and x is the longitudinal distance from the CG to station 2 (positive)

Notional relative motion was defined as

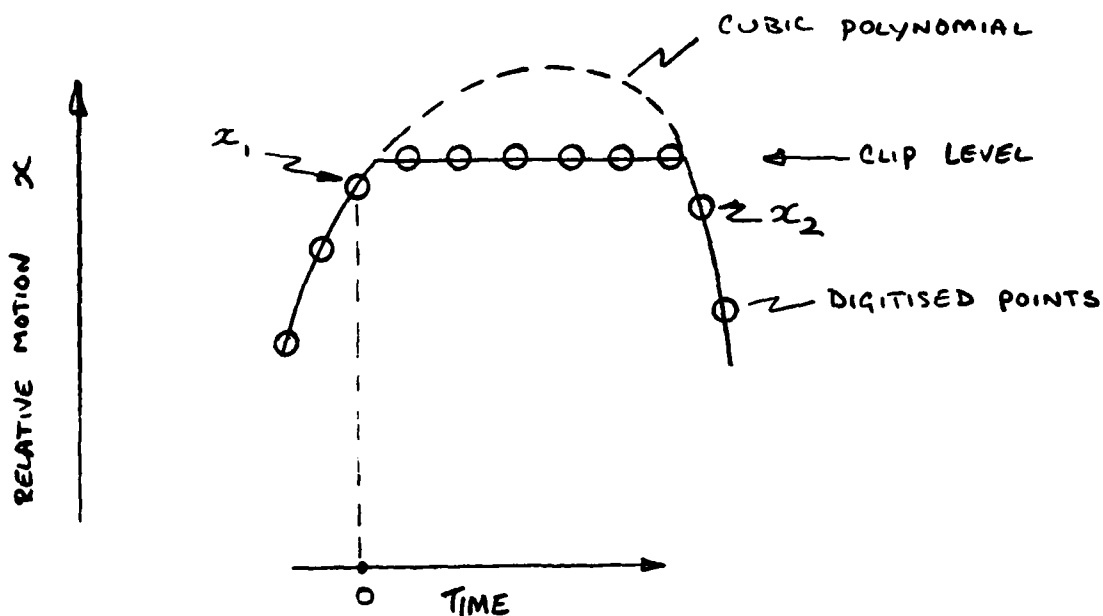
$$S_{\text{NOT}} = -a - \zeta \text{ (positive bow up)}$$

where ζ is the wave elevation alongside station 2.

Files PTCH.AL and NRBM.AL used the same version numbers as the raw data files.

4. Program CLIP

Program CLIP operated on the five relative motion time histories RBM1.AL - RBM5.AL and was used to replace "missing" peaks and troughs arising from deck submergence and keel emergence. In order to simplify the identification of the missing peaks and troughs the program was arranged to clip the signals at levels slightly less than the measured freeboard and draught. The peaks and troughs were then replaced by cubic polynomials arranged to fare in with the original records as shown below.



Suppose the last point before the clip is x_1 and the first point after the clip is x_2 . Suppose also that the slopes at these points are given by \dot{x}_1 and \dot{x}_2 respectively. Then the "missing" peak is given by

$$x = a_0 + a_1 t + a_2 t^2 + a_3 t^3$$

where t is measured from an origin at x_1 .

It can be shown that

$$a_3 = \frac{\dot{x}_1 + \dot{x}_2 + 2 \frac{(x_1 - x_2)}{t_2}}{t_2^2}$$

$$a_2 = \frac{x_1 - x_2}{t_2^2} + \frac{\dot{x}_2}{t_2} - 2 a_3 t_2$$

$$a_1 = \dot{x}_2 - 2 a_2 t_2 - 3 a_3 t_2^2$$

$$a_0 = x_2 - a_1 t_2 - a_2 t_2^2 - a_3 t_2^3$$

Hence the missing peak can be interpolated from a knowledge of x_1 , x_2 , \dot{x}_1 and \dot{x}_2 .

The CLIP program created five new "corrected" relative motion time histories with names CBM1.AL - CBM5.AL. Version numbers for these files are listed in Tables A2.1 and A2.2.

5. Program WETANA

Program WETANA was run to analyse the motion time histories. The program read the files CBM1 - CBM5, ENCW and NRBM and analysed the data to obtain the mean value, the rms value and a histogram of peaks and troughs for each time history. All results were converted to metres at ship scale and written to a file named according to the following system:

	WG	22	A	.B30	;1
Wave Time History Name	_____	_____	_____	_____	_____
Speed in Knots	_____	_____	_____	_____	_____
Output of WETANA	_____	_____	_____	_____	_____
Bow Identification	_____	_____	_____	_____	_____
Version Number	_____	_____	_____	_____	_____

Calm water runs used "CALM" as the wave identifier. The knuckle bow used "BK" as the bow identifier for the time histories analysed in the usual way. "BK1" was used to identify the analysis with the relative motions clipped at the knuckle line.

Version numbers are listed in Tables A2.1 and A2.2.

6. Program WETANB

Program WETANB was run to analyse the pressure data. The impact pressure peaks were sorted into histograms and mean and significant pressures were calculated for each pressure transducer. The total number of impacts and the impact times and recorded pressures were also listed individually. The program also sorted the data into successive wetness events by correlating the impact times for each transducer and related the results to the times at which the relative motions exceeded the freeboard.

Output of WETANB was filed under a name according to the convention already described for WETANA and the same version numbers were used.

In practice it was found that the results of WETANB could not be trusted without extensive checking by hand since the pressure signals were often noisy and many spurious "impacts" featured in the analysis. These were readily identified because they generally appeared only on one channel : nevertheless their elimination was a time consuming exercise.

7. Program WETANC

After all the runs with a given bow and wave spectrum had been completed Program WETANC was used to amalgamate all the data to produce a collated result for all runs. It was first necessary to rename all the files produced by programs WETANA and WETANB according to the following system:

Bow 30 . A ; 1

Bow Identifier _____

WETANA _____

Version Number _____

Version numbers are listed in Table A2.1. Program WETANC calculated:

- a. Average mean relative motion and wave elevation weighted according to individual run times.
- b. Average rms relative motion and wave elevation calculated by weighting the individual variances according to individual run times.
- c. Minimum and maximum individual mean and rms motions.
- d. Probability distributions of peaks and troughs of relative motions and encountered waves.
- e. Corresponding theoretical probability distributions based on the calculated mean rms motions and wave elevations.
- f. Total number of recorded motion and wave peaks and troughs.
- g. Pressure histograms for each transducer.
- h. Mean and significant pressures for each transducer.
- i. Total number of recorded impacts.
- j. Total number of freeboard exceedances and freeboard exceedances at each station.
- k. Total run time.
- l. Impacts and freeboard exceedances per hour.
- m. Bow efficiency.

Output of program WETANC was listed in files named PROB.PDP.

Table A2.1 (a)

EXPERIMENT RUNS AND FILE VERSION NUMBERS

30 Degrees Bow Discpack 1 $H_{1/3} = 5.5 \text{ m}$ $T_o = 12.4 \text{ sec}$

Date	Time	Wave	Delay Sec	Data File Version No	CBM File Version No	Result File Version No	Renamed Result File Version No
19 July 1983	1322	WG	120	145	72	1	1
	1400		158	146	73	2	2
	1440		194	147	74	3	3
	1505		229	150	75	4	4
	1527		265	151	76	5	5
	1548		301	152	77	6	6
	1620	WH	120	153	100	1	7
	1640		172	154	101	2	10
	1707		207	155	102	3	11
	1730		242	156	103	4	12
	1804	WU	277	157	104	5	13
	1830		312	160	105	6	14
	1923		120	161	106	1	15
	1941		174	162	107	2	16
	2003		209	163	110	3	17
	2026		244	164	111	4	20
	2047		279	165	112	5	21
	2107		314	166	113	6	22

Table A2.1 (b)

EXPERIMENT RUNS AND FILE VERSION NUMBERS

30 Degrees Bow (Repeat)

Discpack

 $H_{1/3} = 5.5 \text{ m}$ $T_o = 12.4 \text{ sec}$

Date	Time	Wave	Delay Sec	Data File Version No	CBM File Version No	Result File Version No	Renamed Result File Version No
11 Jan 1984	0900	WG	120	222	222	1	1
	0948		158	223	223	2	2
	1013		194	224	224	3	3
	1108		229	225	225	4	4
	1129		265	226	226	5	5
	1204		301	227	227	6	6
	1318	WH	120	230	230	1	7
	1342		172	231	231	2	10
	1406		207	232	232	3	11
	1430		242	233	233	4	12
	1457		277	234	234	5	13
	1529		312	235	235	6	14
12 Jan 1984	0954	WU	120	236	236	1	15
	1031		174	237	237	2	16
	1052		209	240	240	3	17
	1123		244	241	241	4	20
	1149		279	242	242	5	21
	1452		314	243	243	6	22

Table A2.1 (c)

EXPERIMENT RUNS AND FILE VERSION NUMBERS

35 Degrees Bow Discpack 1 $H_{1/3} = 5.5 \text{ m}$ $T_o = 12.4 \text{ sec}$

Date	Time	Wave	Delay Sec	Data File Version No	CBM File Version No	Result File Version No	Renamed Result File Version No	
5 July 1983		WG	120	4	1	1	1	
			150	5	2	2	2	
			194	6	3	3	3	
			229	7	4	4	4	
			265	10	5	5	5	
			301	11	6	6	6	
WH		120	12	7	1	7		
		172	13	10	2	10		
6 July 1983		WU	207	14	116	3	11	
			242	15		4	12	
			277	16	117	5	13	
			312	17	13	6	14	
			120	20	14	1	15	
			174	21	15	2	16	
7 July 1983			0839	209	22	16	3	17
			0930	244	23	17	4	20
	0945		279	24	20	5	21	
	1015		314	25	21	6	22	

Table A2.1 (d)

EXPERIMENT RUNS AND FILE VERSION NUMBERS

40 Degrees Bow

Discpack 1

 $H_{1/3} = 5.5 \text{ m}$ $T_0 = 12.4 \text{ sec}$

Date	Time	Wave	Delay Sec	Data File Version No	CBM File Version No	Result File Version No	Renamed Result File Version No	
8 July 1983		WG	120	27	22	1	1	
			158	30	23	2	2	
			194	31	24	3	3	
12 July 1983		WH	229	100	25	4	4	
			265	101	26	5	5	
			301	102	27	6	6	
120			103	30	1	7		
172			104	31	2	10		
207			105	32	3	11		
242			106	33	4	12		
277			107	34	5	13		
13 July 1983			WU	312	110	35	6	14
				120	111	36	1	15
	174	112		37	2	16		
	209	113		40	3	17		
	244	114		41	4	20		
	279	115		42	5	21		
1227	314	116	43	6	22			

Table A2.1 (e)

EXPERIMENT RUNS AND FILE VERSION NUMBERS40 Degrees Bow
(repeat)

Discpack 2

 $H_{1/3} = 5.5 \text{ m}$ $T_o = 12.4 \text{ sec}$

Date	Time	Wave	Delay Sec	Data File Version No	CBM File Version No	Result File Version No	Renamed Result File Version No
26 July 1983	1700	WG	120	76	76	1	1
	1729		158	77	77	2	2
	1752		194	100	100	3	3
	1815		248*	101	101	4	4
	1835		265	102	102	5	5
	1855		301	103	103	6	6
	1910	WH	120	104	104	1	7
	1935		172	105	105	2	10
	1956		207	106	106	3	11
	2015		242	107	107	4	12
	2035	WU	277	110	110	5	13
	2050		312	111	111	6	14
	2110		120	112	112	1	15
	2135		174	113	113	2	16
	2155		209	114	114	3	17
	2210		244	115	115	4	20
	2230		279	116	116	5	21
	2249		314	117	117	6	22

* Late Start

Table A2.1 (f)

EXPERIMENT RUNS AND FILE VERSION NUMBERS

45 Degrees Bow Discpack 2 $H_{1/3} = 5.5 \text{ m}$ $T_0 = 12.4 \text{ sec}$

Date	Time	Wave	Delay Sec	Data File Version No	CBM File Version No	Result File Version No	Renamed Result File Version No
20 July 1983	1443	WG	120	1	2	1	1
	1525		158	2	1	2	2
	1600		194	3	3	3	3
	1650		229	4	4	4	4
	1710		265	5	5	5	5
	1732		301	7	6	6	6
	1750	WH	120	10	7	1	7
	1812		172	11	10	2	10
	1835		207	12	11	3	11
	1857		242	13	12	4	12
	1920		277	14	13	5	13
	2005		312	15	14	6	14
	2030	WU	120	16	15	1	15
	2048		174	17	16	2	16
	2107		209	20	17	3	17
	2128		244	21	20	4	20
	2147		279	22	21	5	21
	2207		314	23	22	6	22

Table A2.1 (g)

EXPERIMENT RUNS AND FILE VERSION NUMBERS

45 Degrees Bow Discpack $H_{1/3} = 5.5 \text{ m}$ $T_o = 12.4 \text{ sec}$
(Repeat)

Date	Time	Wave	Delay Sec	Data File Version No	CBM File Version No	Result File Version No	Renamed Result File Version No
6 Jan 1984	1417	WG	120	200	200	1	
5 Jan 1984	0853		158	173	173	2	
	1048		194	174	174	3	
6 Jan 1984	1113		229	175	175	4	
	1201		265	176	176	5	
	1337		301	177	177	6	
	1444	WH	120	201	201	1	
	1511		172	202	202	2	
	1545		207	203	203	3	
	1624		242	204	204	4	
9 Jan 1984	0920		277	205	205	5	
	0949		312	206	206	6	
	1028	WU	120	210	207	1	
	1046		174	211	211	2	
	1107		209	212	212	3	
	1129		244	213	213	4	
	1211		279	215	215	10	
	1532		314	216	216	6	

Table A2.1 (h)

EXPERIMENT RUNS AND FILE VERSION NUMBERS

50 Degrees Bow Discpack 2 $H_{1/3} = 5.5 \text{ m}$ $T_o = 12.4 \text{ sec}$

Date	Time	Wave	Delay Sec	Data File Version No	CBM File Version No	Result File Version No	Renamed Result File Version No
25 July 1983	1411	WG	120	52	52	1	1
	1430		158	53	53	2	2
	1500		194	54	54	3	3
	1520		229	55	55	4	4
	1540		265	56	56	5	5
	1611		301	57	57	6	6
		WH	120	60	60	1	7
			172	61	61	2	10
			207	62	62	3	11
	1728		242	63	63	4	12
26 July 1983	0910	WH	277	65	65	5	13
	0928		312	66	66	6	14
	0946	WU	120	67	67	1	15
	1007		174	70	70	2	16
	1030		209	71	71	3	17
	1052		244	72	72	4	20
	1117		279	73	73	5	21
	1140		314	74	74	6	22

Table A2.1 (1)

EXPERIMENT RUNS AND FILE VERSION NUMBERS

55 Degrees Bow Discpack 1 $H_{1/3} = 5.5$ m $T_o = 12.4$ sec

Date	Time	Wave	Delay Sec	Data File Version No	CBM File Version No	Result File Version No	Renamed Result File Version No
14 July 1983	1113	WG	120	120	45	1	1
			158	121	46	2	2
	1339		194	122	47	3	3
	1410		229	123	50	4	4
	1432		265	124	51	5	5
	1510	WH	301	125	52	6	6
	1550		120	126	53	1	7
	1614		172	127	54	2	10
	1630		207	130	55	3	11
	1651		242	131	56	4	12
	1718	WU	277	132	57	5	13
	1739		312	133	60	6	14
	1759		120	134	61	1	15
	1815		174	135	52	2	16
			209	136	63	3	17
	1900		267*	137	64	4	20
	1918		290*	140	65	5	21
			314	141	66	6	22

* Late Start

Table A2.1 (j)

EXPERIMENT RUNS AND FILE VERSION NUMBERS

35/45K Bow Discpack 1 $H_{1/3} = 5.5 \text{ m}$ $T_o = 12.4 \text{ sec}$

					Standard Analysis	RBM Signals Clipped at Knuckle		
Date	Time	Wave	Delay Sec	Data File Version No	CBM Version No	CBM Version No	Result File Version No	Renamed Result File Version No
21 July 1983	1312	WG	120	26	26	162	1	1
	1335		158	27	27	163	2	2
	1357		194	30	30	164	3	3
	1412		229	31	31	165	4	4
	1432		265	32	32	166	5	5
	1447		301	33	33	167	6	6
	1512	WH	138*	34	34	170	1	7
	1540		191*	35	35	171	2	10
	1602		207	36	36	172	3	11
	1626		242	37	37	173	4	12
	1646		277	40	40	174	5	13
	1707		312	41	41	175	6	14
	1729	WU	120	42	42	176	1	15
	1749		174	43	43	177	2	16
	1807		209	44	44	200	3	17
	1827		249	45	45	201	4	20
	1845		279	46	46	202	5	21
	1901		314	47	47	203	6	22

* Late Start

Table A2.1 (k)

EXPERIMENT RUNS AND FILE VERSION NUMBERS

40 Degrees Bow Discpack 2 $H_{1/3} = 6.5 \text{ m}$ $T_o = 12.4 \text{ sec}$

Date	Time	Wave	Delay Sec	Data File Version No	CBM File Version No	Result File Version No	Renamed Result File Version No
27 July 1983	0856	WI	120	121	121	1	1
	0919		156	122	122	2	2
			192	123	123	3	3
	1028		228	124	124	4	4
	1052		264	125	125	5	5
	1117		300	126	126	6	6
		WJ	120	127	127	1	7
	1200		156	130	130	2	10
	1230		192	131	131	3	11
	1250		228	132	132	4	12
	1313		264	133	133	5	13
	1337		300	134	134	6	14
28 July 1983	1032	WI	120	155	155	7	-

Table A2.1 (1)

EXPERIMENT RUNS AND FILE VERSION NUMBERS

40 Degrees Bow Discpack 2 $H_{1/3} = 5.5 \text{ m}$ $T_o = 13.8 \text{ sec}$

Date	Time	Wave	Delay Sec	Data File Version No	CBM File Version No	Result File Version No	Renamed Result File Version No
27 July 1983	2204 2229	WO	120	141	141	1	1
			156	142	142	2	2
			192	143	143	3	3
			228	144	144	4	4
			264	145	145	5	5
			300	146	146	6	6
28 July 1983	0849 0914 0932 0955 1014	WP	120	147	147	1	7
			156	150	150	2	10
			192	151	151	3	11
			228	152	152	4	12
			264	153	153	5	13
			300	154	154	6	14

Table A2.1 (m)

EXPERIMENT RUNS AND FILE VERSION NUMBERS

40 Degrees Bow Discpack 2 $H_{1/3} = 5.5 \text{ m}$ $T_o = 15.0 \text{ sec}$

Date	Time	Wave	Delay Sec	Data File Version No	CBM File Version No	Result File Version No	Renamed Result File Version No
27 July 1983		WQ	120	135	135	1	1
			156	136	136	2	2
			192	137	137	3	3
			228	140	140	4	4

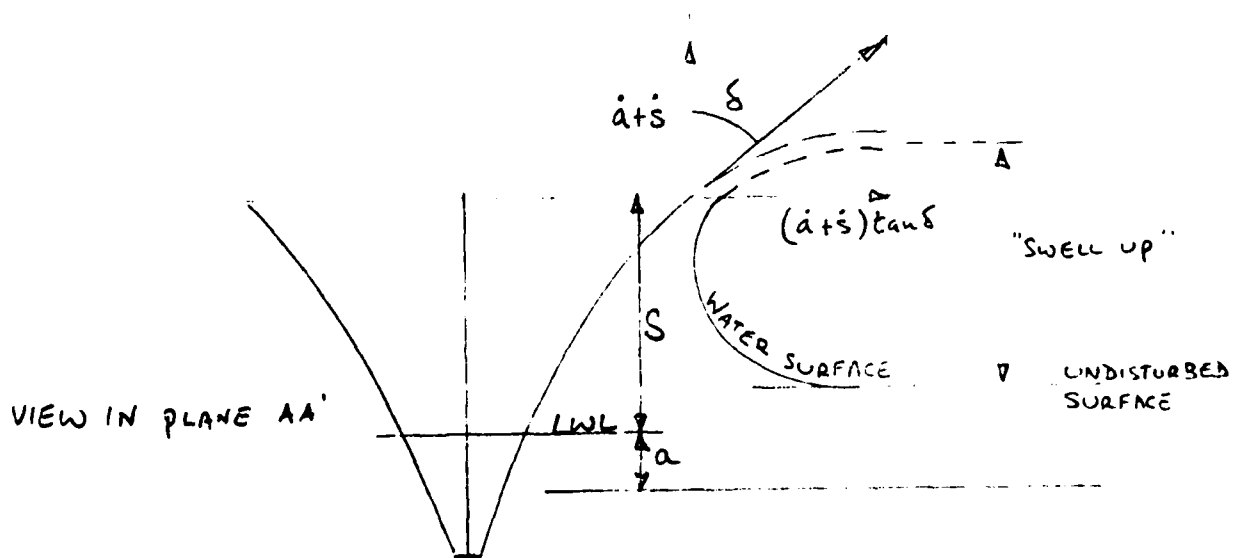
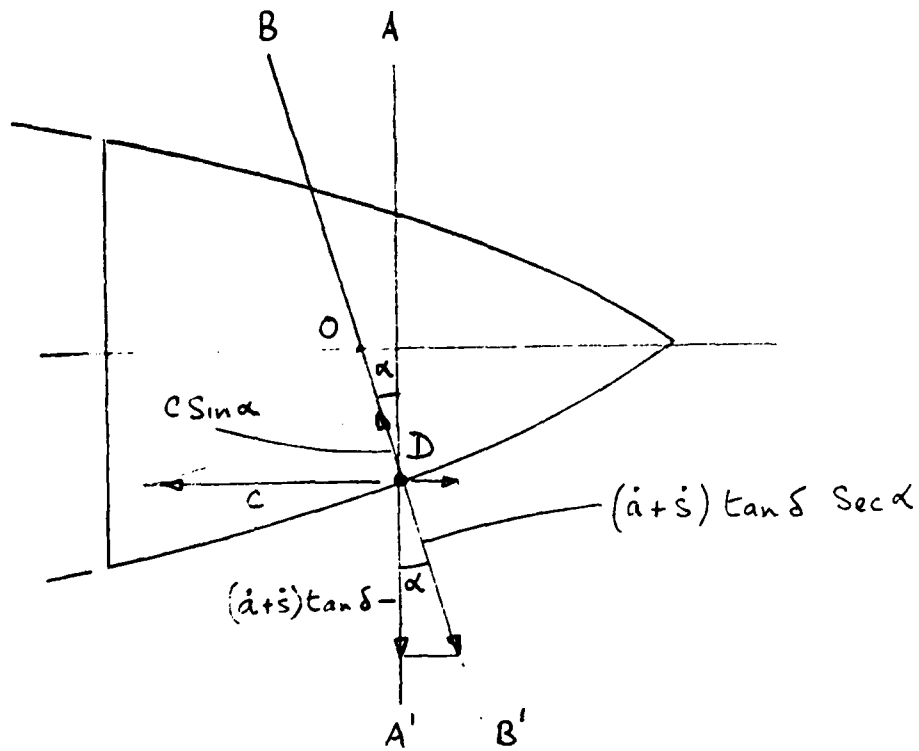
Table A2.2

CALM WATER EXPERIMENTS AND FILE VERSION NUMBERS

Bow	Date	Time	Discpack	Data File Version No	CBM File Version No	Result File Version No
30 Degrees	19 July 1983	1258	1	144	71	1
	10 Jan 1984	1700		211	211	
35 Degrees	7 July		1	170	115	1
40 Degrees	13 July	1315	1	117	44	1
	26 July	1650	2	75	75	1
	27 July	0812	2	120	120	2
45 Degrees	20 July		1	167	114	1
	20 July	2227	2	24	25	1
	9 Jan 1984	1616		220		
50 Degrees	25 July	1350	2	51	51	2
	26 July	0820	2	64	64	3
55 Degrees	14 July		1	142	67	1
	15 July	0810	1	143	70	2
35/45 K	21 July	1247	2	25	24	1
	21 July	1933	2	50	50	2

Appendix 3

CRITICAL VELOCITY



Consider the ship's bow from the point of view of a stationary observer in the plane AA^1 . Suppose that the relative motion exceeds the freeboard at D at some particular instant of time.

The absolute displacement of the bow is a (positive up) from its calm water datum and the relative motion of the water surface at the instant of freeboard exceedance is S (positive up). In this instance $S = F$.

The vertical component of the velocity of the water surface at this instant is $\dot{a} + \dot{s}$ (positive up) relative to the earth. The horizontal component of the velocity of the water surface in the plane AA^1 is $(\dot{a} + \dot{s}) \tan \delta$.

We now assume that in the absence of waves and forward speed the water leaves the vicinity of the ship's side in a direction normal to the deck edge (ie in the plane BB^1).

Hence the total horizontal velocity component is

$$(\dot{a} + \dot{s}) \tan \delta \sec \alpha$$

normal to the ship's side. α is the angle between the deck edge and the ship's axis when viewed in plan.

In head waves the water surface will have an additional velocity in the longitudinal direction. If we call this velocity c its component in the plane BB^1 will be $c \sin \alpha$ towards the ship's axis.

There will, in addition, be a bodily outward motion of the water surface due to the forward speed of the ship and the expansion of the dimension DO as the tapered bow passes through the plane BB^1 . If DO has length y' this will result in an outward water surface velocity \dot{y}' .

A wetting will occur if the total outward water surface velocity is less than the rate of expansion of the dimension y' . ie a wetting will occur if

$$(\dot{a} + \dot{s}) \tan \delta \sec \alpha - c \sin \alpha + \dot{y}' < \dot{y}'$$

or

$$(\dot{a} + \dot{s}) < \frac{c \sin \alpha \cos \alpha}{\tan \delta}$$

In irregular waves the velocity of the wave crest c will be a random quantity. We assume that c is given approximately by the celerity of the regular wave corresponding to the peak relative motion response. Hence $c = g/\omega$ and strip theory calculations (using the programs described in Reference 9) show that

$\omega \approx 0.65$ radians per second for the FFG7 form at a speed of 22 knots.

Hence a wetting should occur if

a. The relative motion exceeds the freeboard at some station.

and b. The absolute vertical velocity of the water surface at the instant of freeboard exceedance is less than $\dot{\zeta}_{CRIT}$

where

$$\dot{\zeta}_{CRIT} = \frac{g \sin \alpha \cos \alpha}{\omega \tan \delta}$$

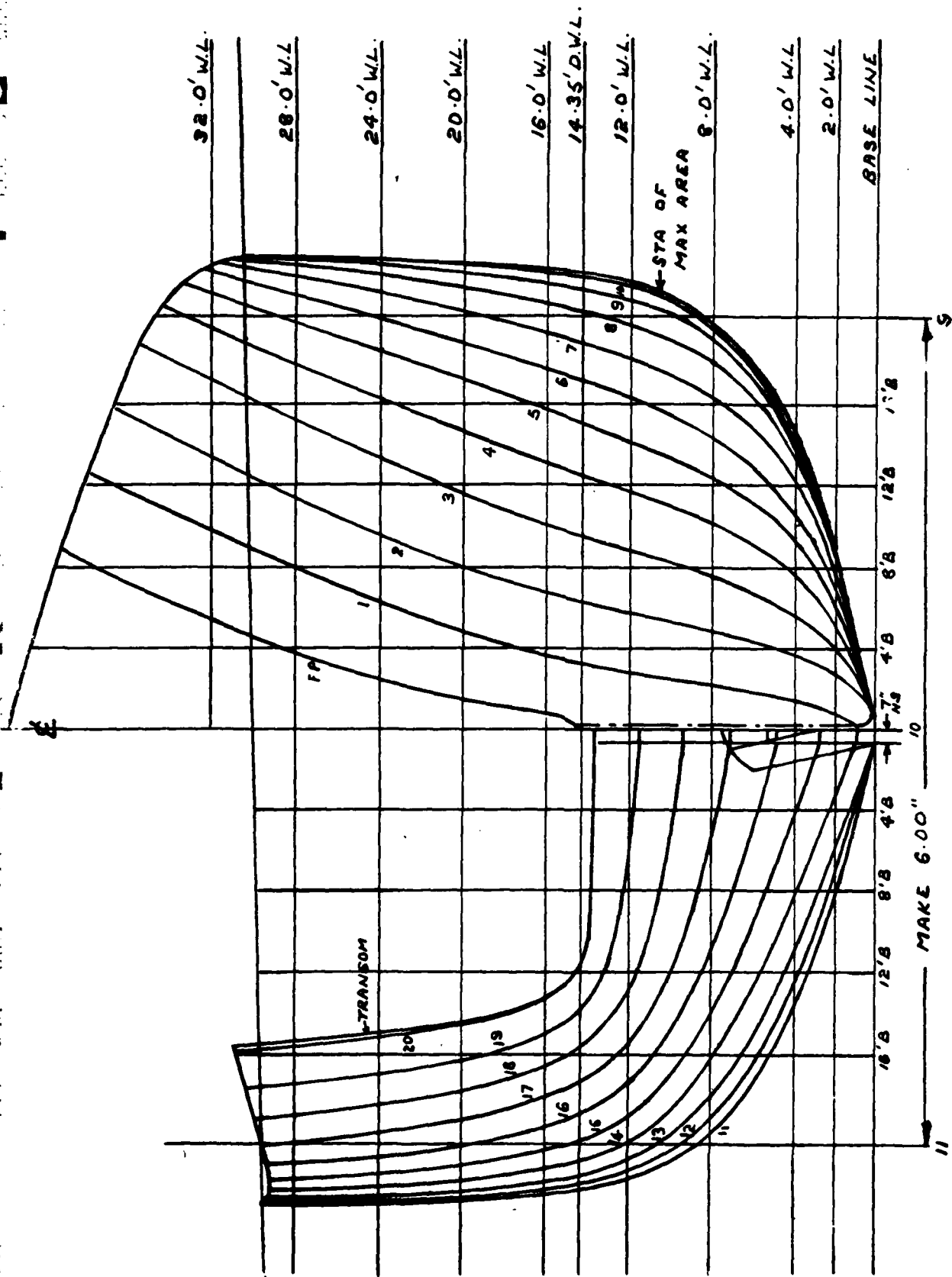


FIG. 1. FFG7 BODY PLAN

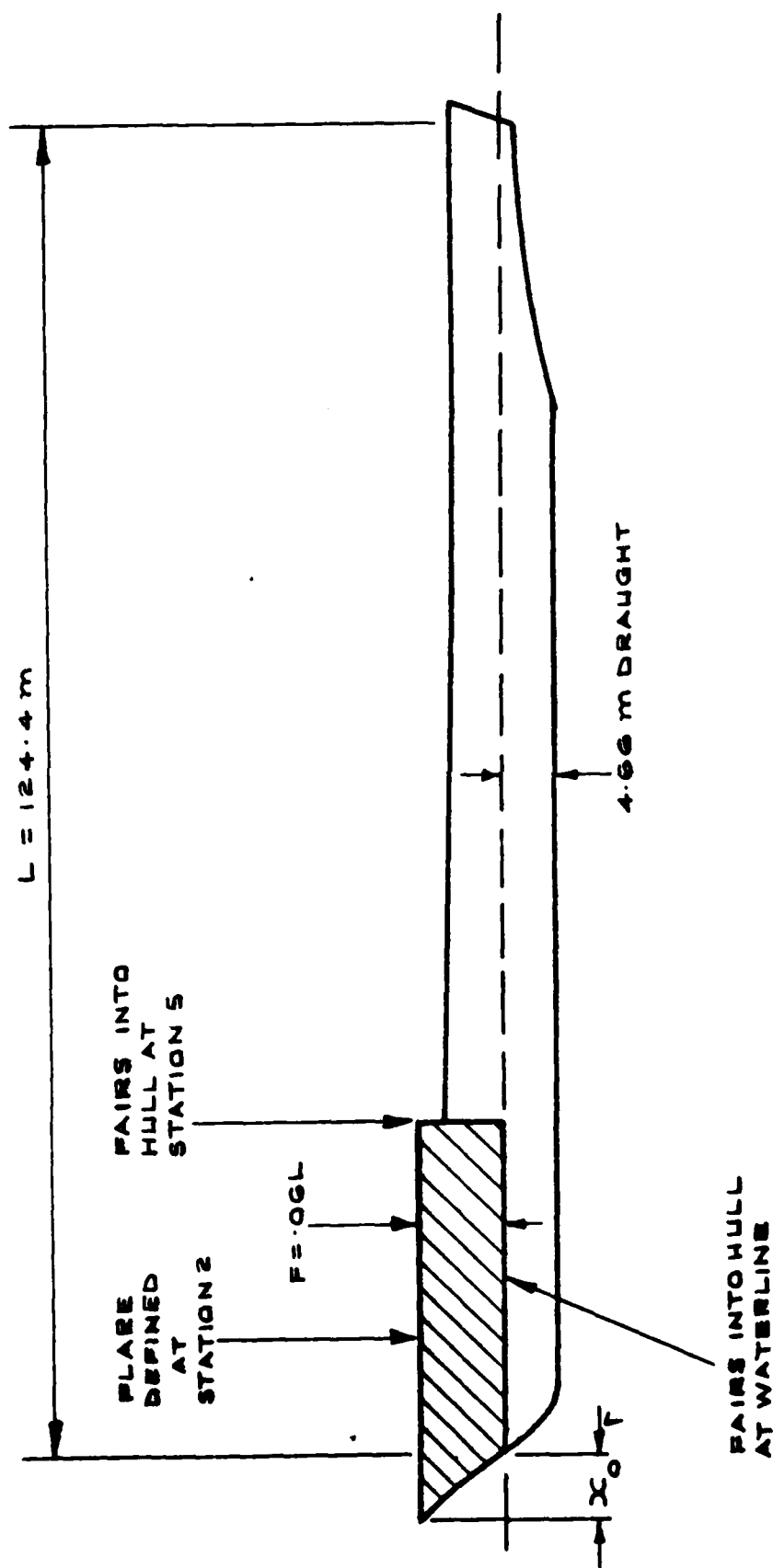
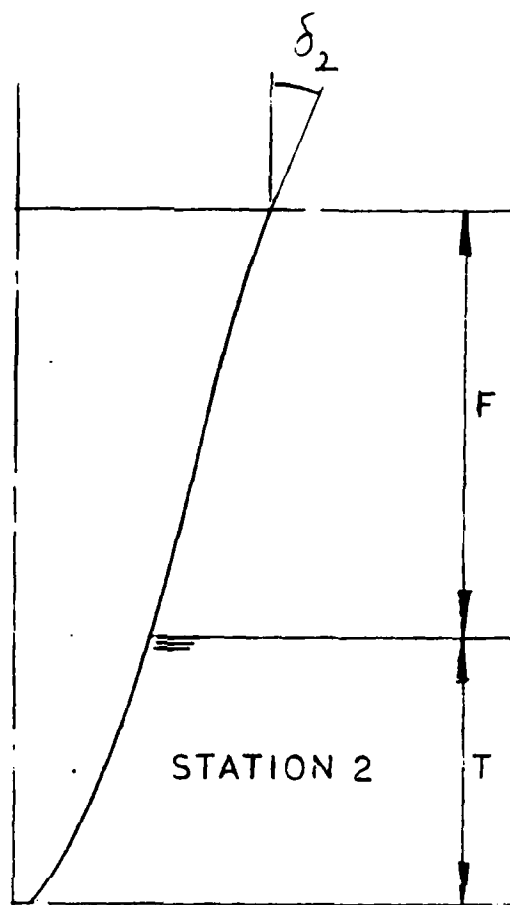


FIG. 2 FFG7 BOW FORM SERIES

SIMPLE
FLARE



KNUCKLE

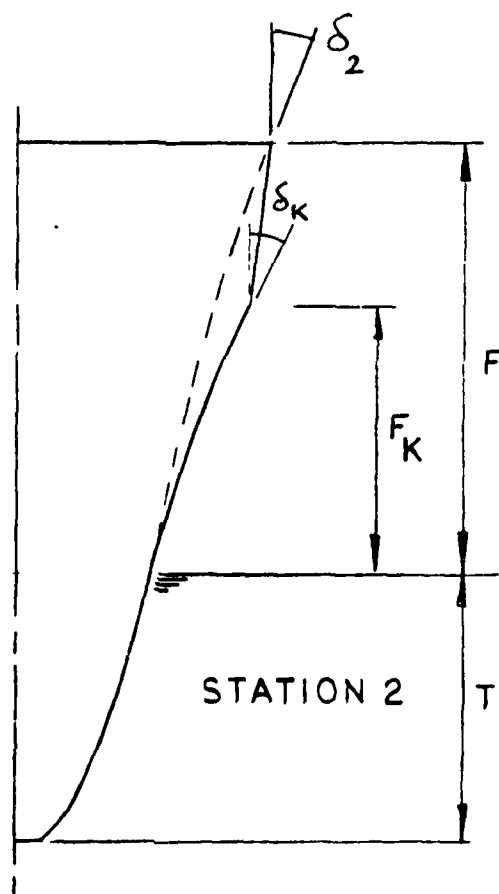


FIG. 3 NOTATION

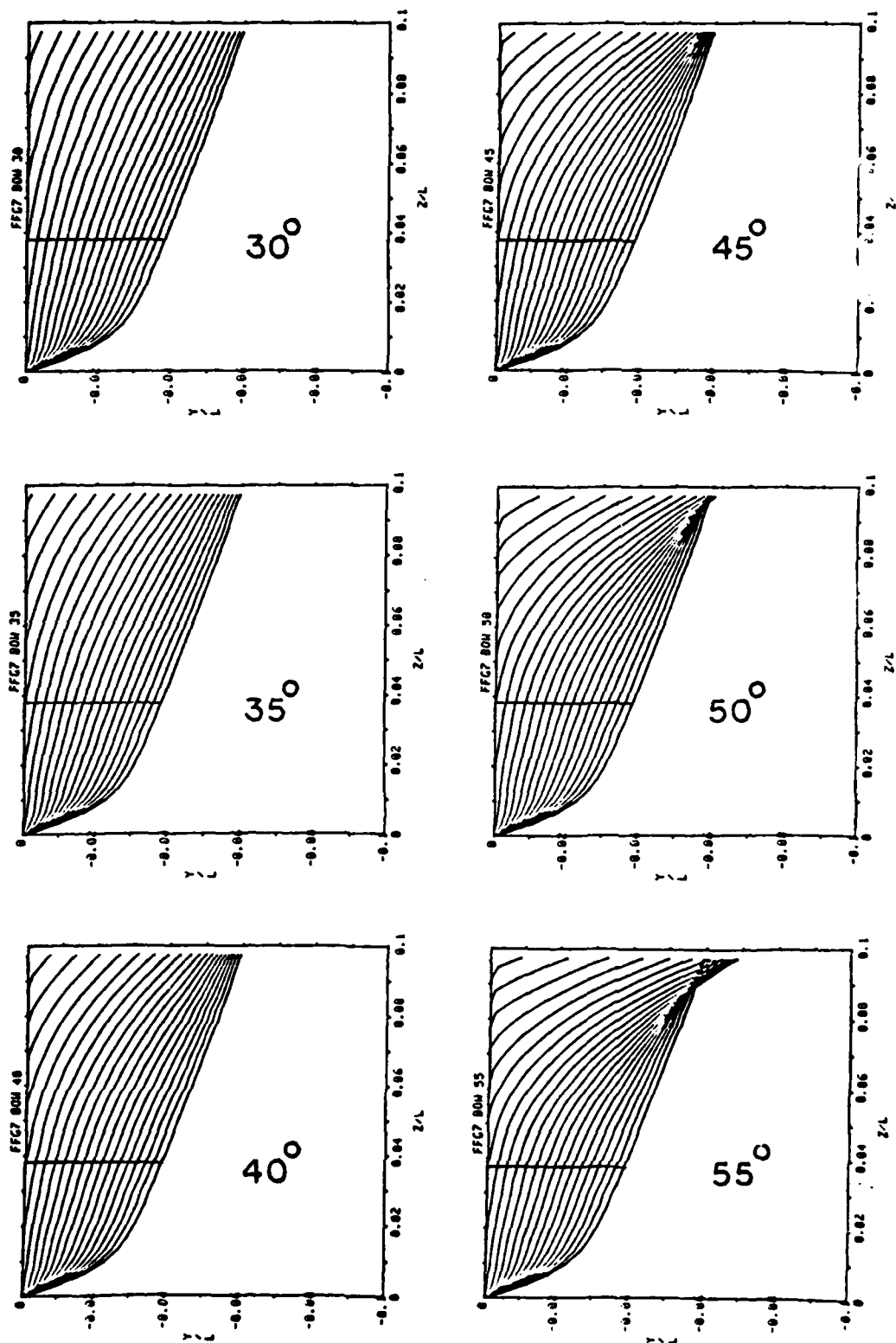


FIG 4 USNA BOW FORMS

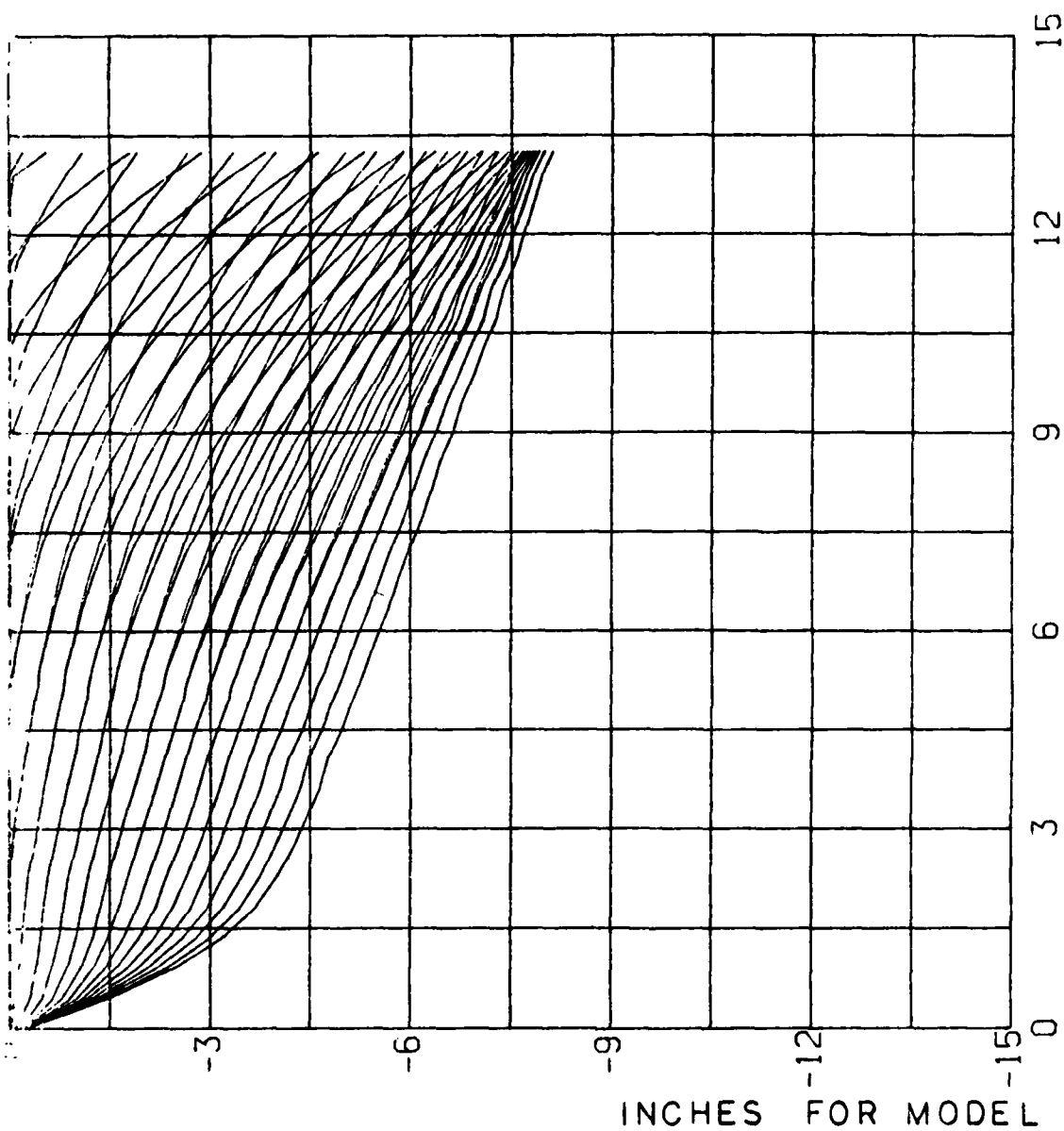


FIG 5 35° AND 45° BOW
BODY PLANS

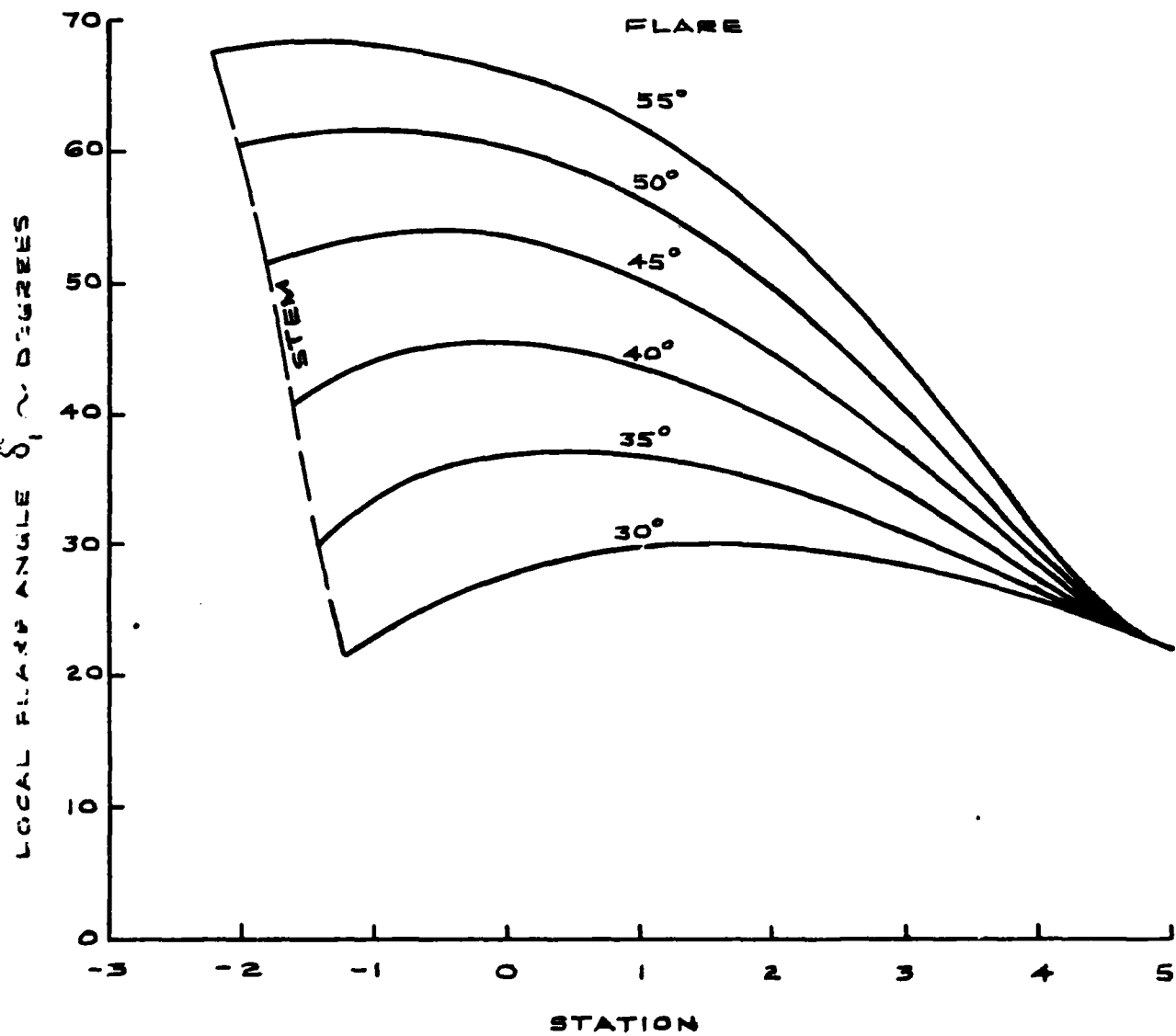


FIG.6 VARIATION OF LOCAL FLARE ANGLE

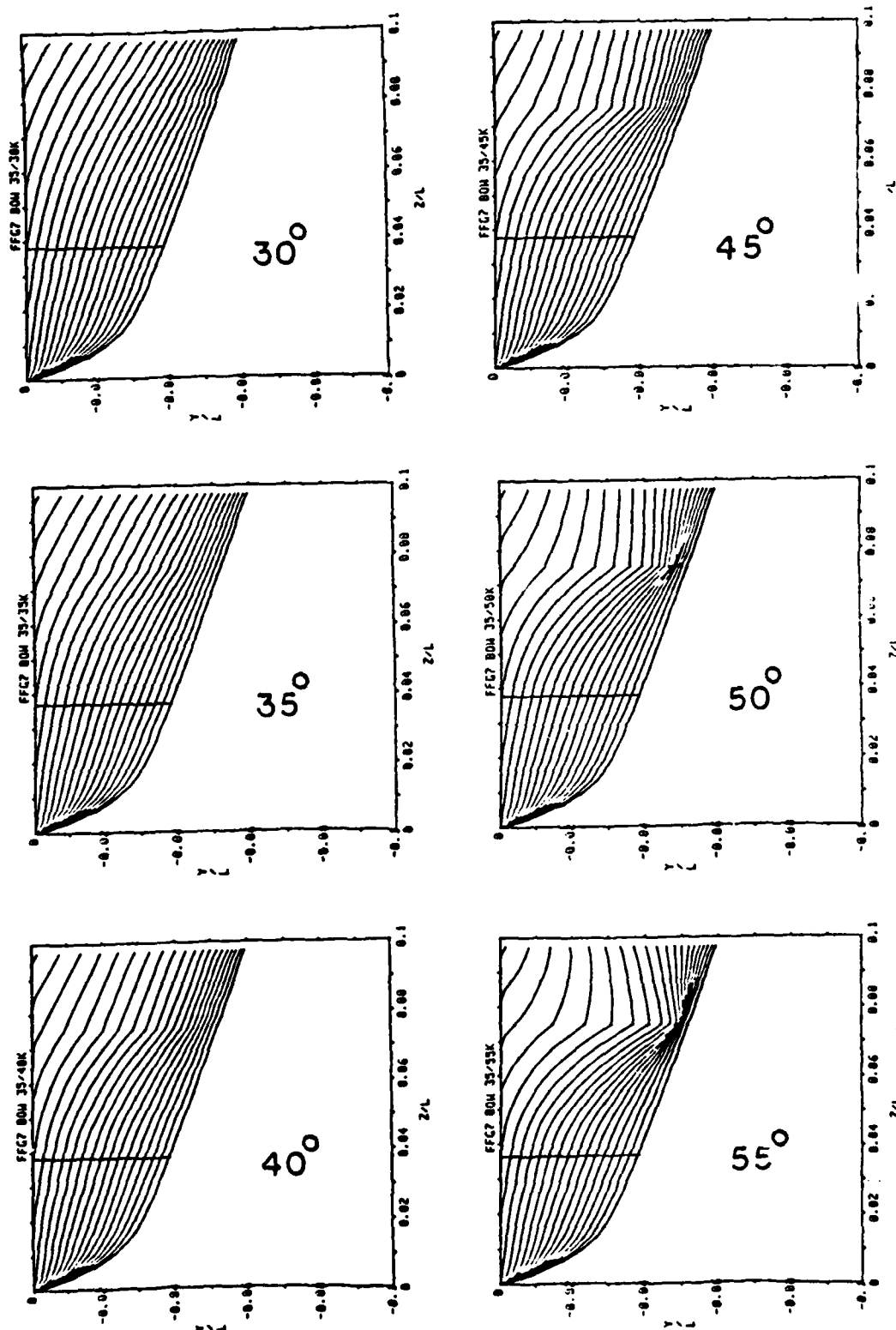


FIG 7 USNA KNUCKLE BOWS

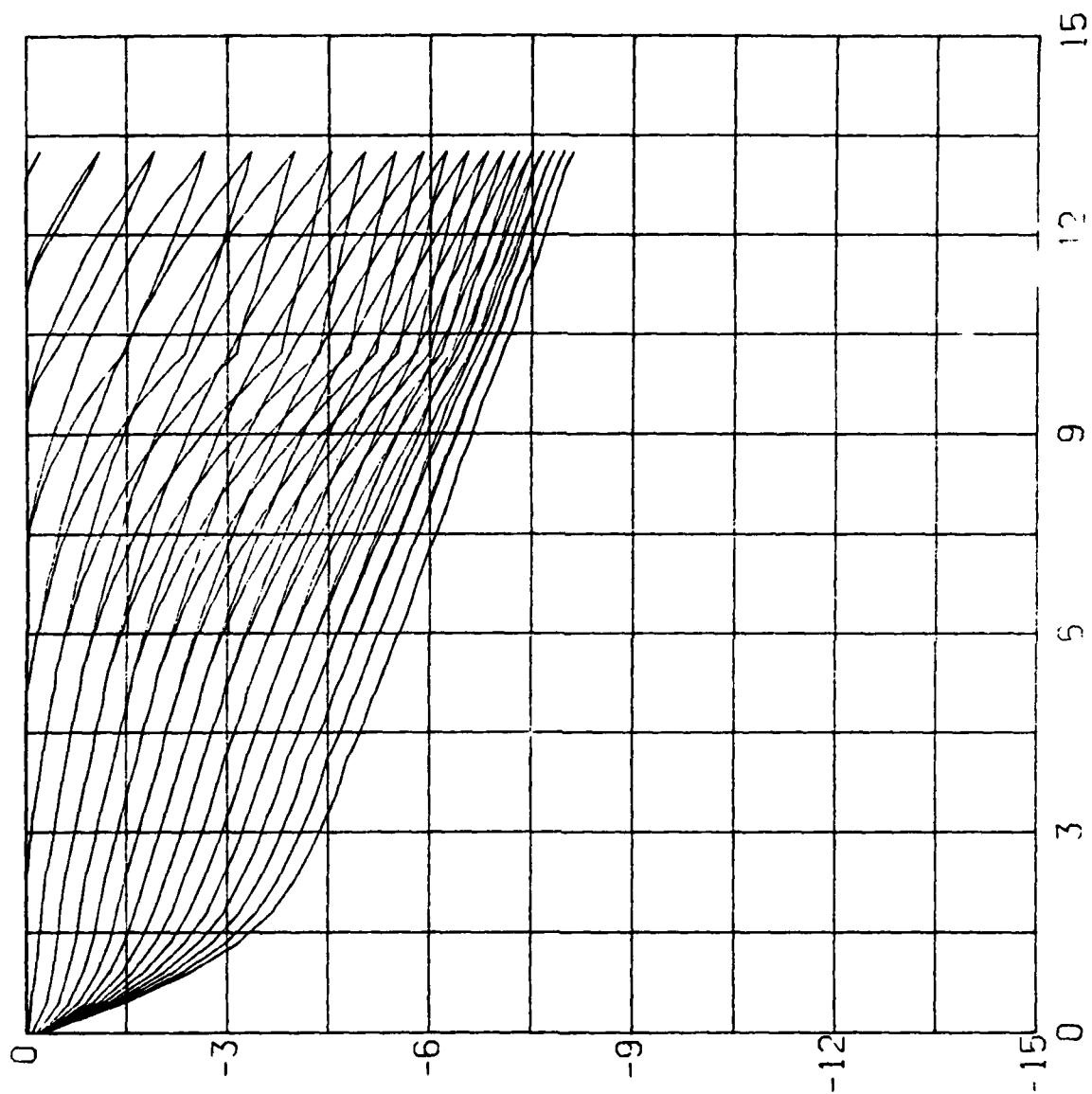


FIG 8 35° FLARE AND 35°/45°
KNUCKLE BODY PLANS

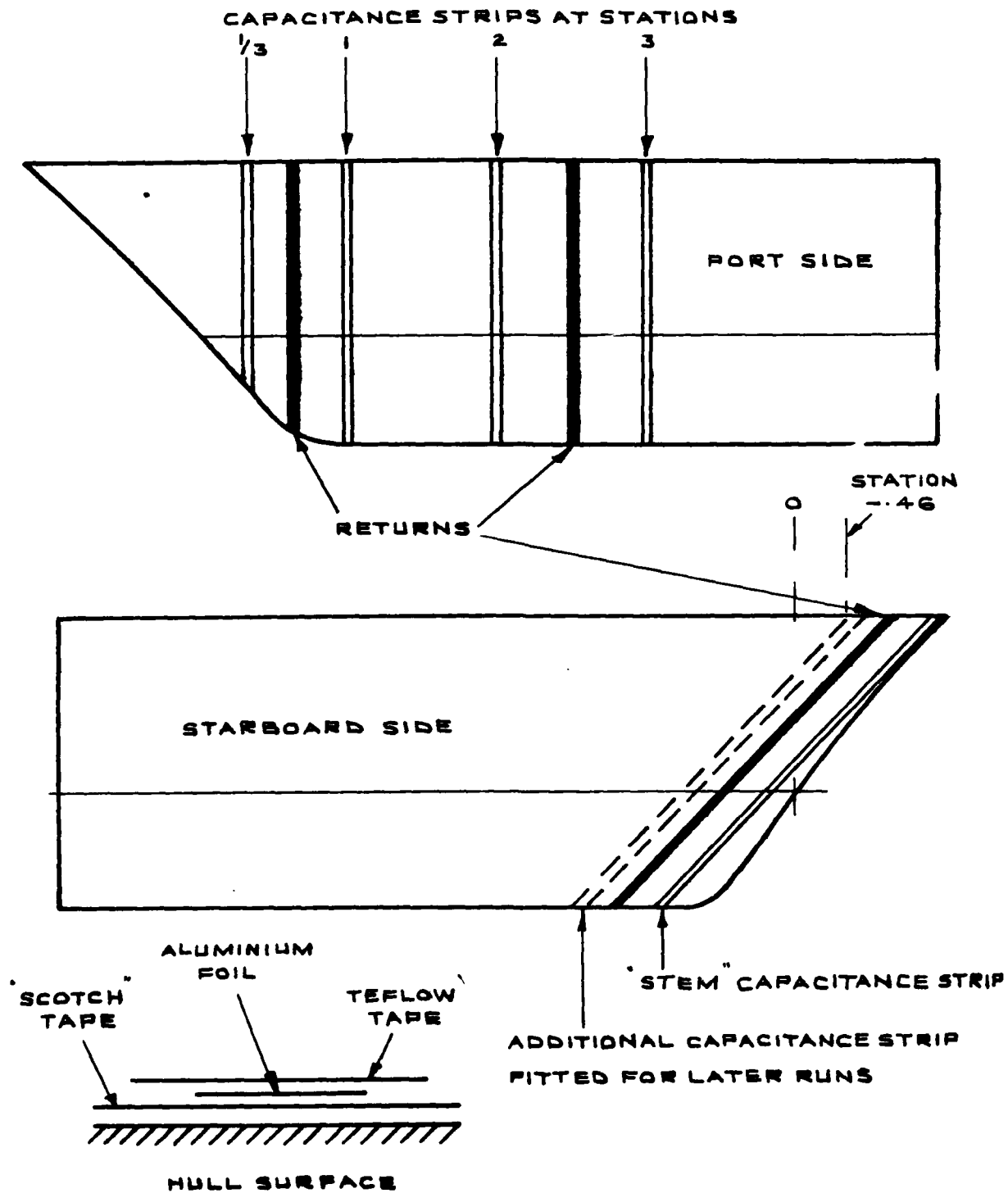


FIG.9 RELATIVE BOW MOTION CAPACITANCE STRIPS

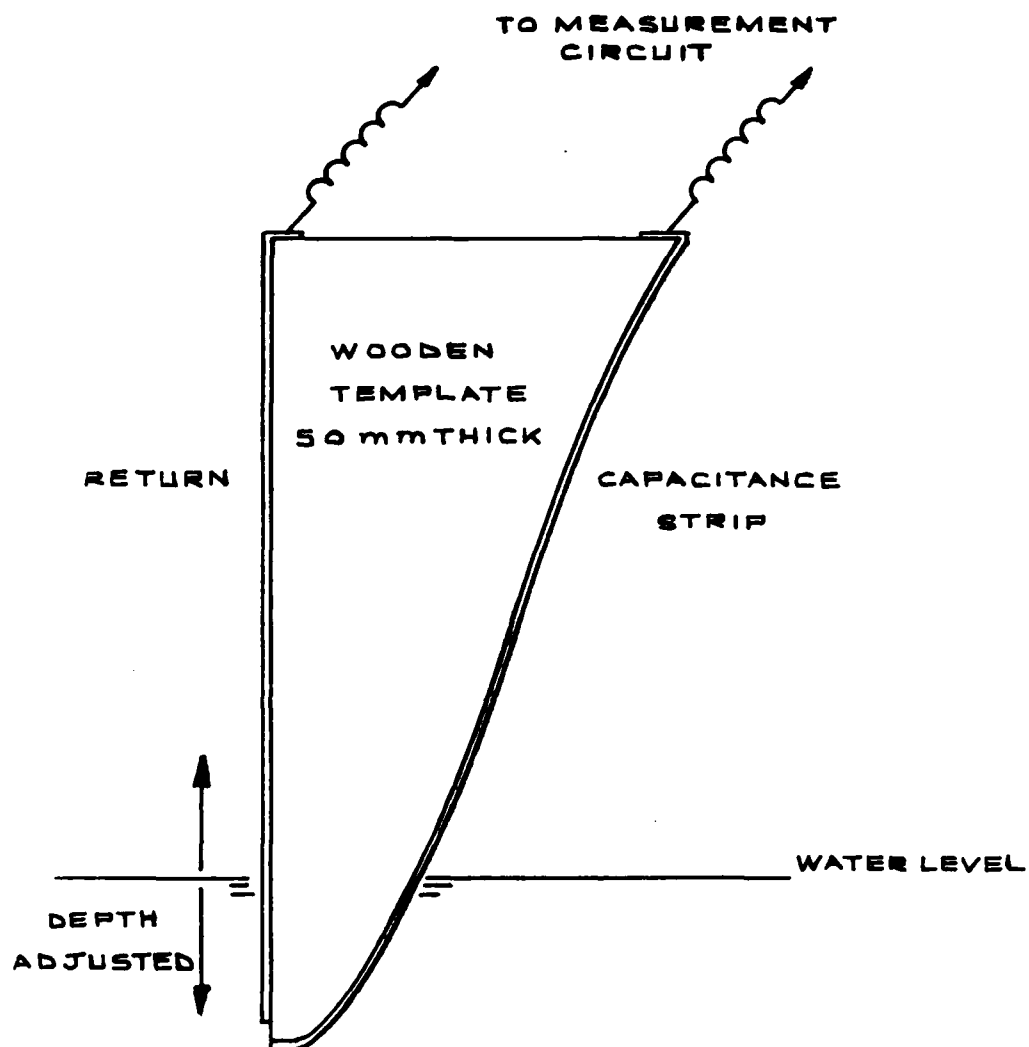


FIG.10 CALIBRATION OF RELATIVE MOTION
CAPACITANCE STRIPS

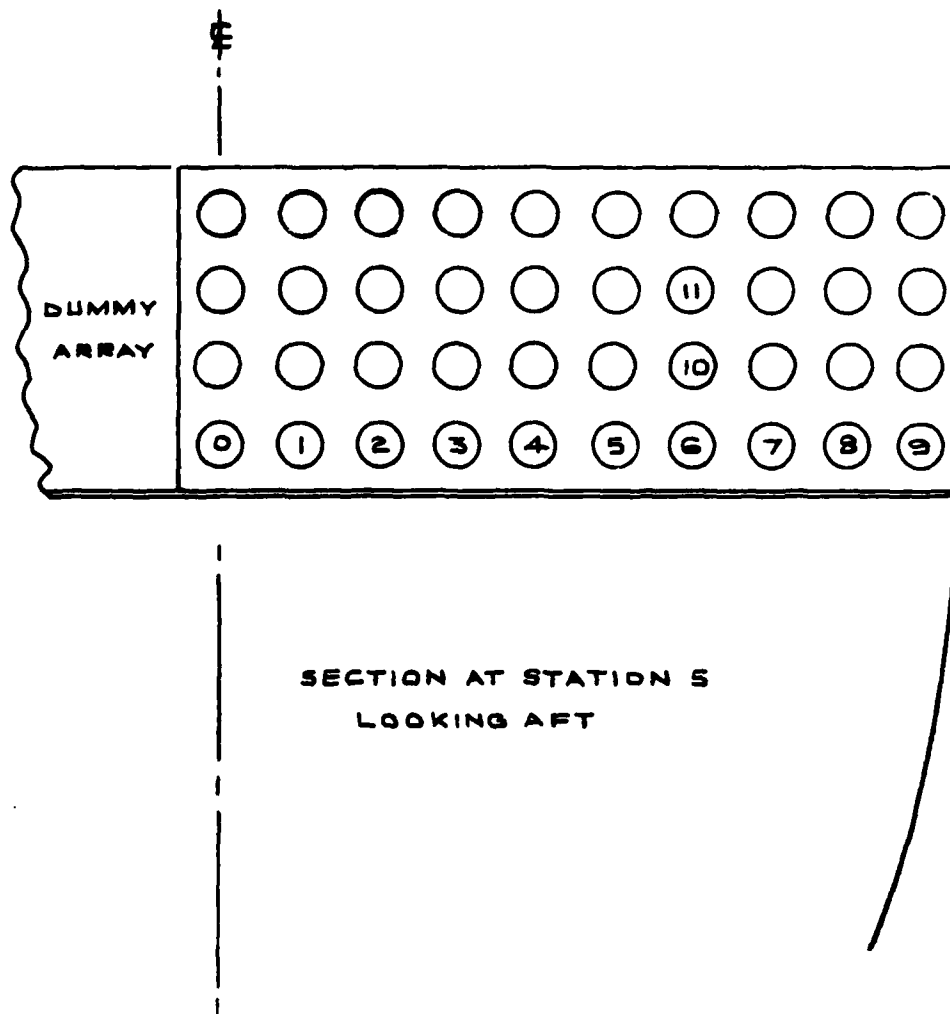
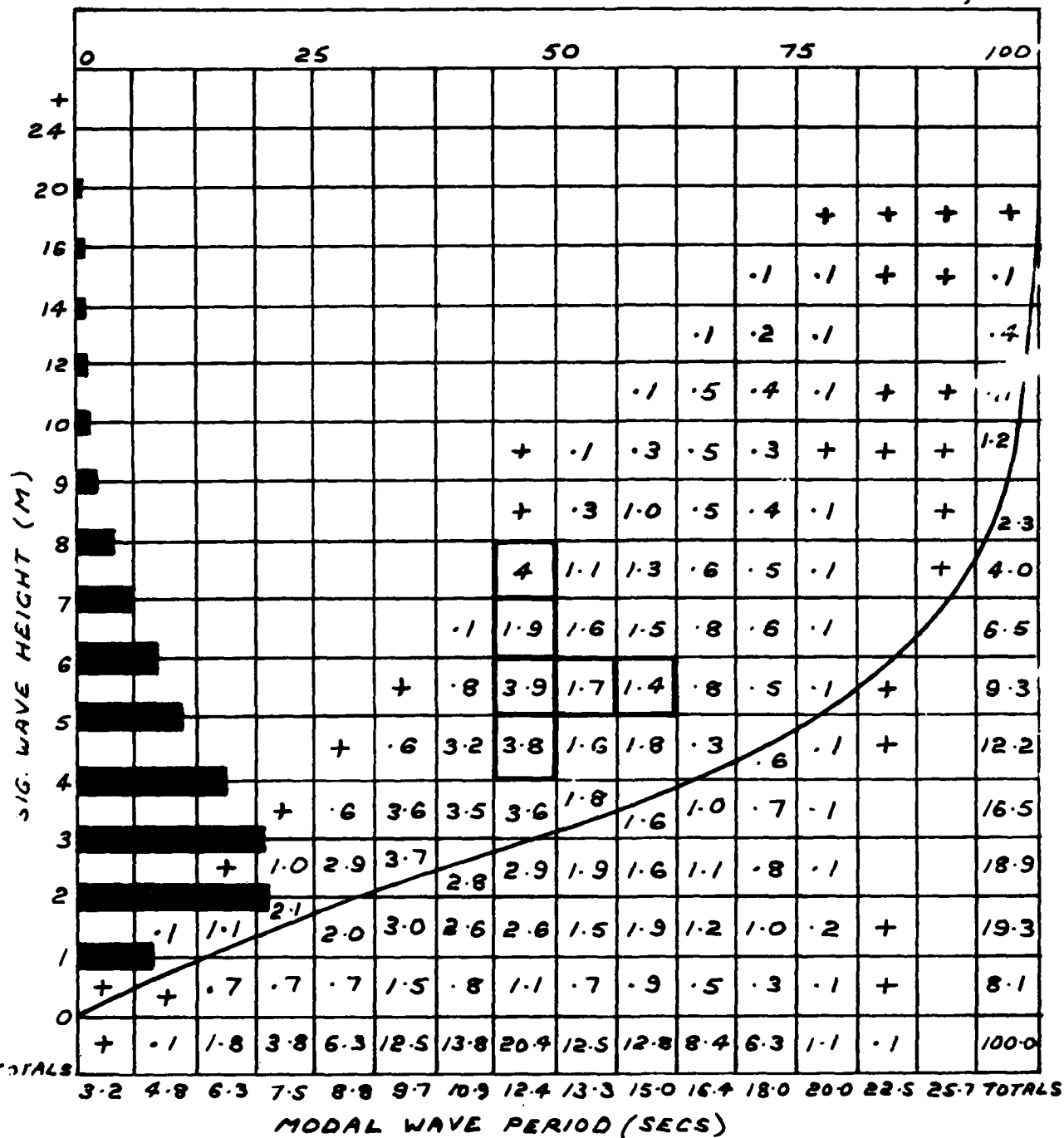


FIG.11 IMPACT PRESSURE ARRAY

WINTER AREA NORTH ATLANTIC TOTAL SAMPLES 35,590



ST
IJ
CH
U OP AR
BC

WAVE SPECTRA USED
IN EXPERIMENTS

FIG.12 SIGNIFICANT WAVE HEIGHT BY MODAL WAVE PERIOD

O DESIRED SPECTRUM
Δ ACHIEVED SPECTRUM

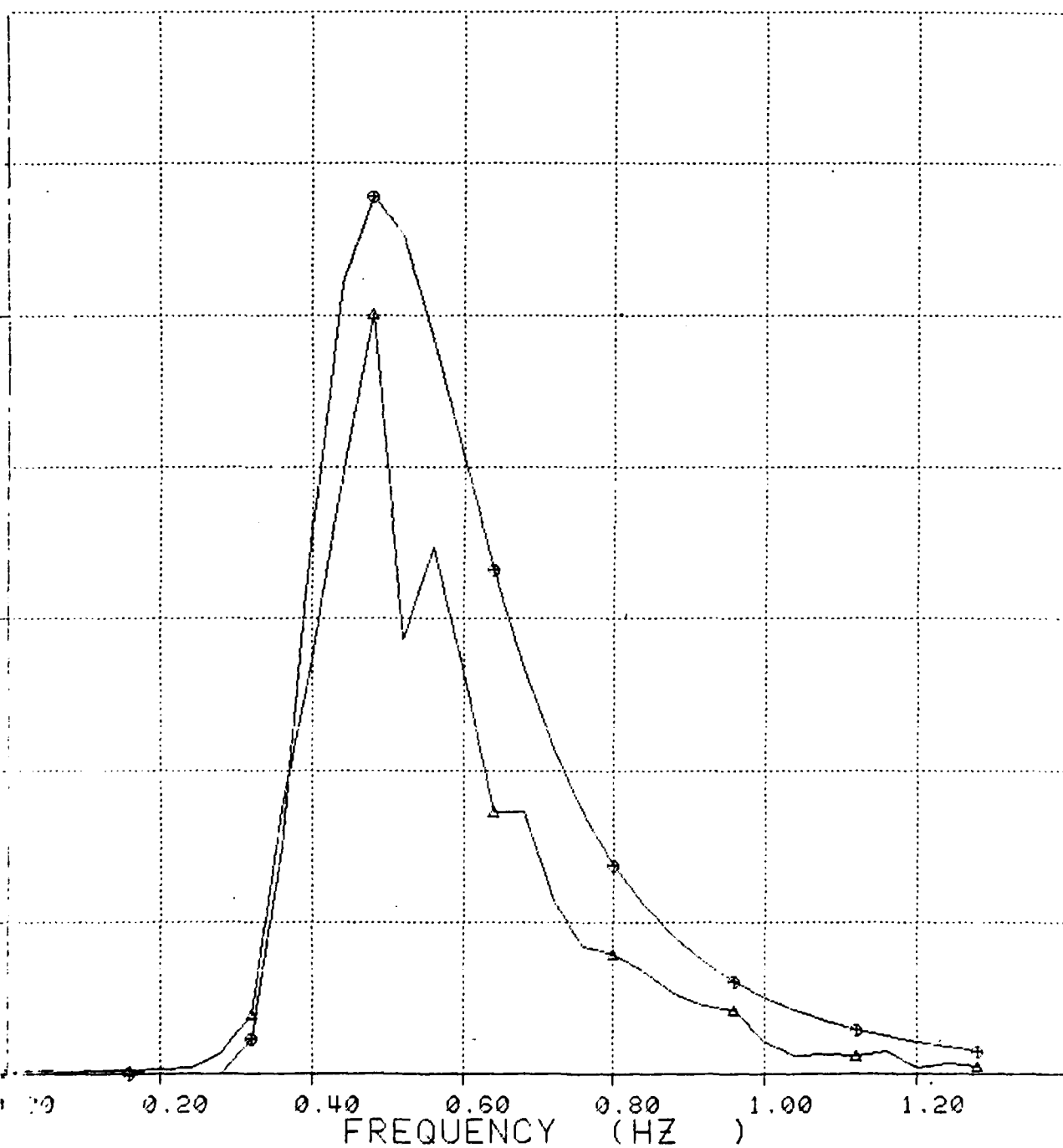


FIG.13 WAVE SPECTRUM WG FIRST ATTEMPT

○ DESIRED SPECTRUM
 ▲ ACHIEVED SPECTRUM

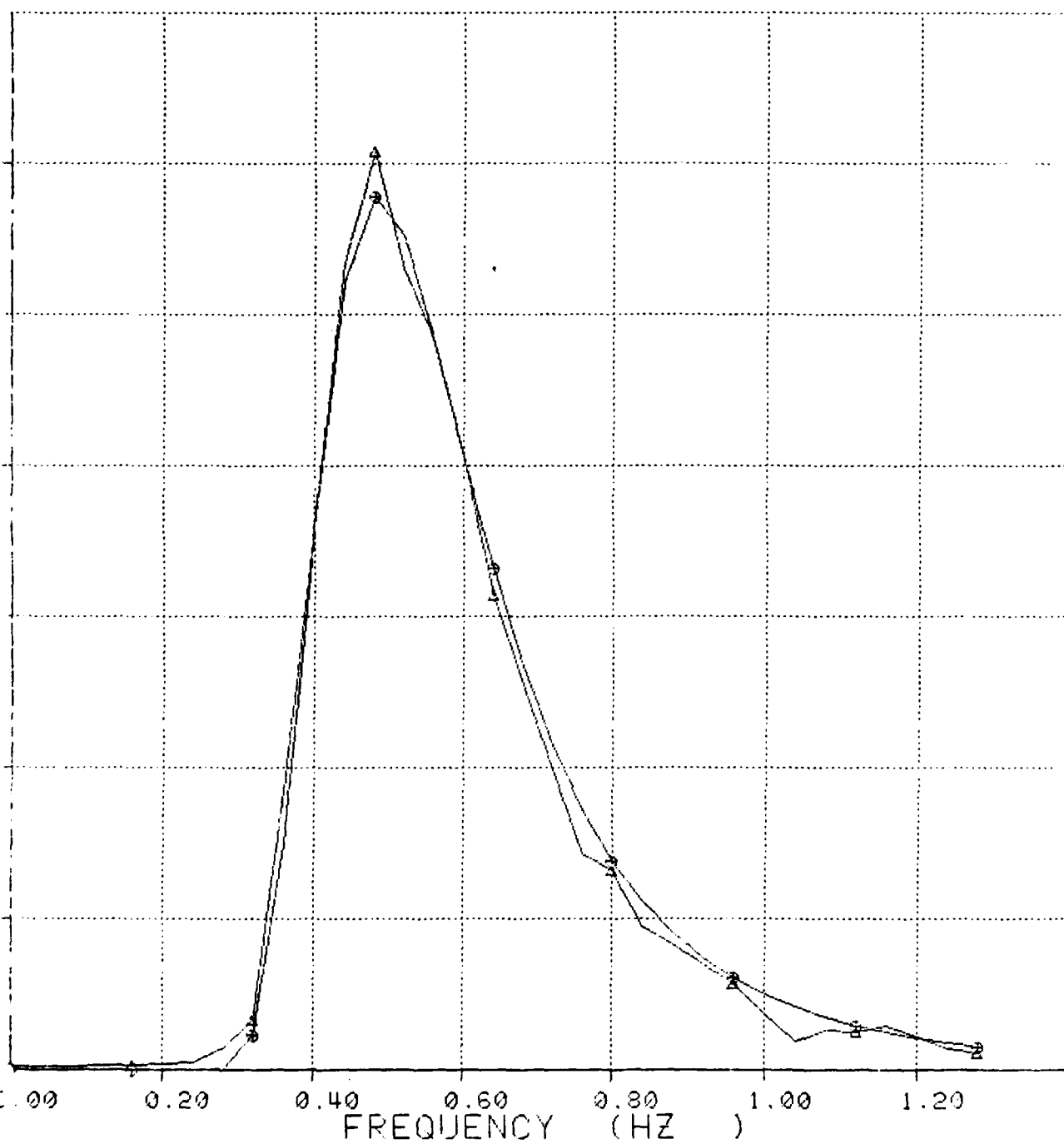


FIG.14 WAVE SPECTRUM WJG SECOND ATTEMPT

O DESIRED SPECTRUM
Δ ACHIEVED SPECTRUM

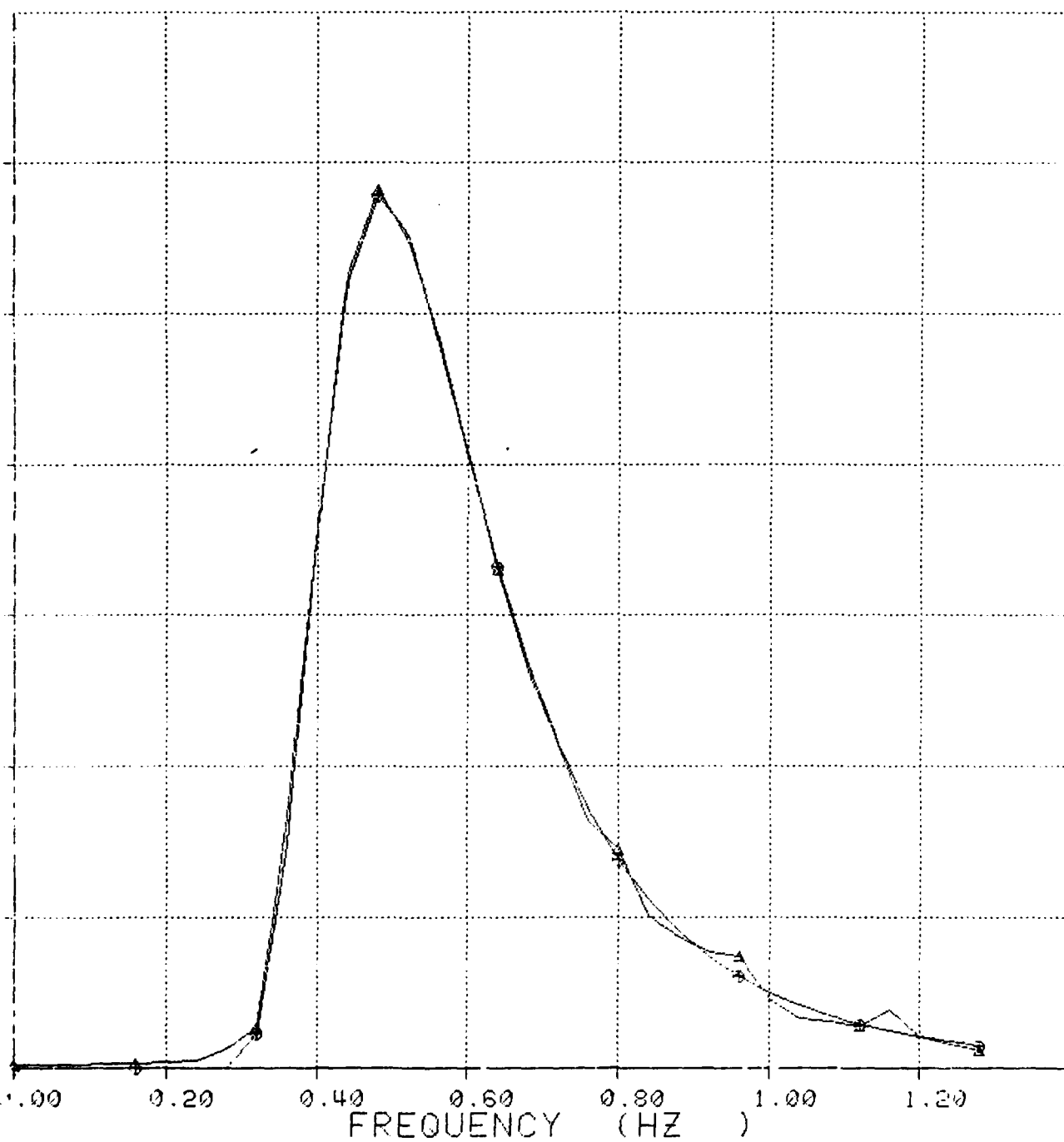


FIG.15 WAVE SPECTRUM WG THIRD ATTEMPT

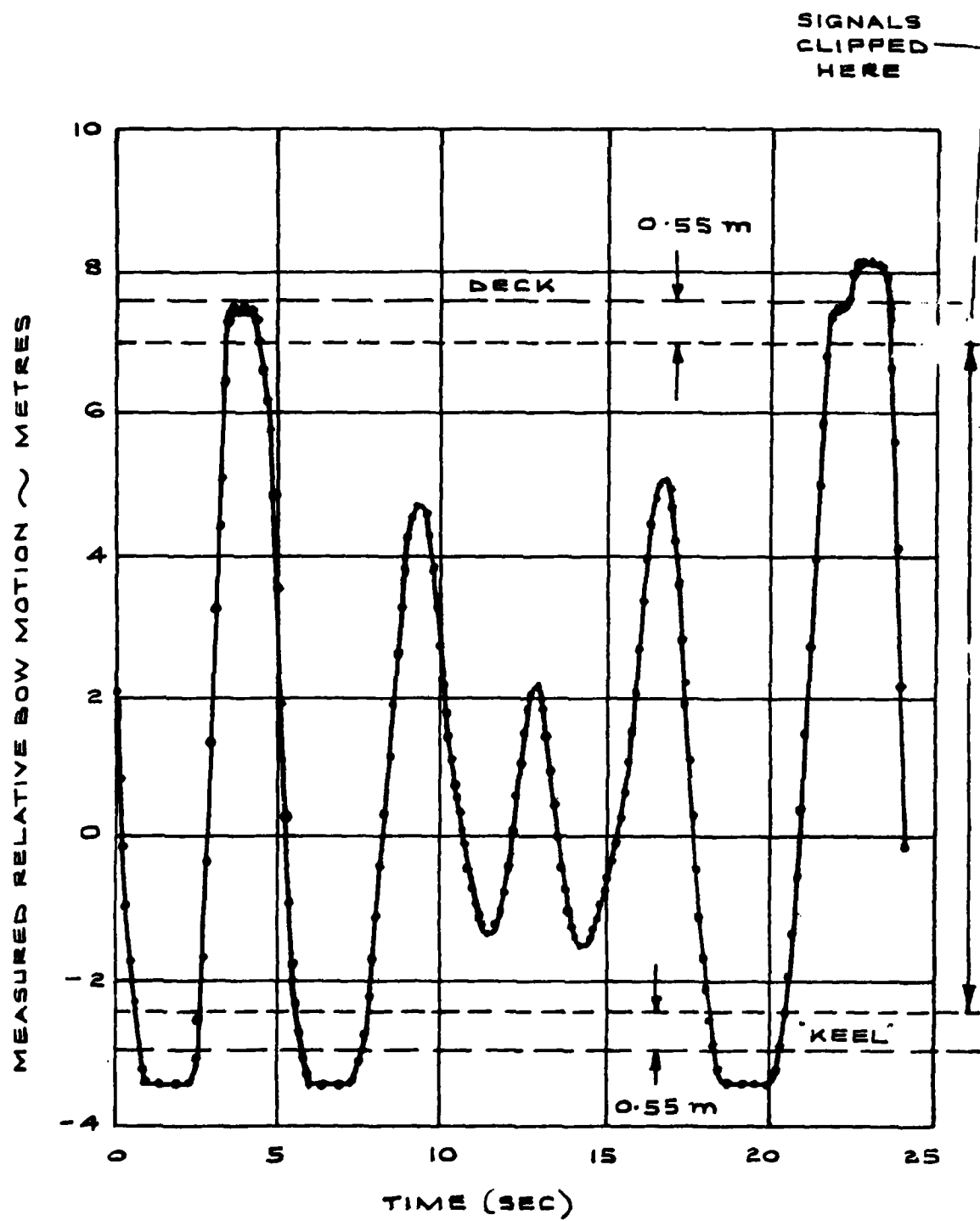


FIG.16 TYPICAL RELATIVE MOTION SIGNAL

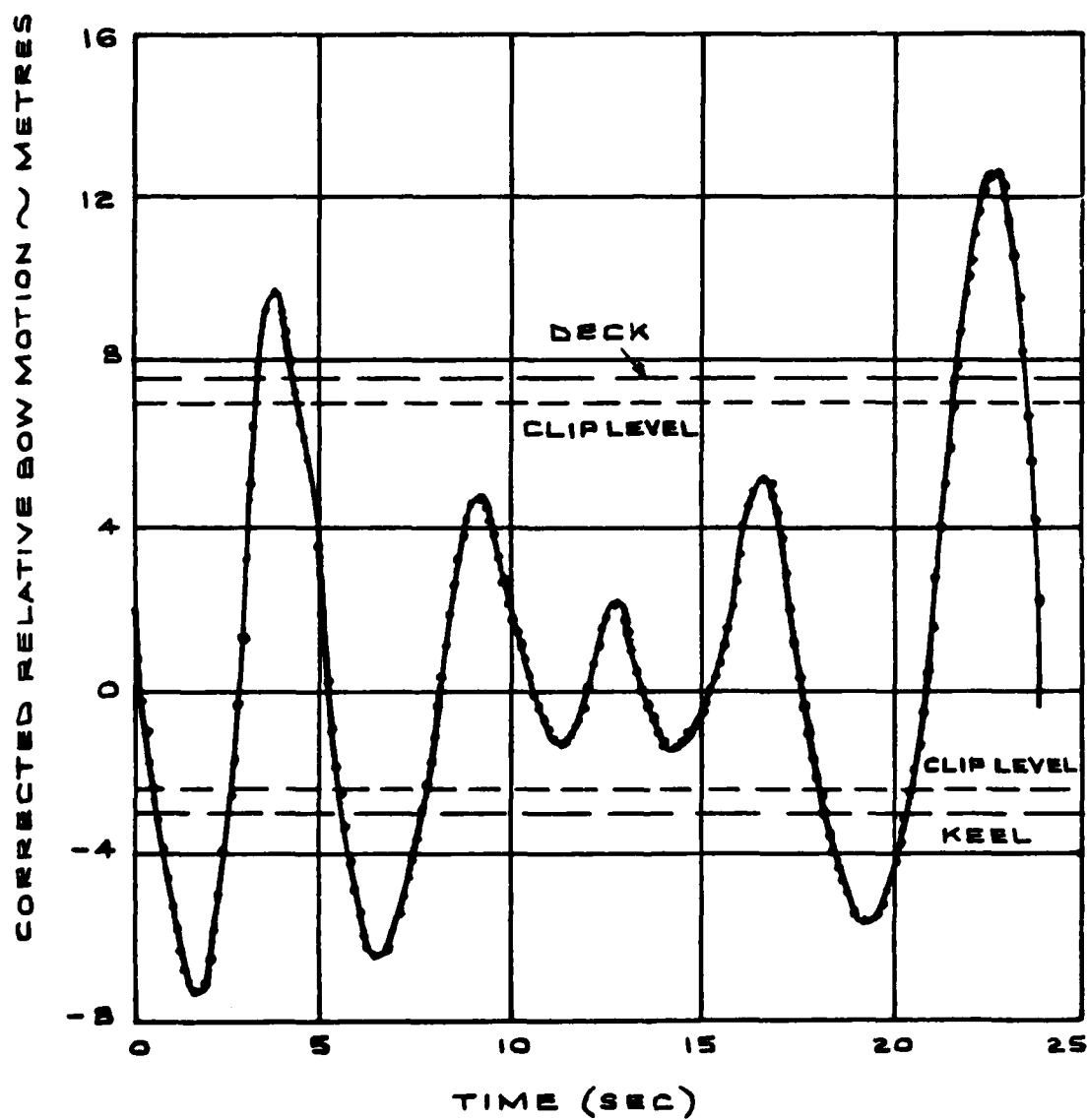


FIG.17 TYPICAL 'CORRECTED' RELATIVE MOTION SIGNAL

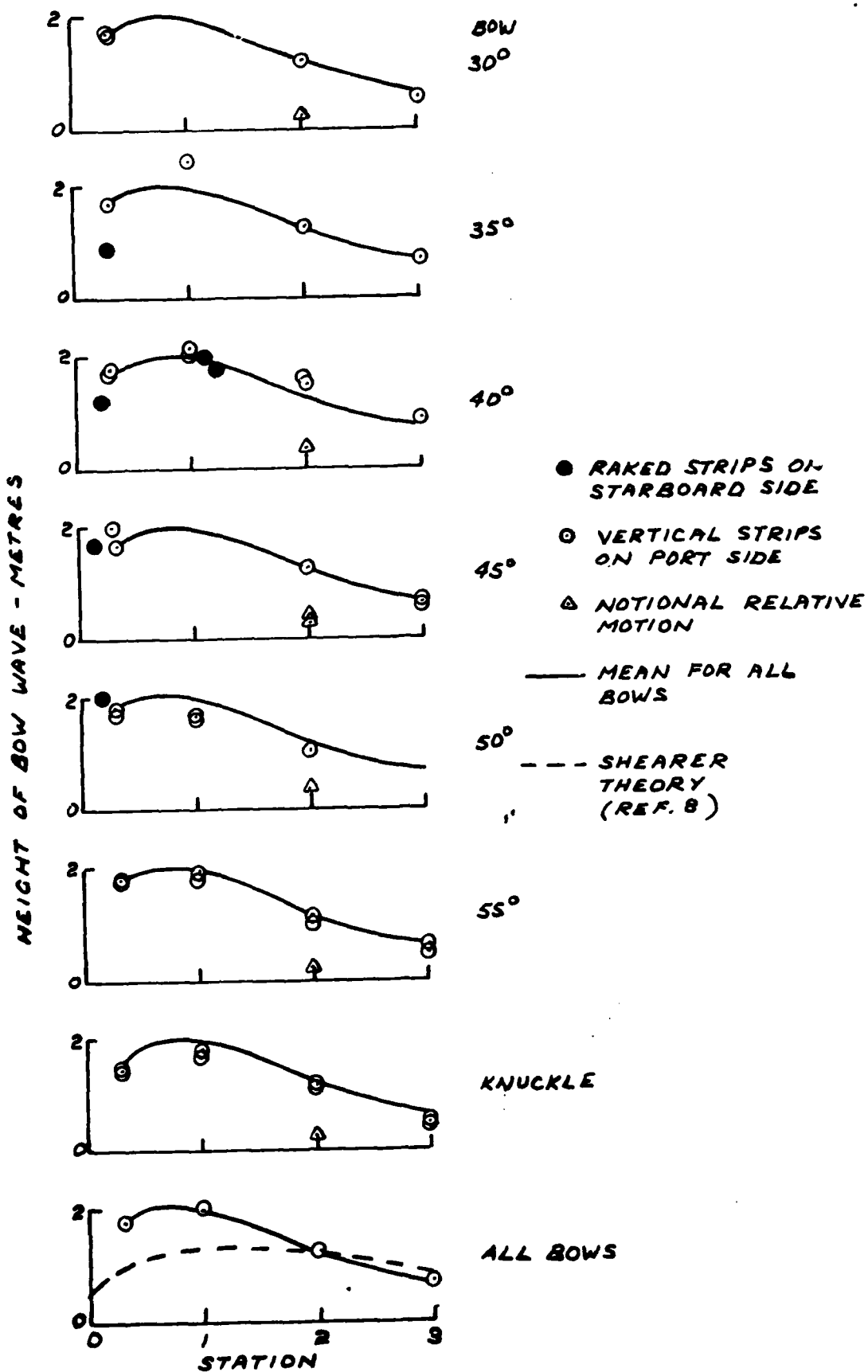


FIG.18 CALM WATER BOW WAVE PROFILES

WAVES $W_G/W_H/W_U$

$H_{1/3} = 5.5$ METRES

$T_0 = 12.4$ SECONDS

○ EXPERIMENT

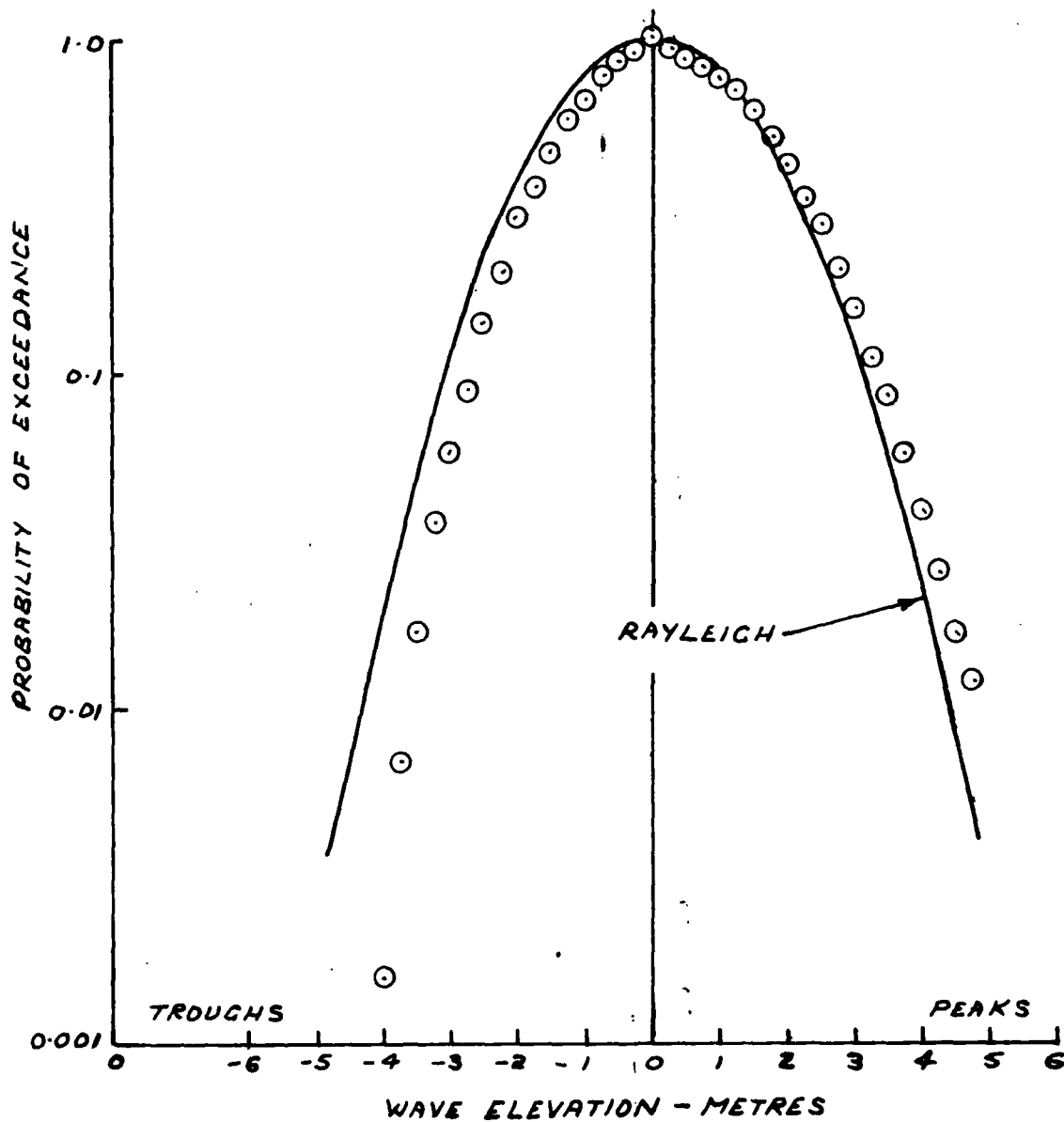


FIG.19 PROBABILITY DISTRIBUTION OF WAVE PEAKS AND TROUGHs

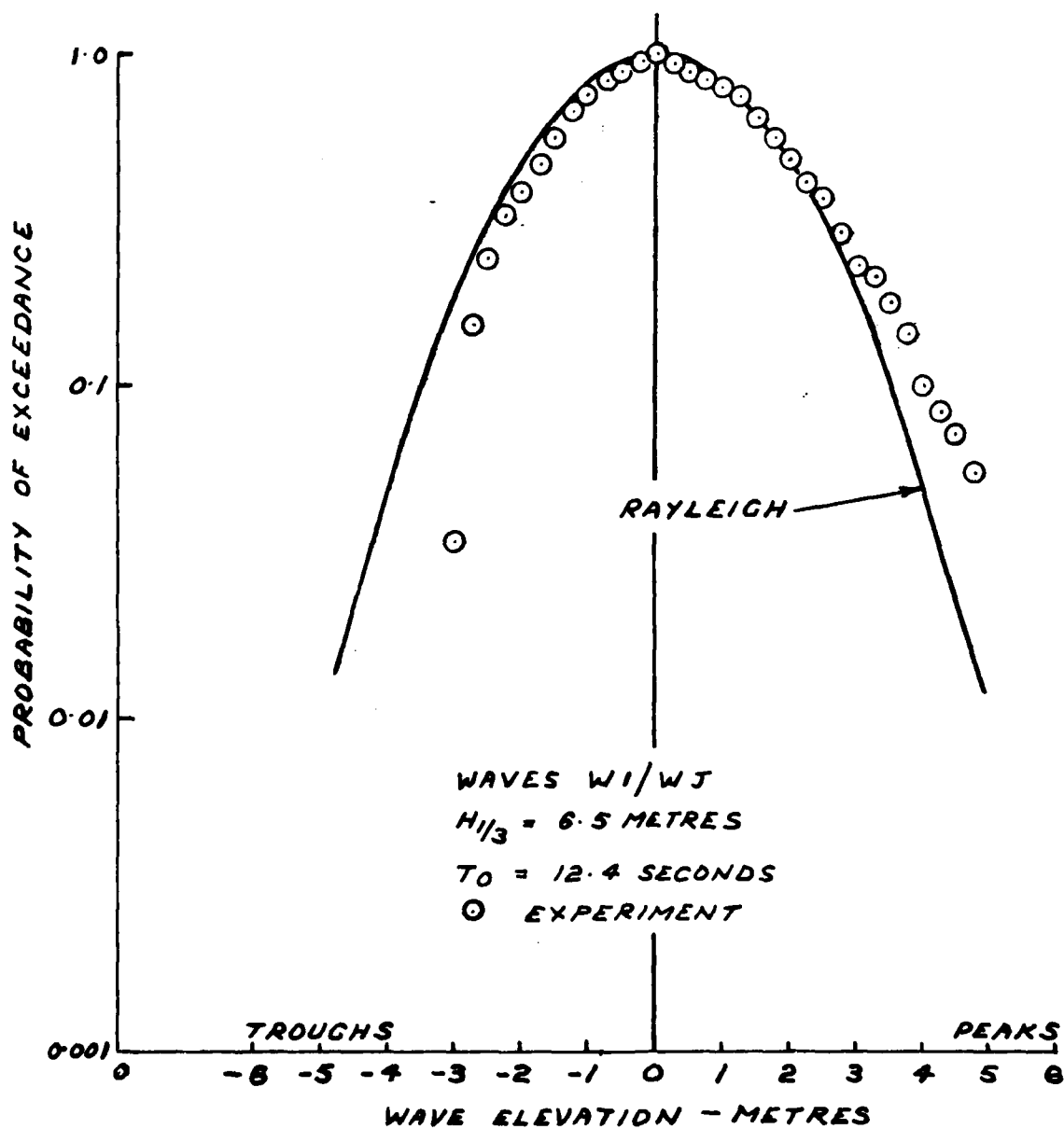


FIG. 20 PROBABILITY DISTRIBUTION OF
WAVE PEAKS AND TROUGHs

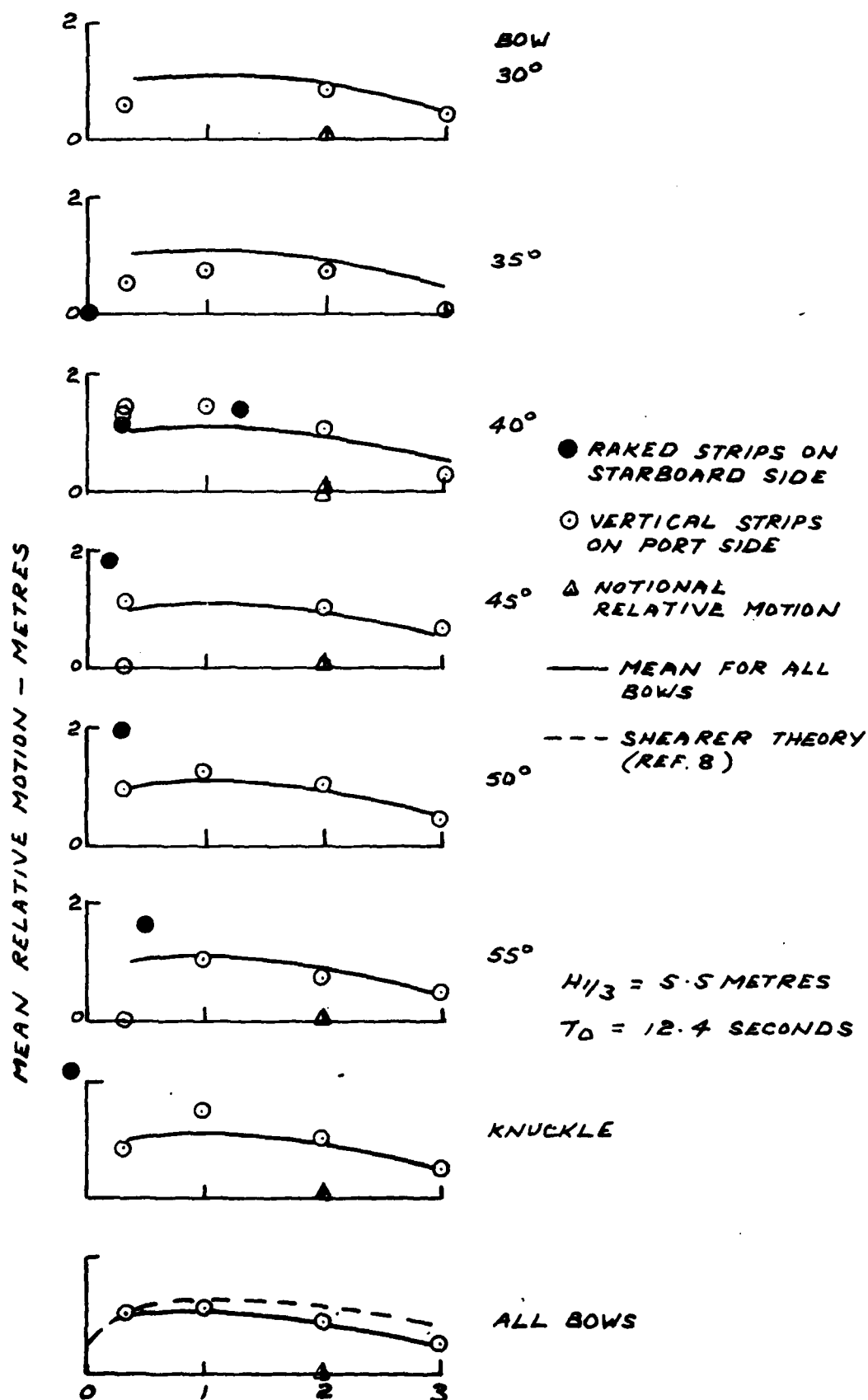


FIG. 21 MEAN RELATIVE MOTION IN WAVES

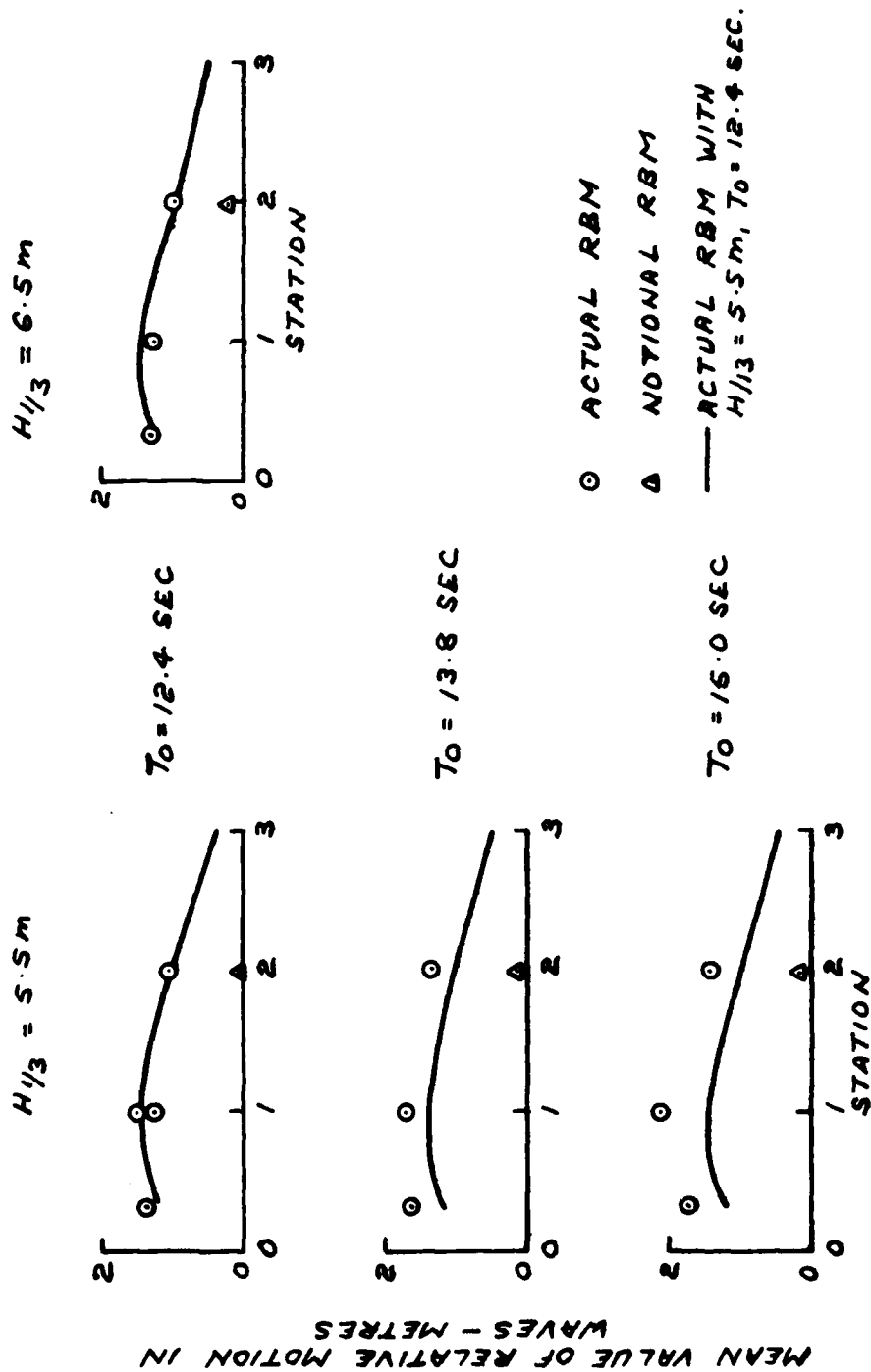
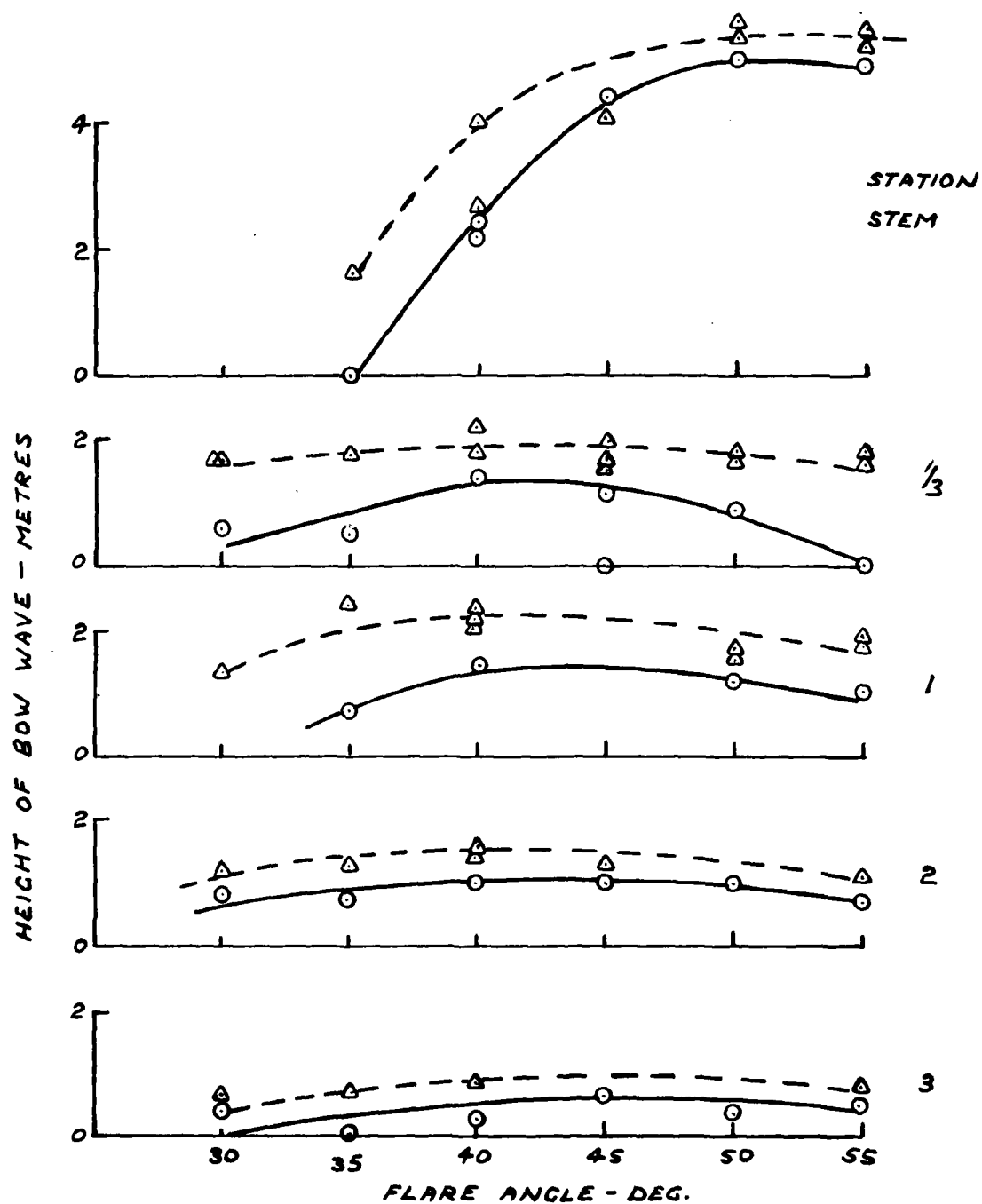


FIG 22 MEAN VALUE OF RELATIVE MOTION IN VARIOUS WAVE SPECTRA
40° BOW



○ MEAN RELATIVE MOTION IN WAVES
 $H_{1/3} = 5.5\text{m}$; $T_0 = 12.4\text{ SECONDS}$

▲ CALM WATER

FIG.23 BOW WAVE PROFILE

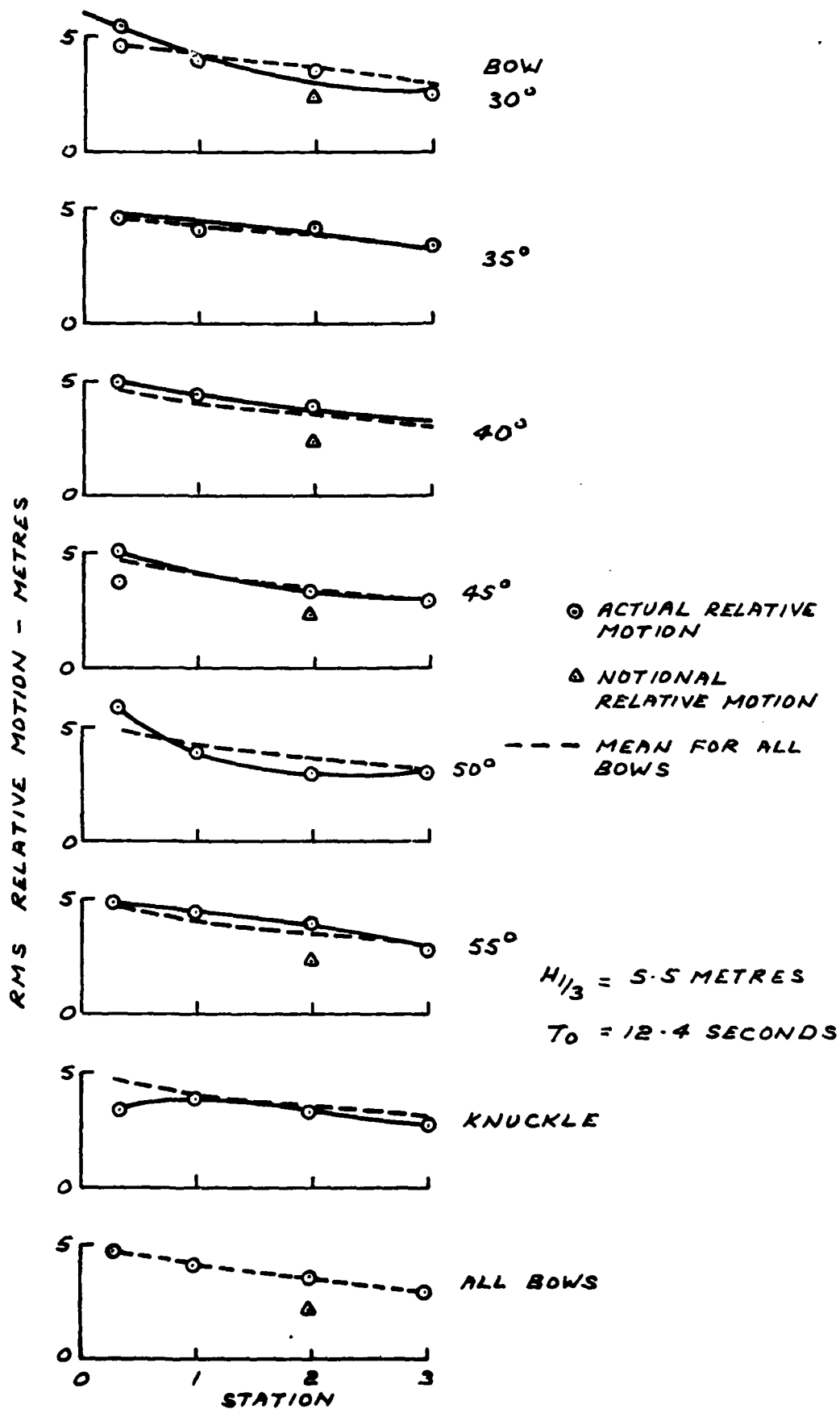


FIG. 24 Rms RELATIVE MOTIONS

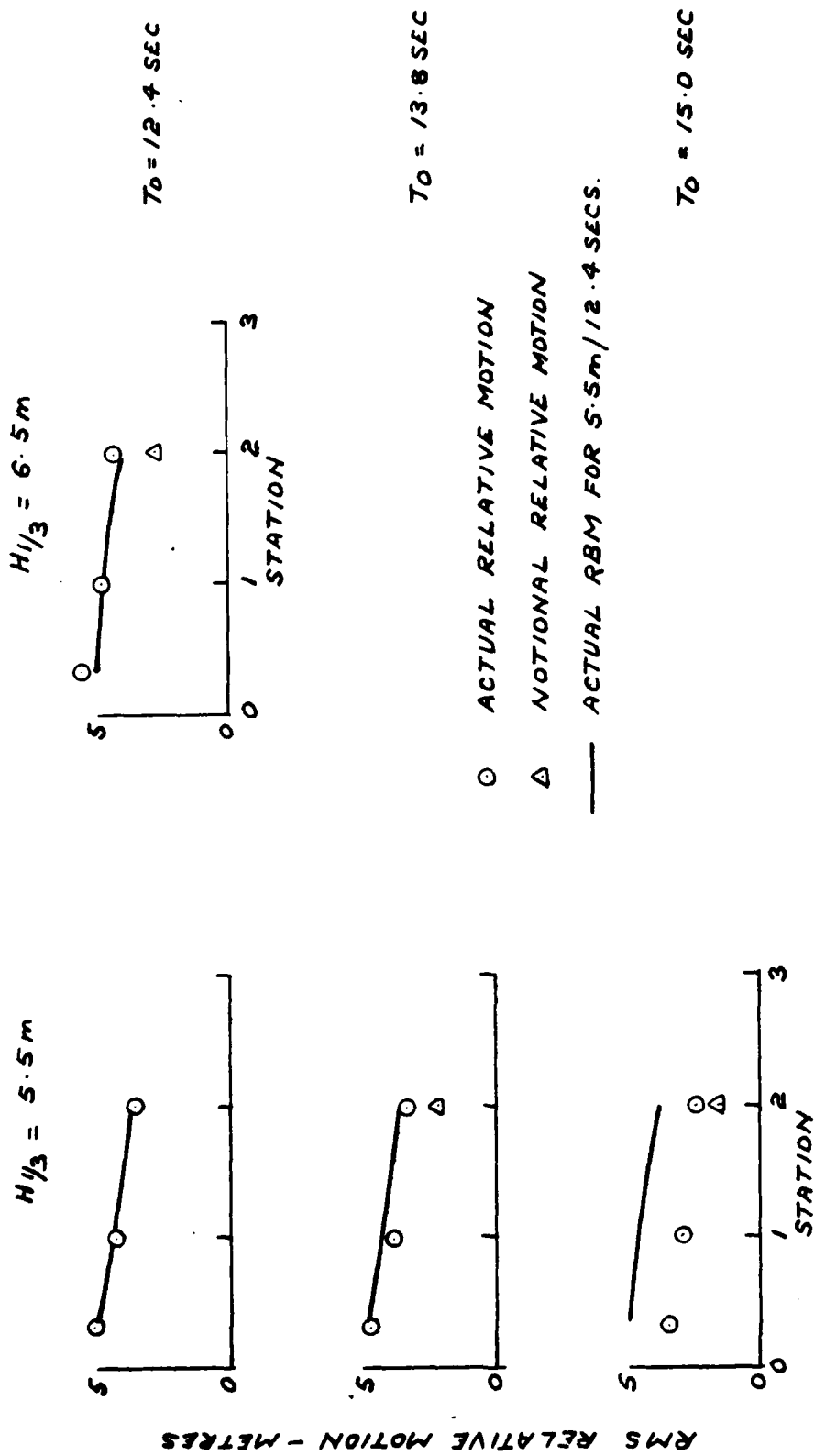


FIG.25 RMS RELATIVE MOTION IN VARIOUS WAVE SPECTRA 40° RCW

AD-A146 719

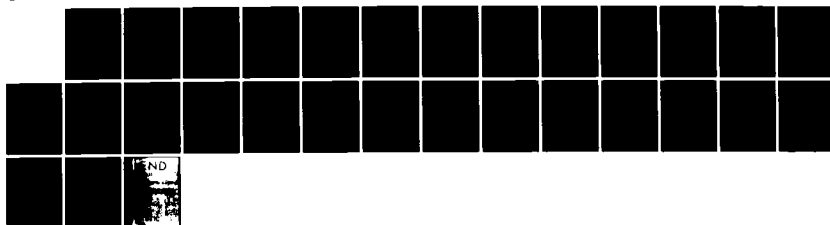
THE EFFECT OF BOW SHAPE ON DECK WETNESS IN HEAD SEAS
(U) NAVAL ACADEMY ANNAPOLIS MD DIV OF ENGINEERING AND
WEAPONS A R LLOYD APR 84 USNA-EW-17-84

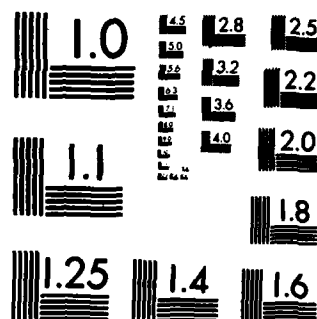
2/2

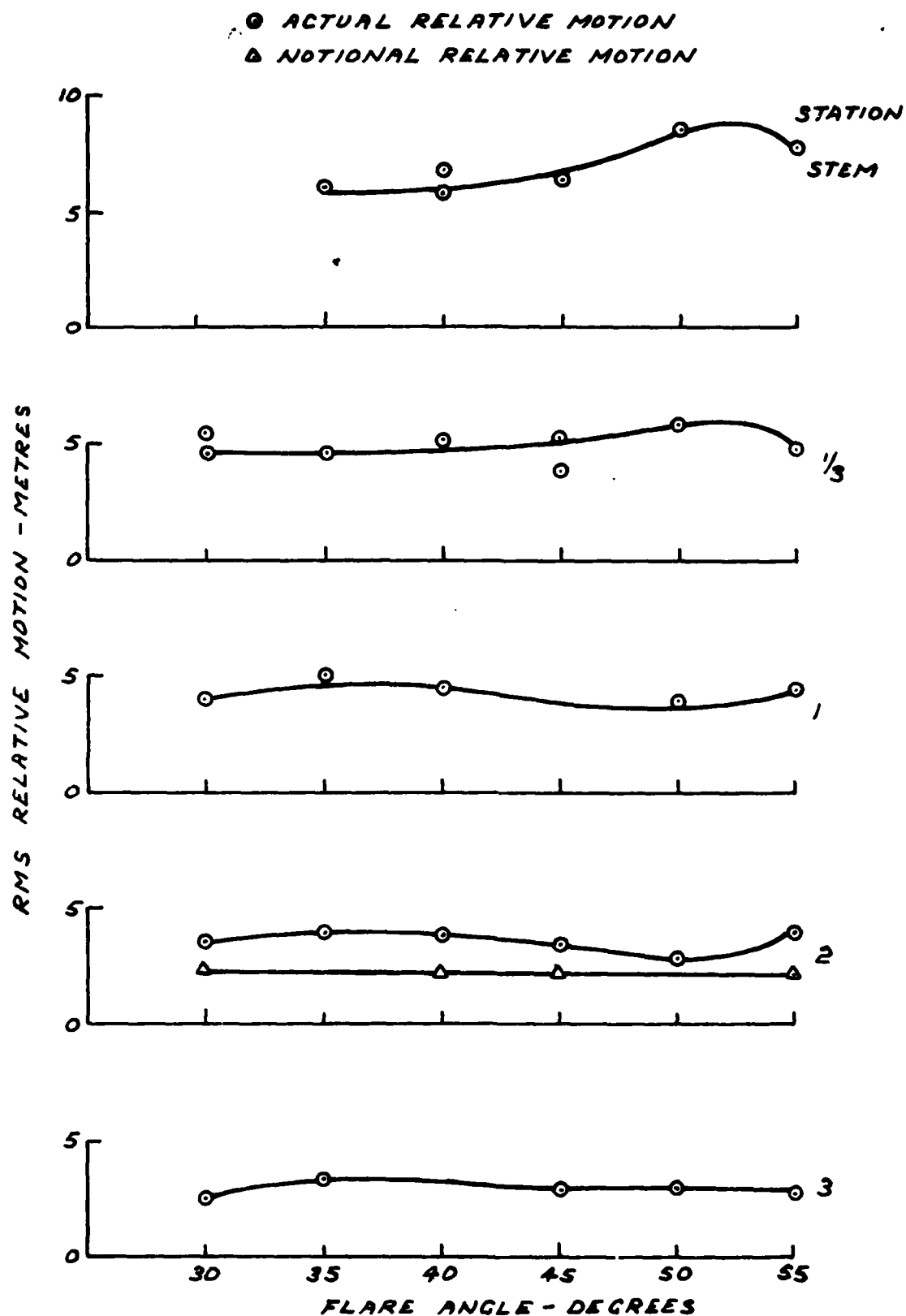
UNCLASSIFIED

F/G 13/10

NL

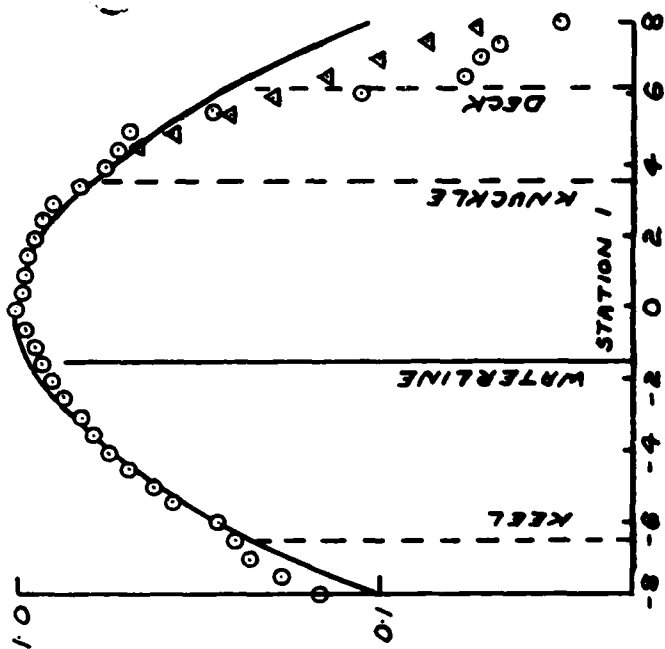
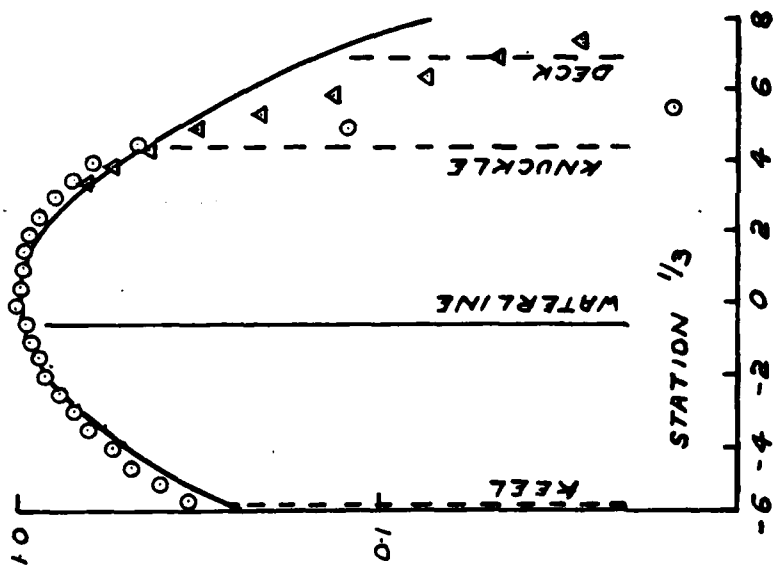
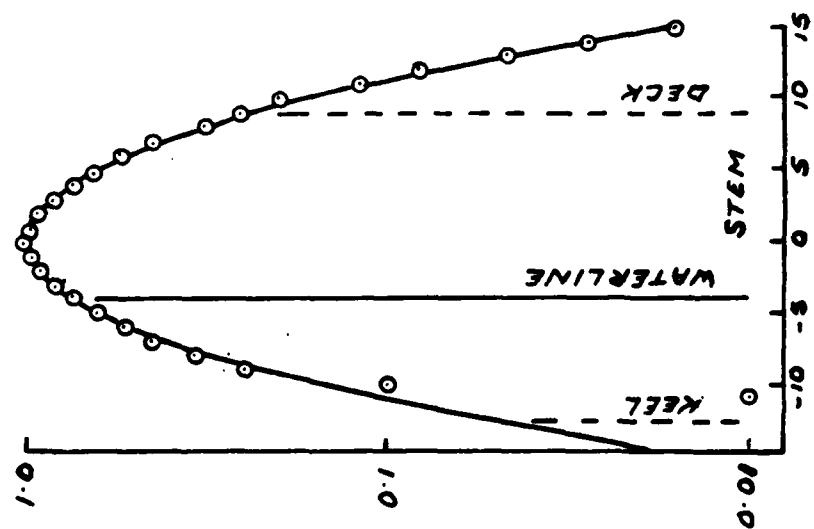






$H/3 = 5.5$ METRES $T_0 = 12.4$ SECONDS

FIG.26 Rms RELATIVE MOTIONS



RELATIVE MOTION AMPLITUDE - METRES

$H_{1/3} = 5.5$ METRES Δ EXPERIMENT - CLIPPED AT KNUCKLE

$T_0 = 12.4$ SECONDS \circ EXPERIMENT - CLIPPED AT DECK

— RAYLEIGH FORMULA

FIG.28 (a) PROBABILITY DISTRIBUTIONS OF RELATIVE BOW MOTION ~ KNUCKLE BOW

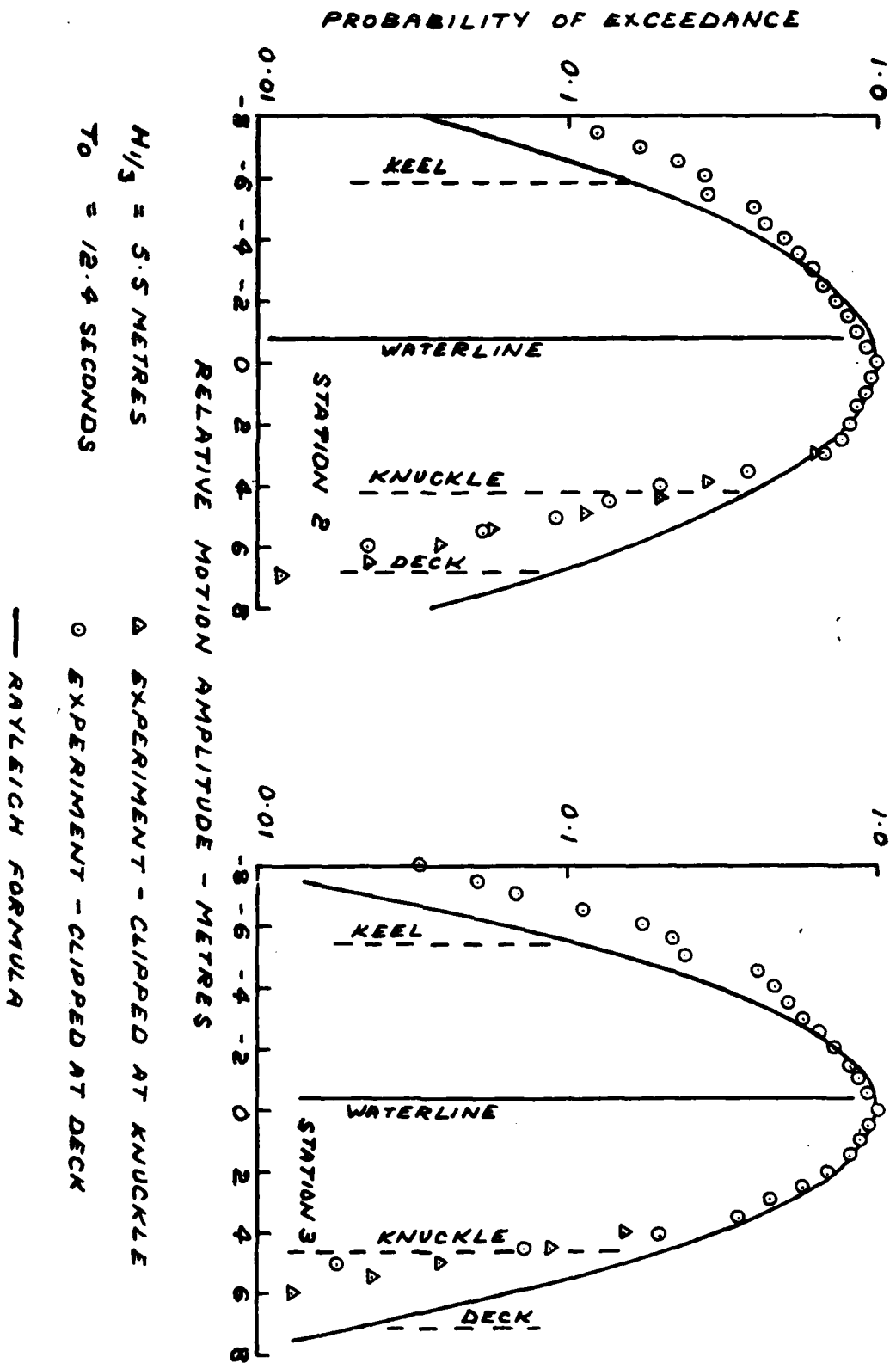


FIG. 28(b) PROBABILITY DISTRIBUTIONS OF RELATIVE BOW MOTION λ_{KN} KNUCKLE BOW

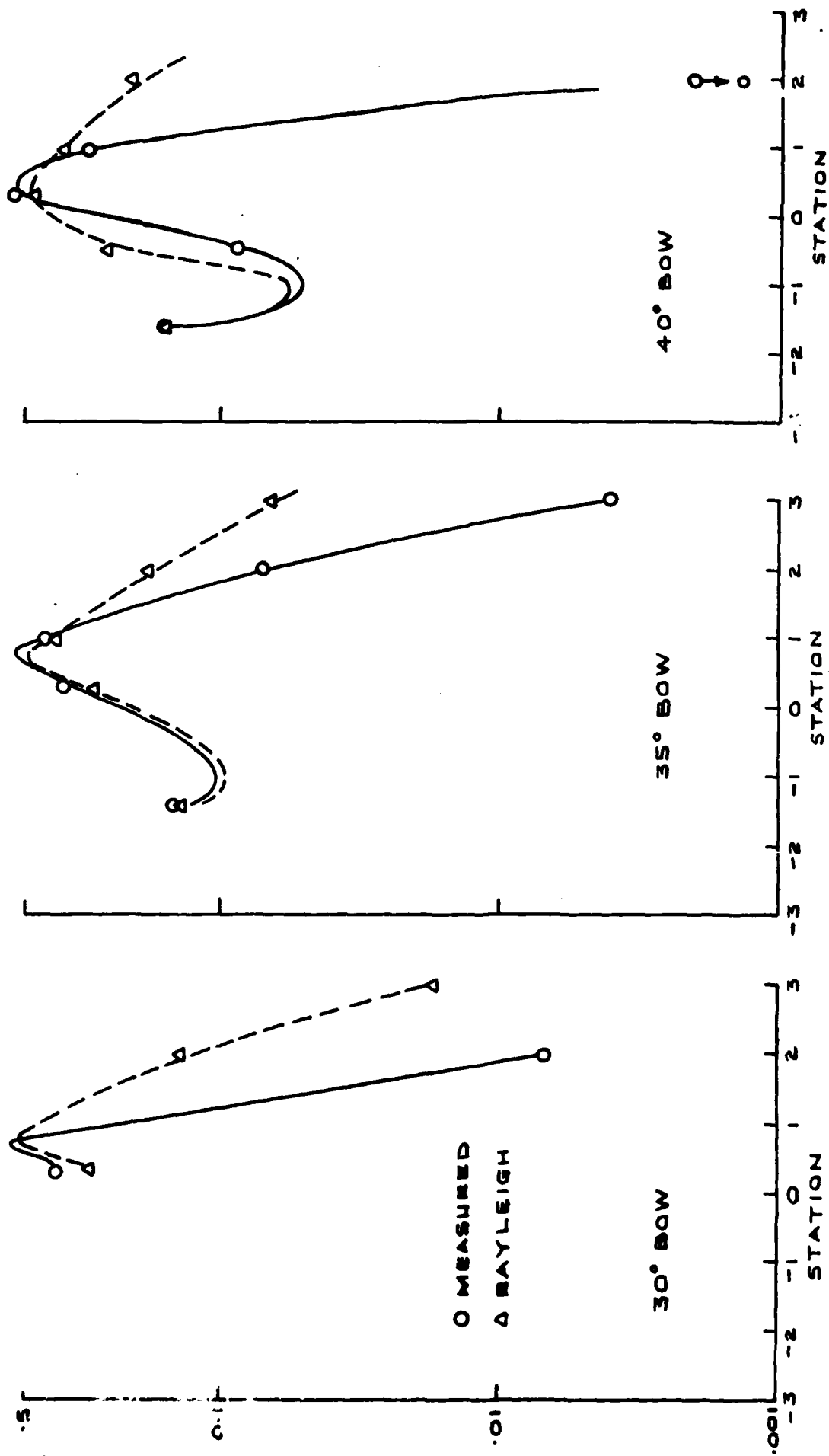


FIG. 29 (a) PROBABILITY OF EXCEEDING FREEBOARD

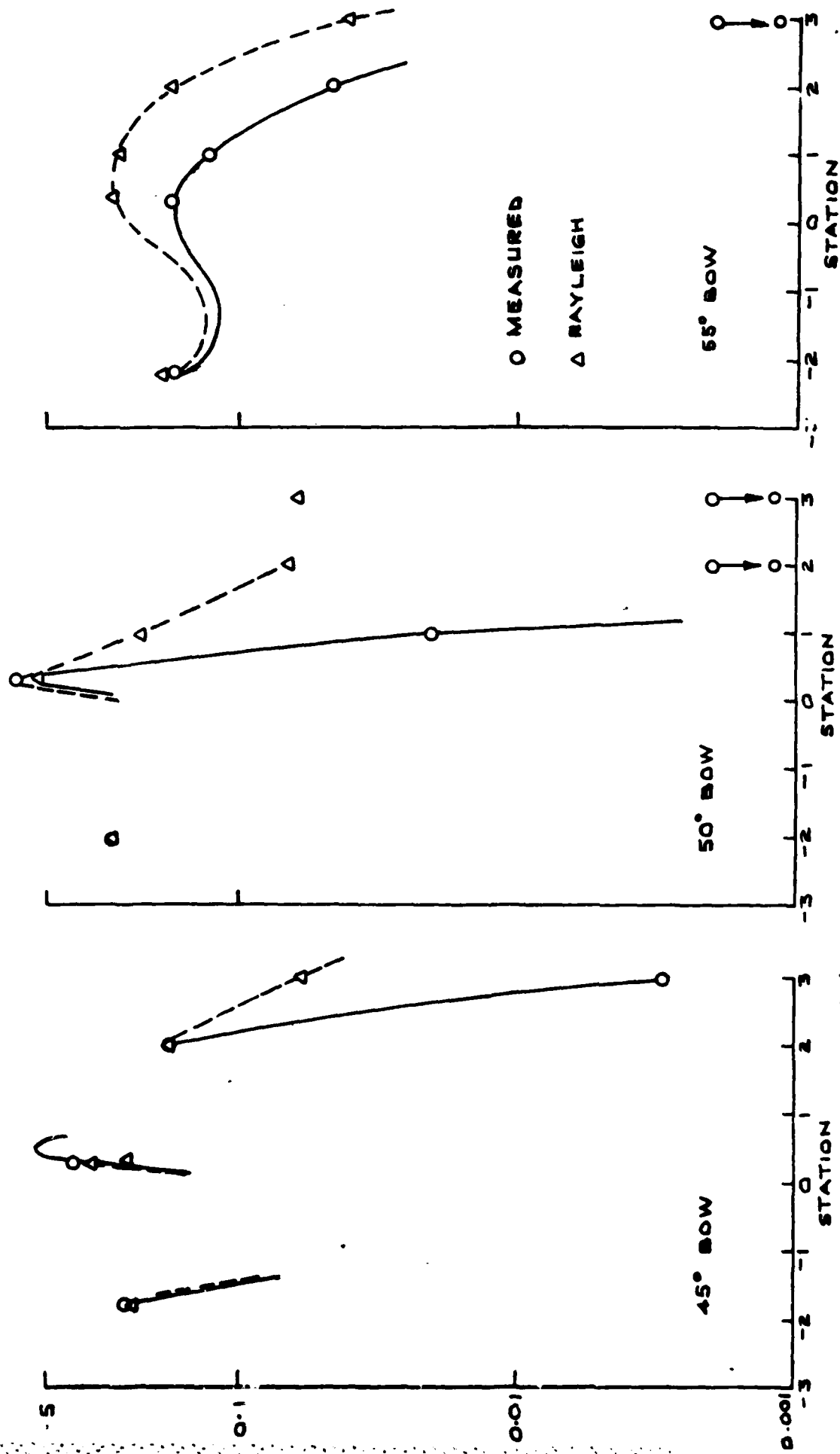


FIG. 29 (b) PROBABILITY OF EXCEEDING FREEBOARD

◇ MEASURED - NO CONTACT WITH HULL

○ MEASURED - IN CONTACT WITH HULL

△ RAYLEIGH

$H_{1/3} = 5.5$ METRES

$T_0 = 12.4$ SECONDS

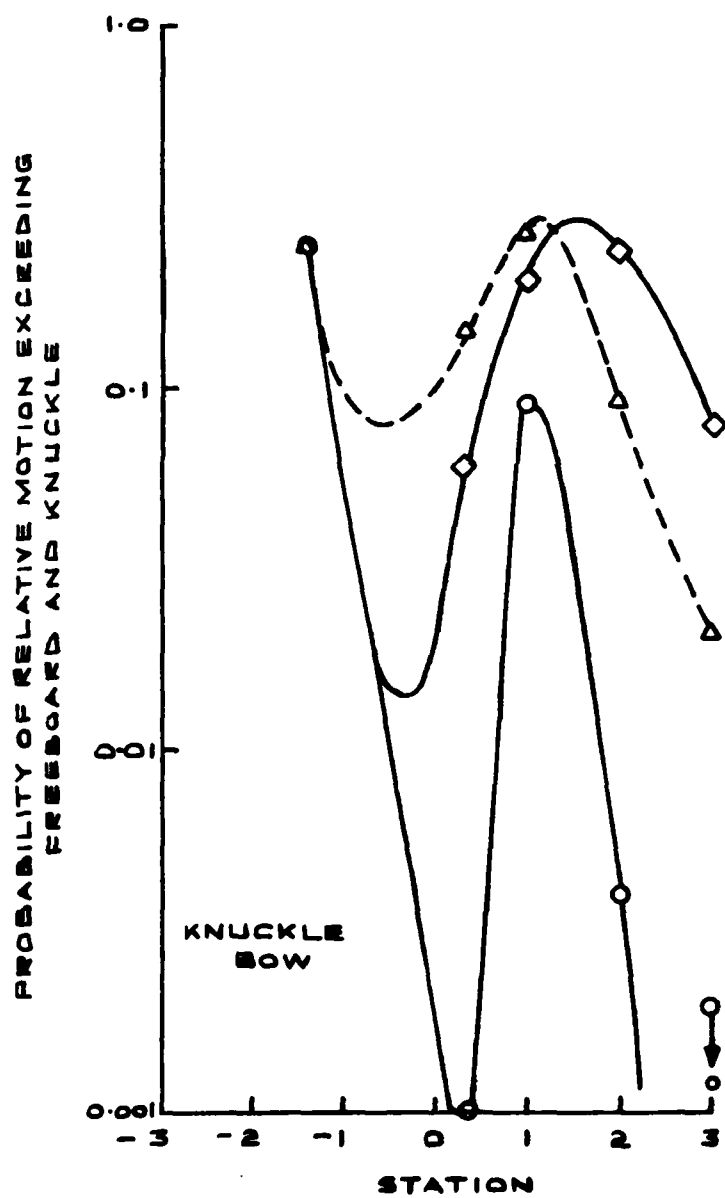


FIG. 29 (c) PROBABILITY OF EXCEEDING FREEBOARD

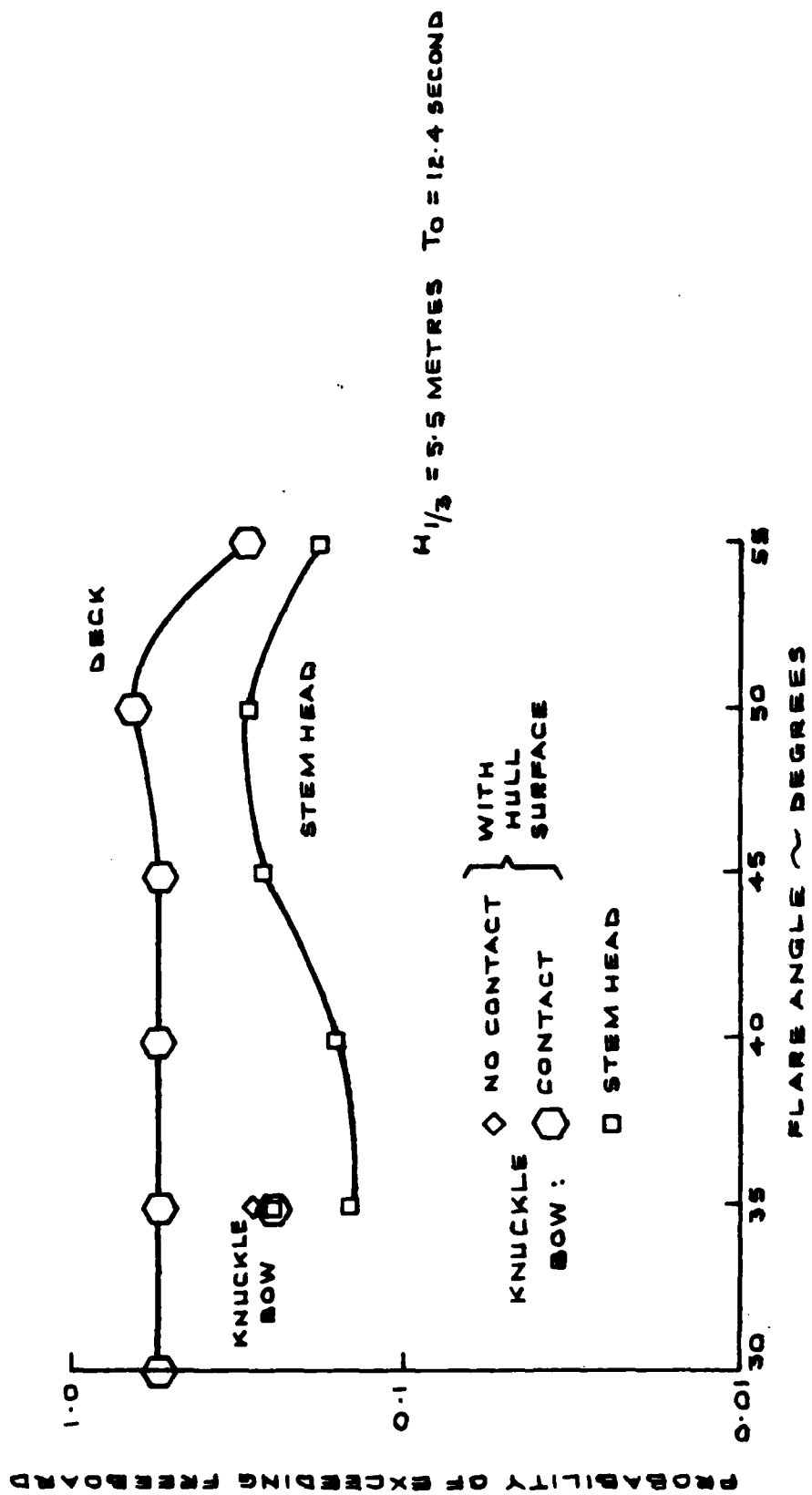


FIG 30 PROBABILITY OF RELATIVE MOTION EXCEEDING FREEBOARD

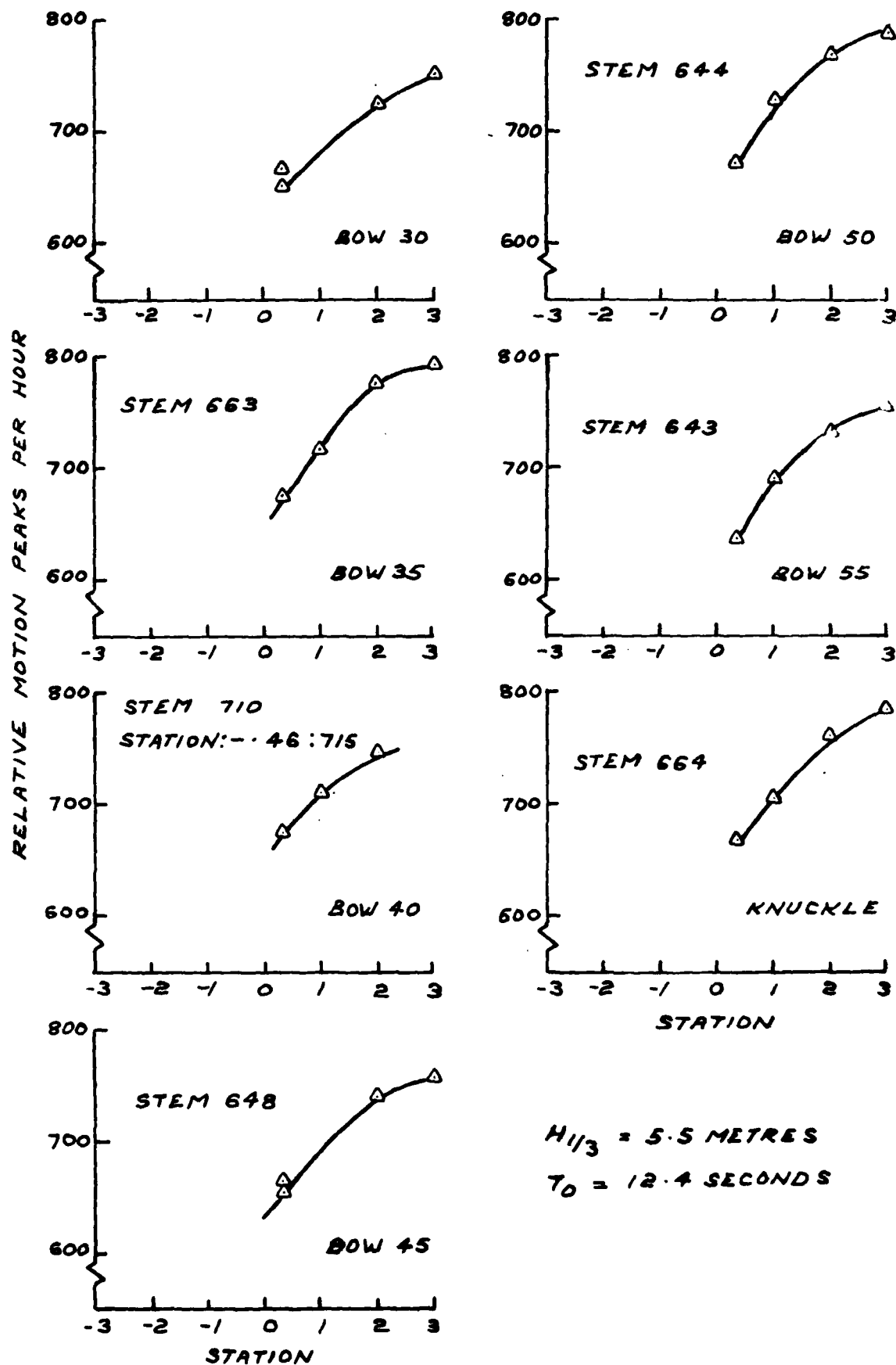
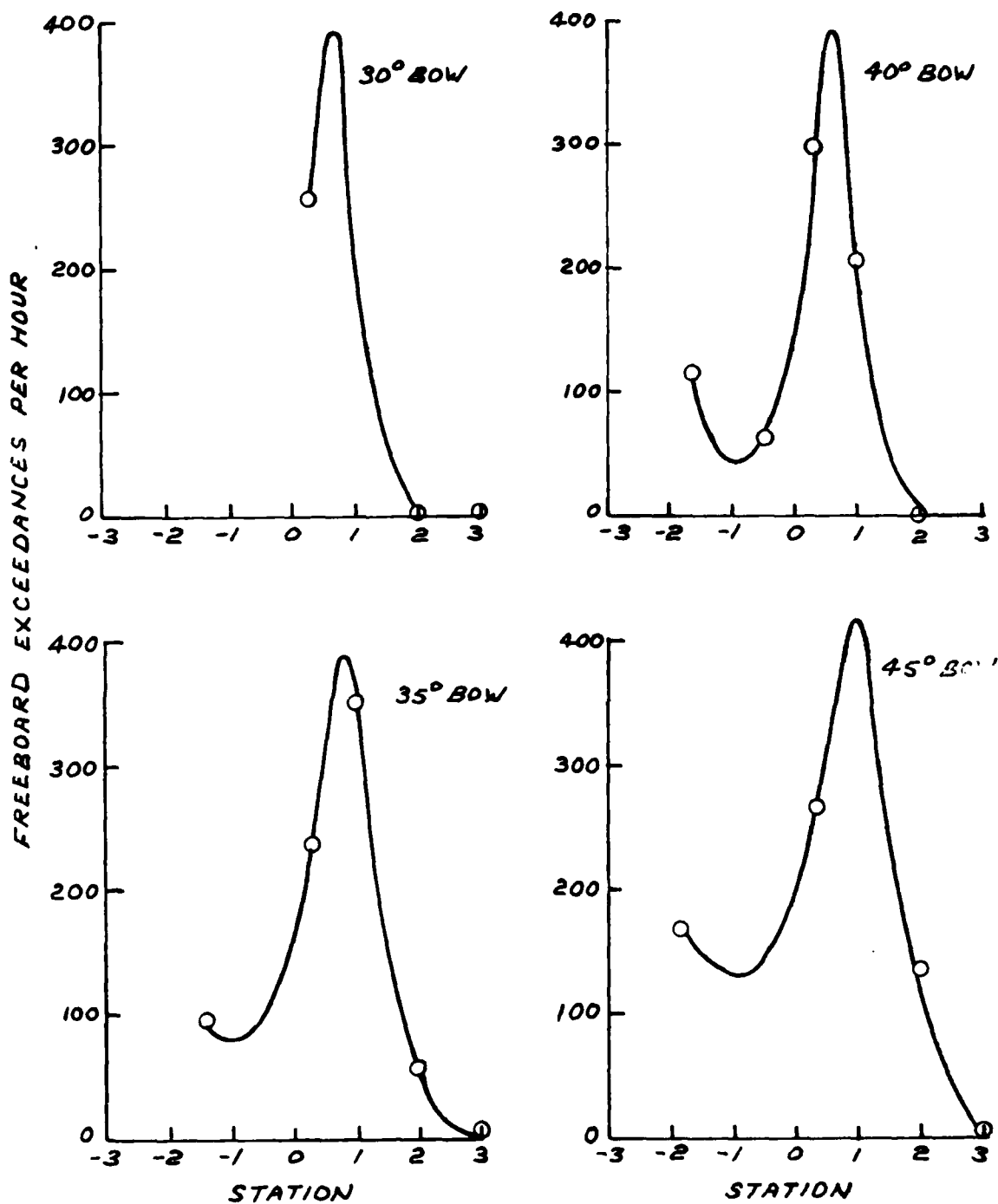
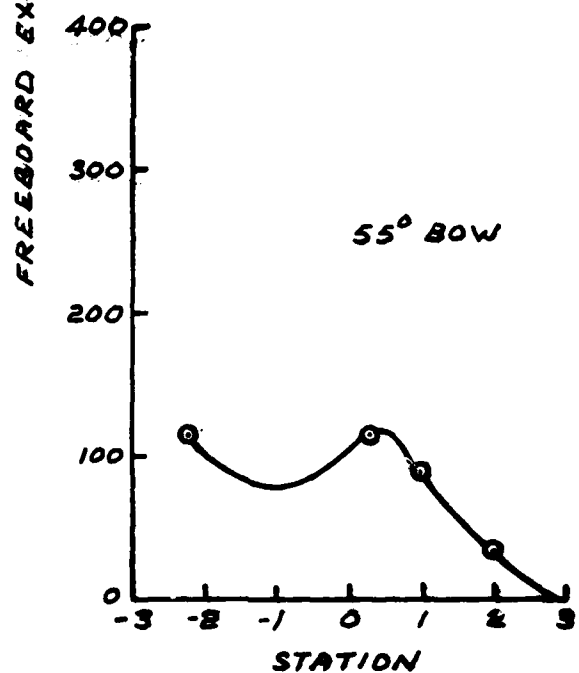
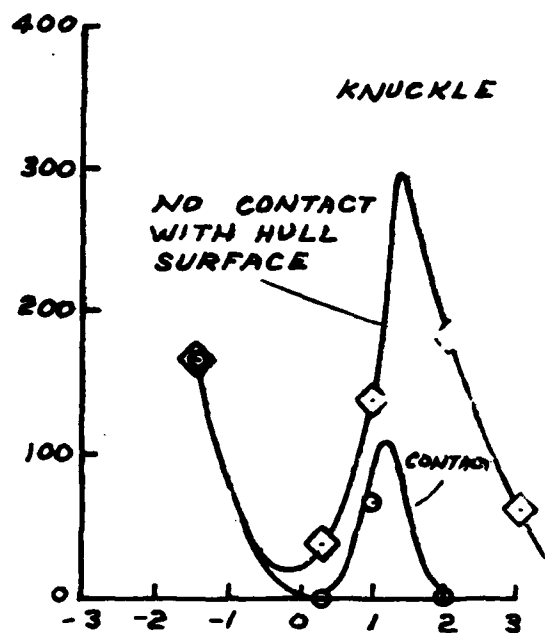
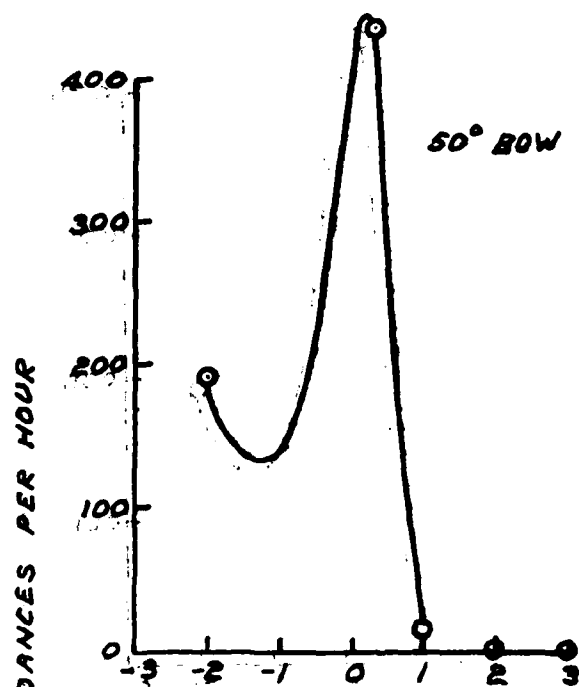


FIG.31 RELATIVE MOTION PEAKS PER HOUR



$H/3 = 5.5 \text{ METRES} \quad T_0 = 12.4 \text{ SECONDS}$

FIG. 32 (a) FREEBOARD EXCEEDANCES PER HOUR



$H_{1/3} = 5.5$ METRES
 $T_0 = 12.4$ SECONDS

FIG. 32(b) FREEBOARD EXCEEDANCES PER HOUR

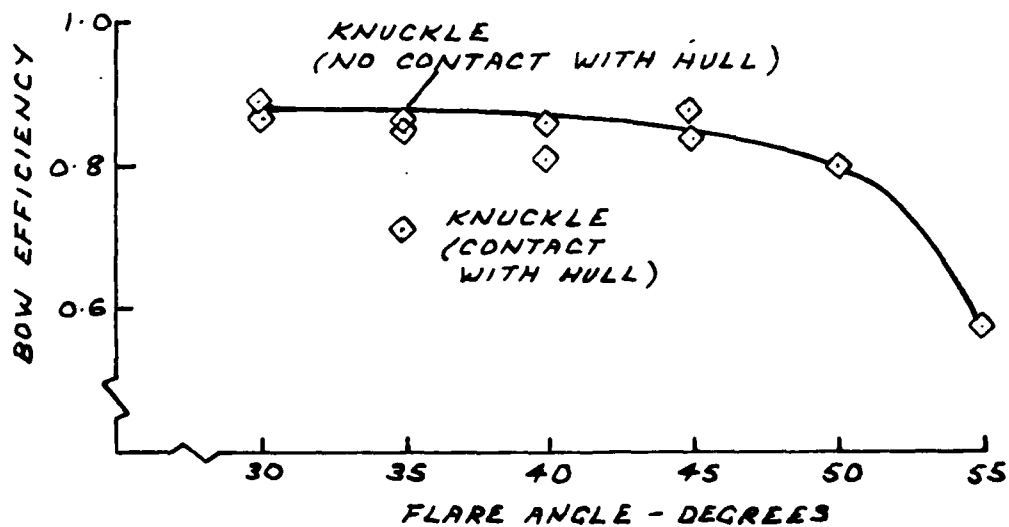
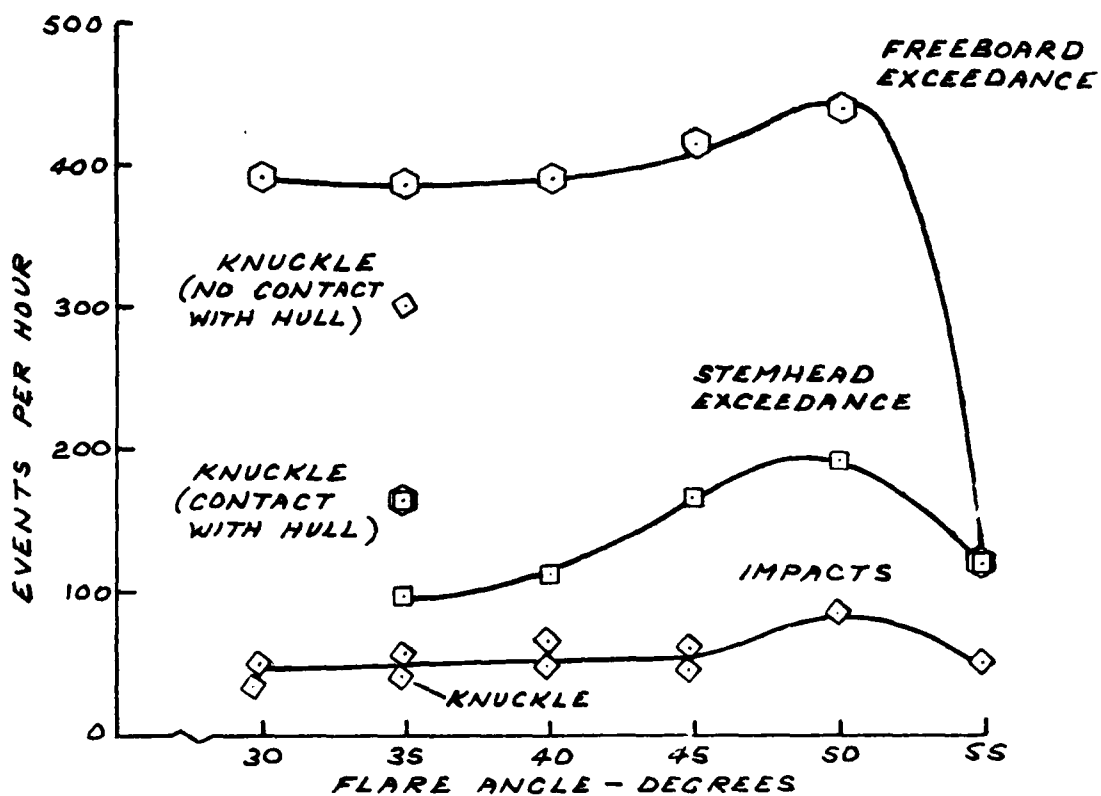
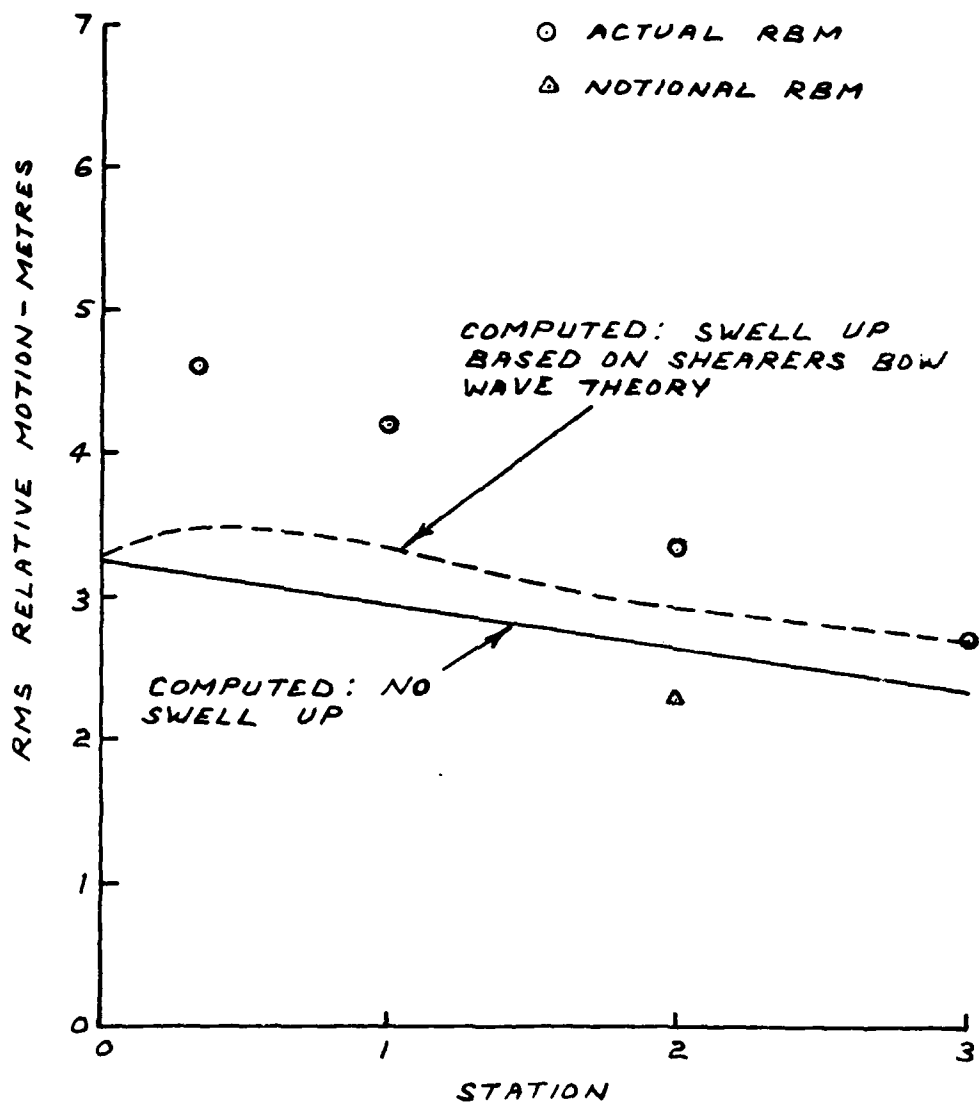


FIG. 33 BOW PERFORMANCE



$H_{1/3} = 5.5$ METRES
 $T_0 = 12.4$ SECONDS
 SPEED = 22 KNOTS

FIG.34 Rms RELATIVE MOTION COMPARISON WITH THEORY

PREDICTED RMS RELATIVE MOTION
 (÷ 1.15 TO ALIGN WITH EXPERIMENT RESULT
 FOR NOMINAL RBM AT STATION 2)

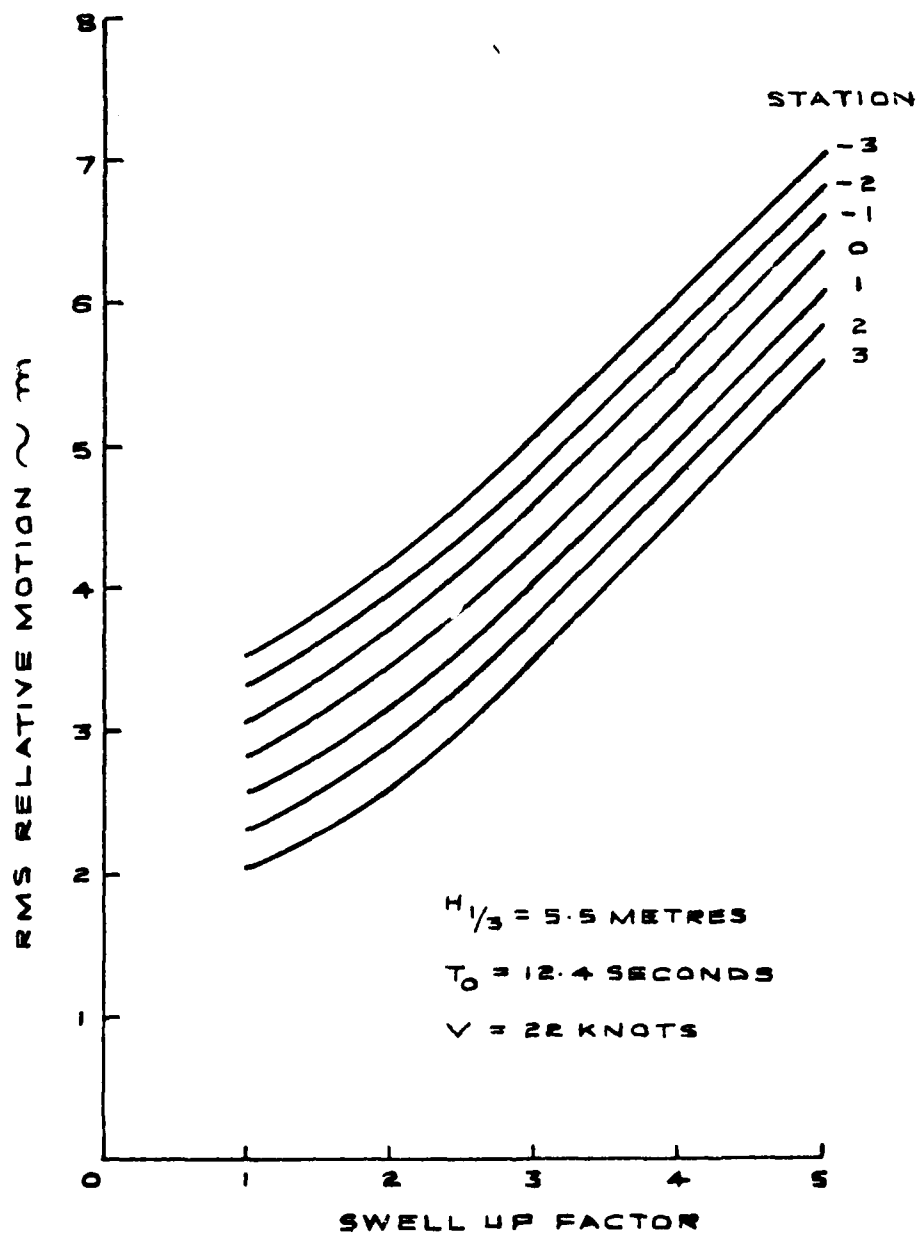


FIG.35 PREDICITED Rms RELATIVE MOTIONS

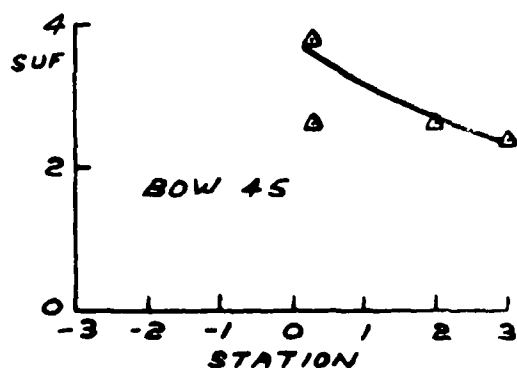
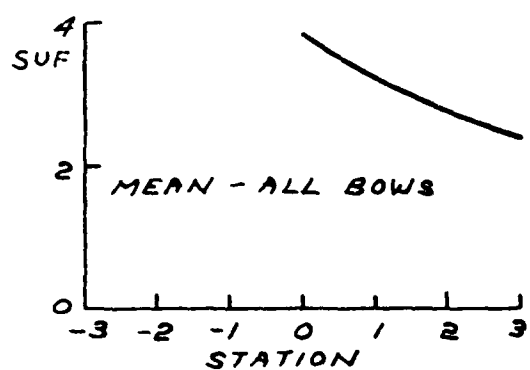
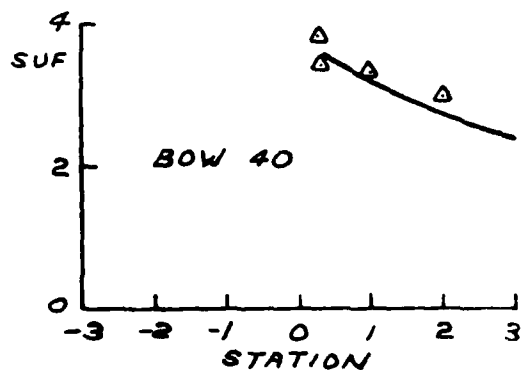
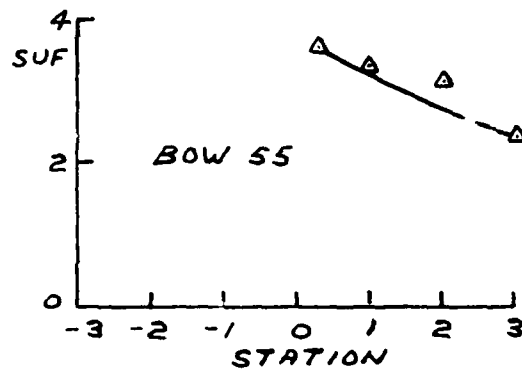
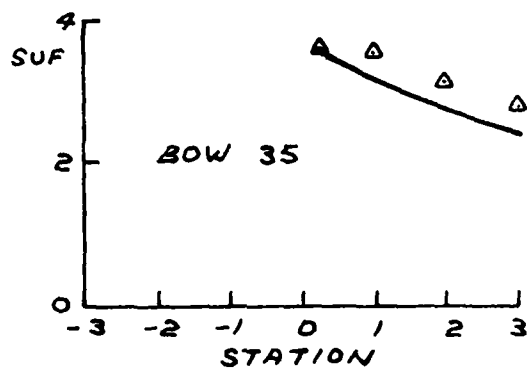
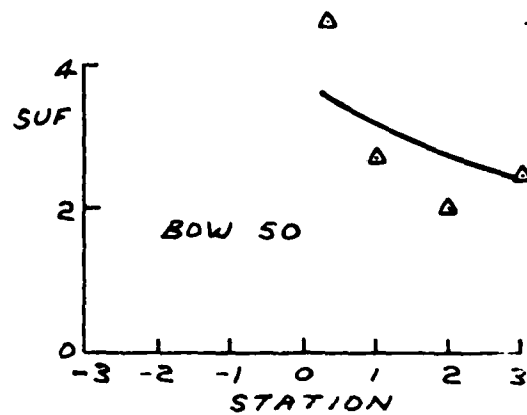
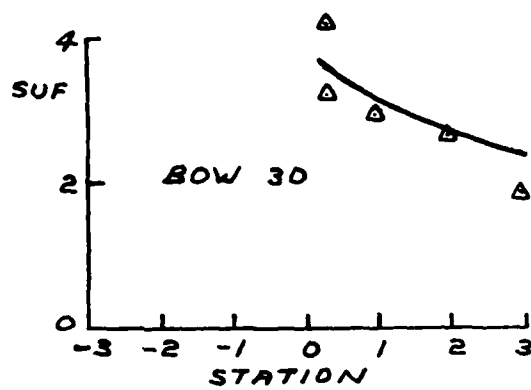


FIG.36 REQUIRED SWELL UP FACTOR

CRITICAL VELOCITY - METRES/SECOND

CRITICAL VELOCITIES

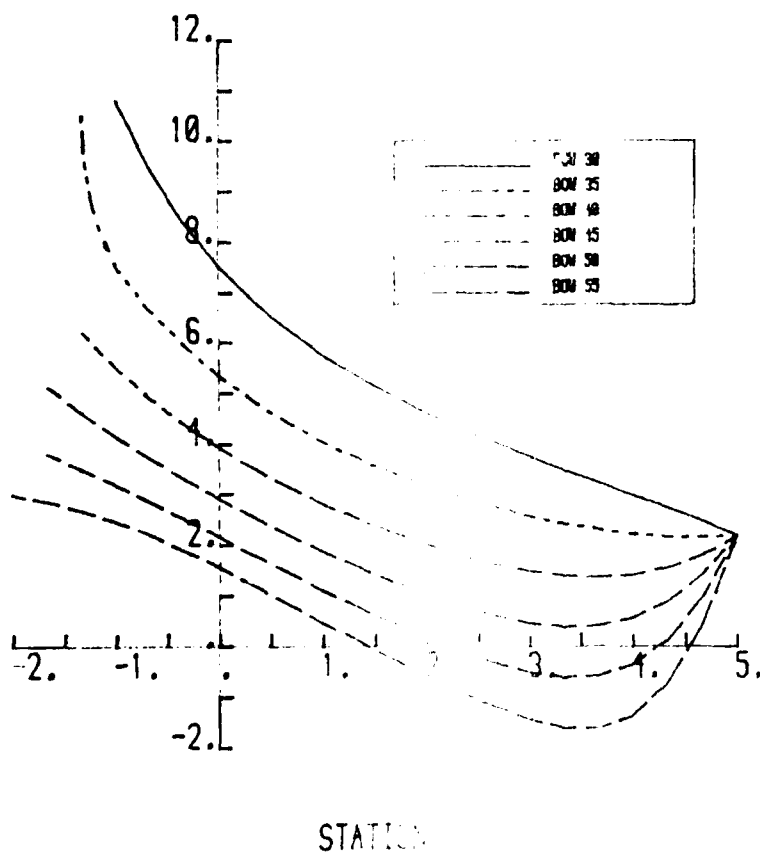


FIG. 37 CRITICAL AND THE VERTICAL WATER VELOCITY

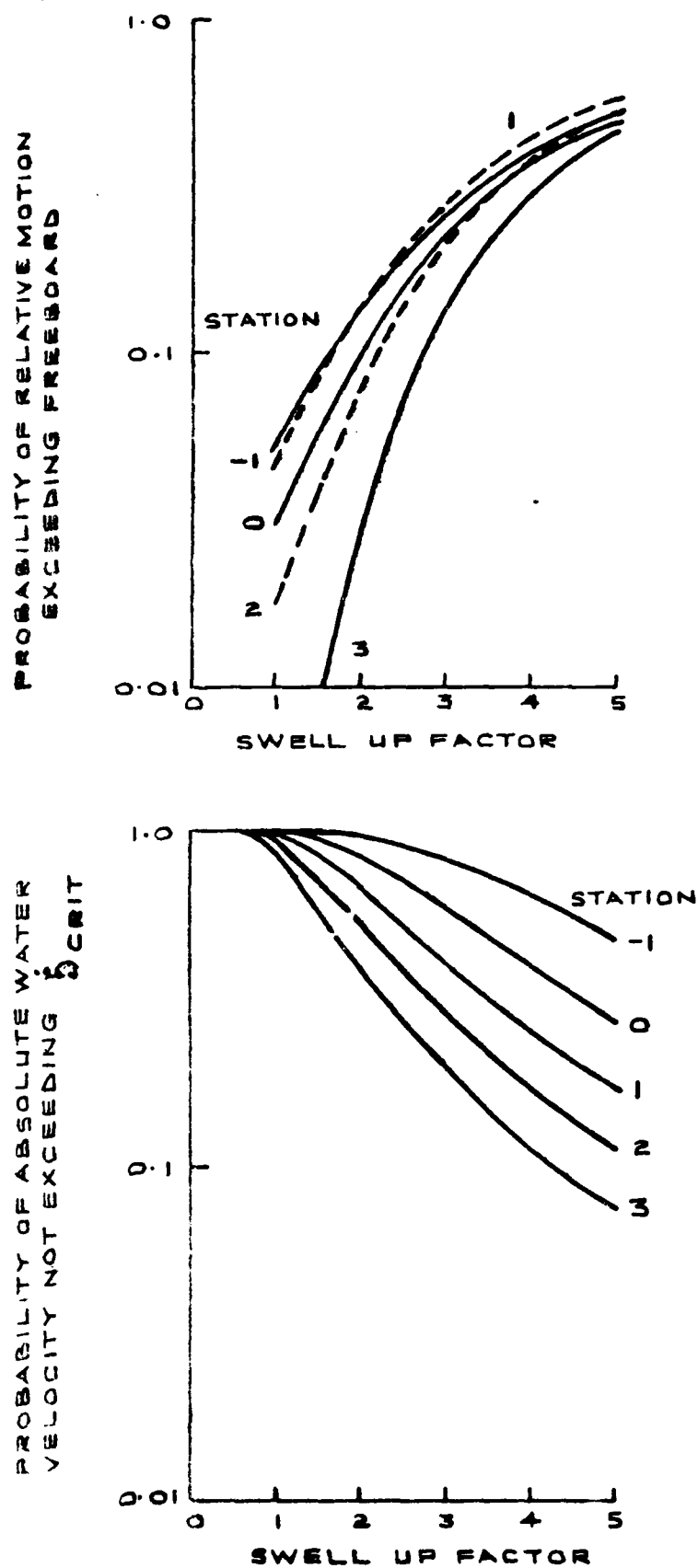


FIG38 PROBABILITIES ASSOCIATED WITH DECK WETNESS
BOW 30

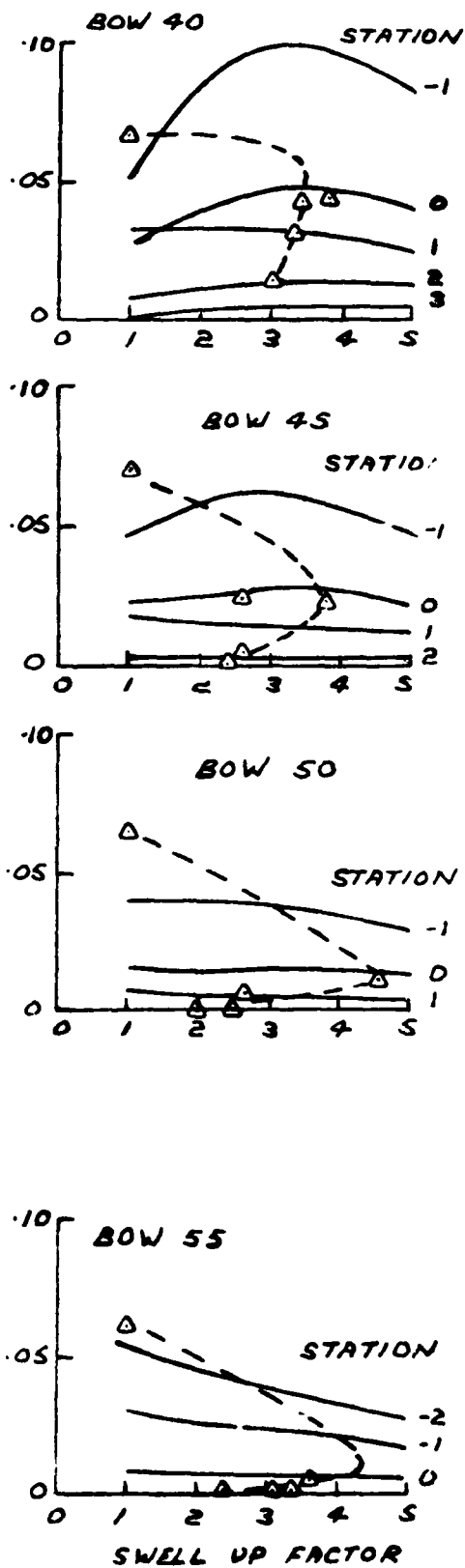
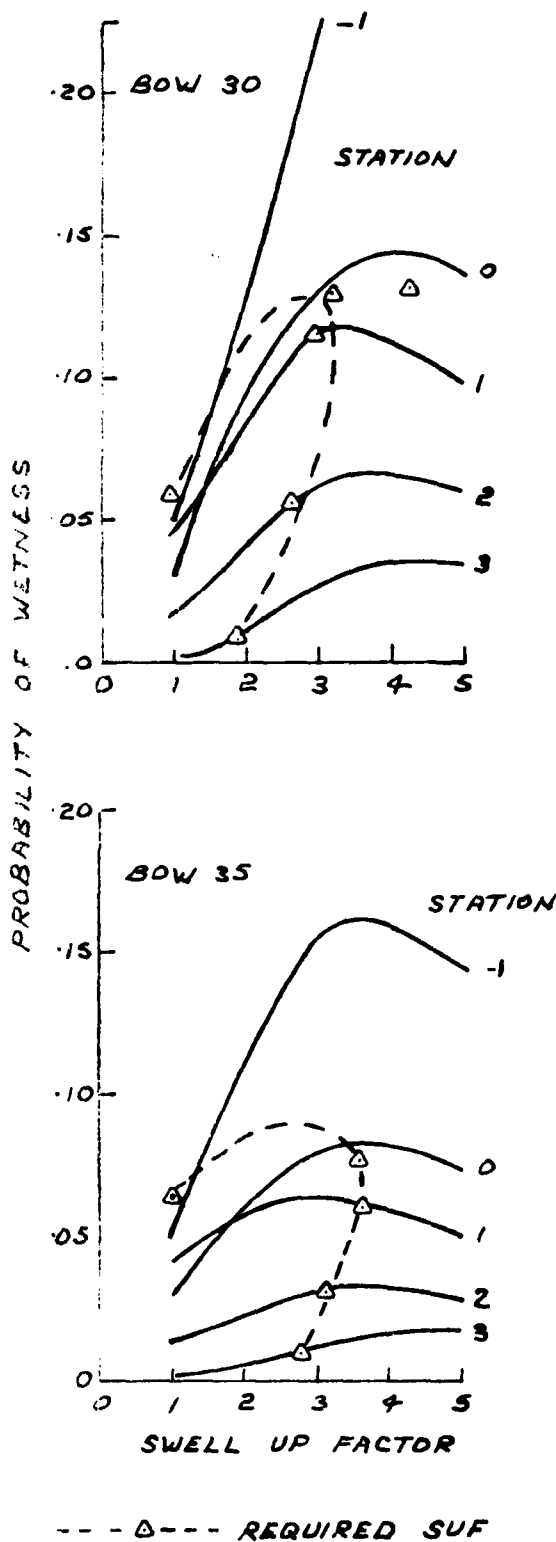
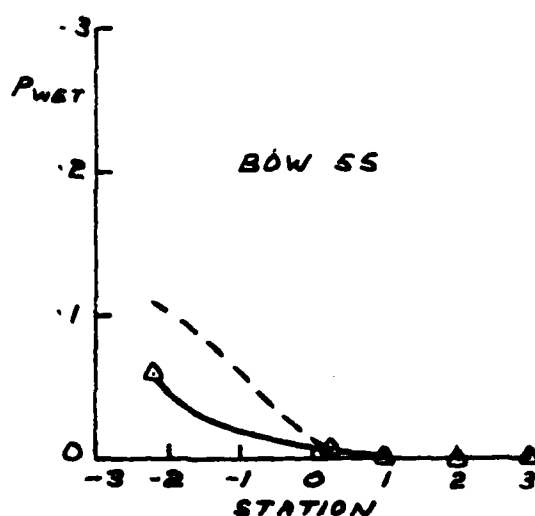
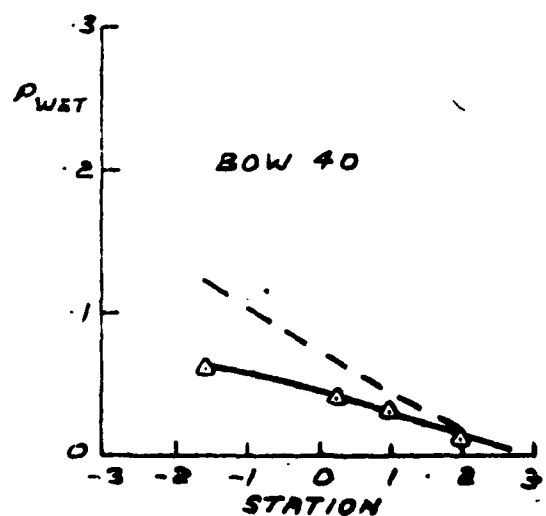
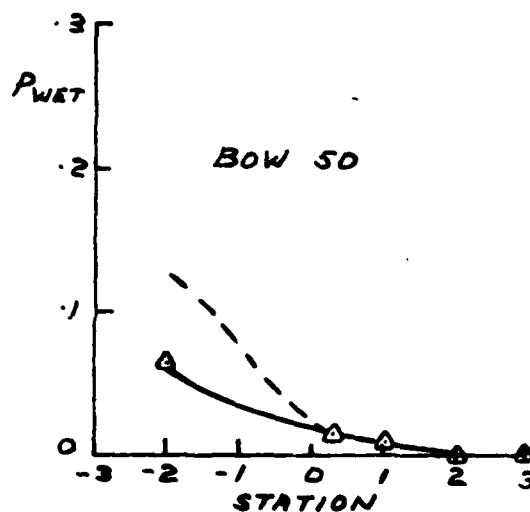
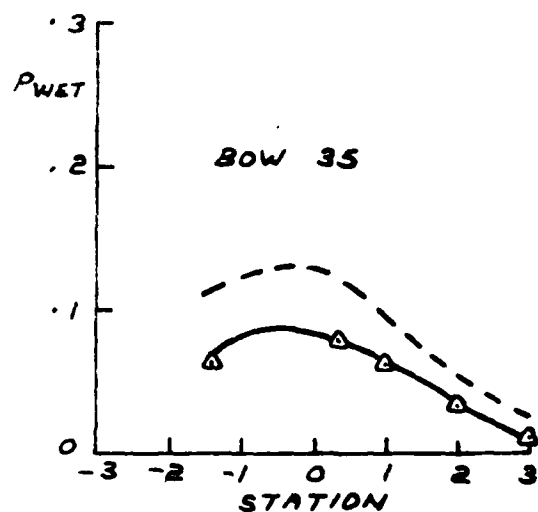
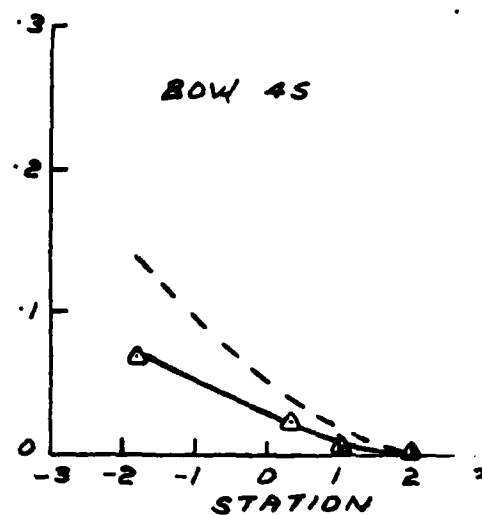
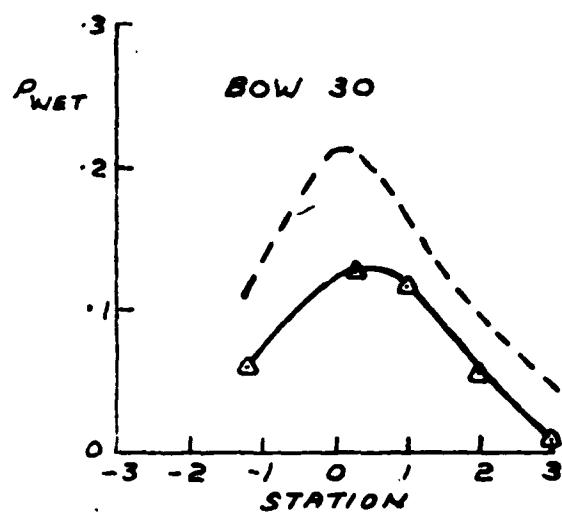
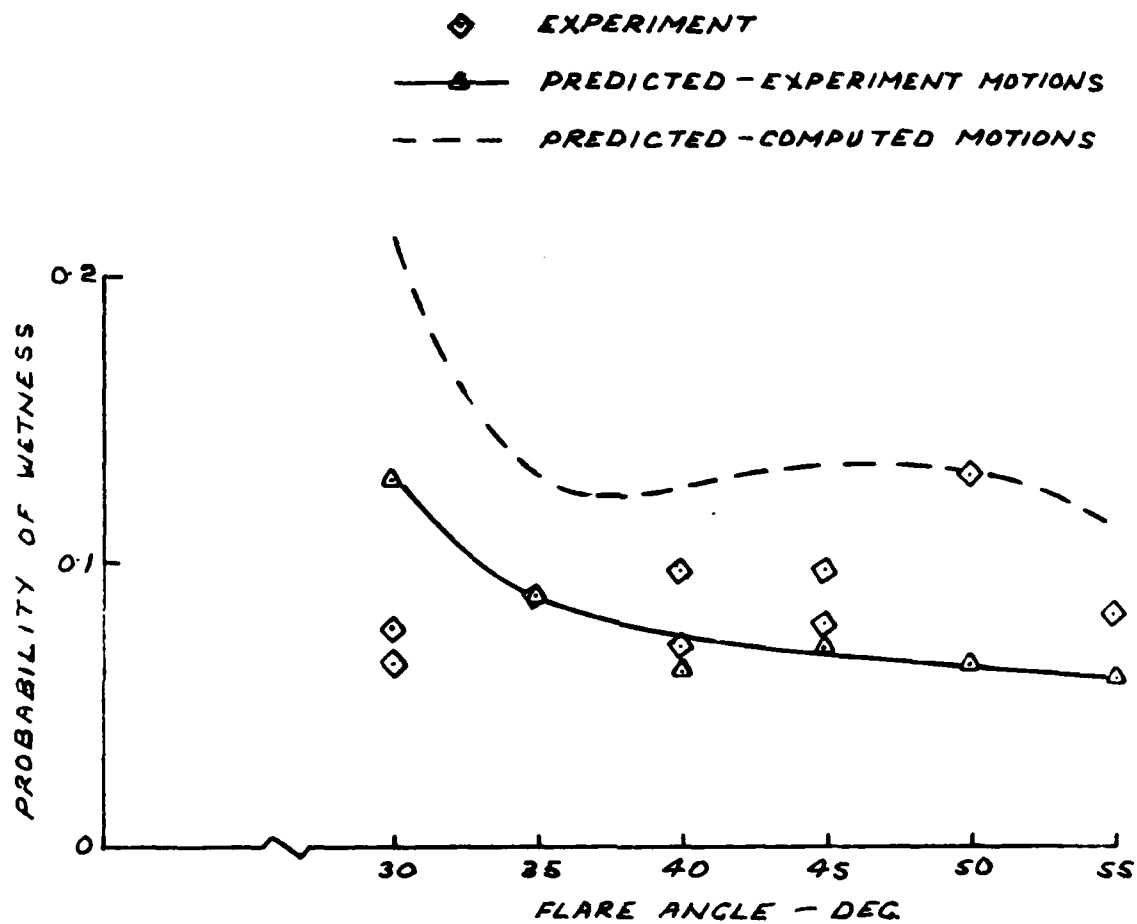


FIG. 39 PROBABILITY OF DECK WETNESS



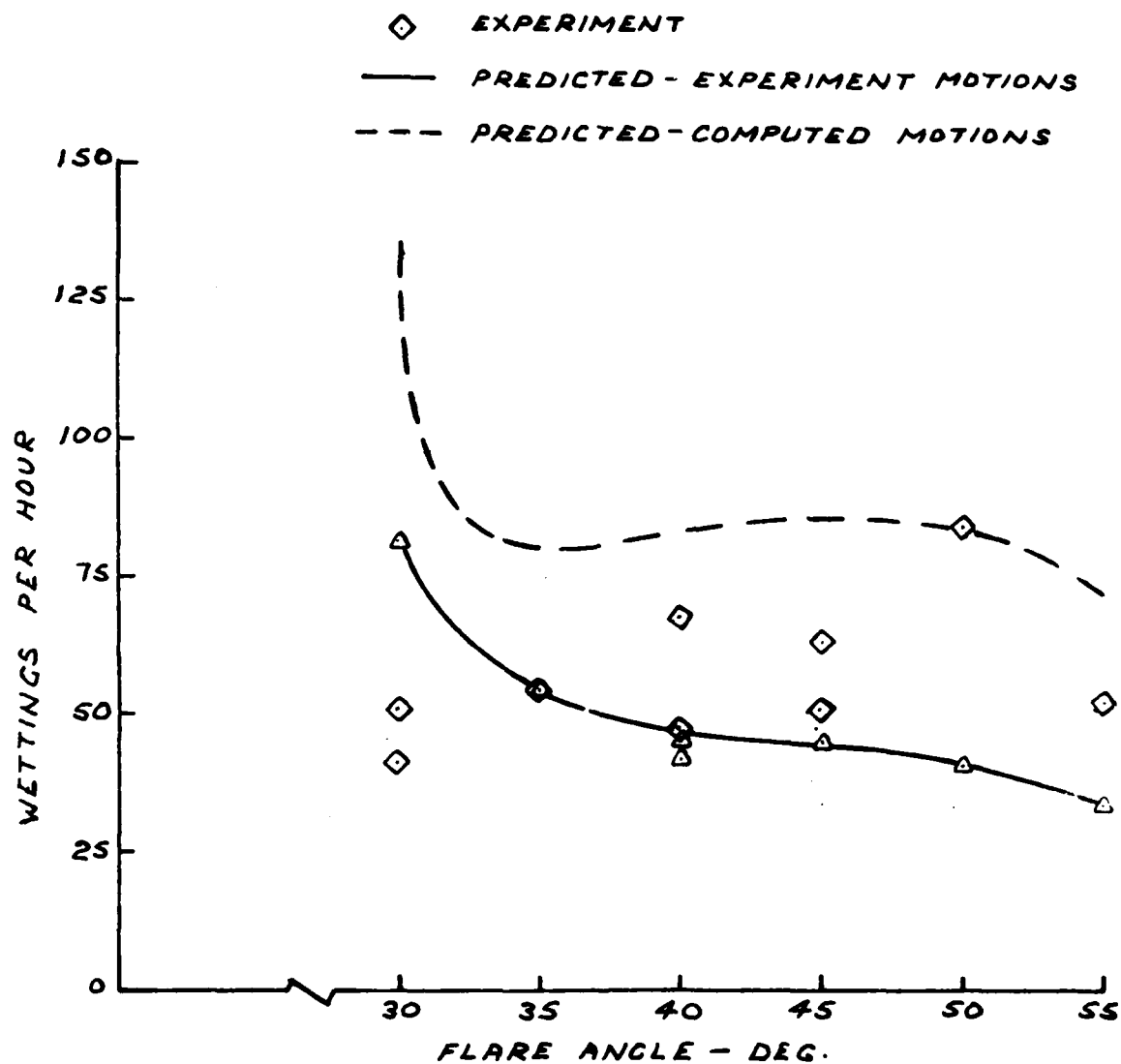
—△— PREDICTED : EXPERIMENT MOTIONS
 --- PREDICTED : COMPUTED MOTIONS

FIG.40 ESTIMATED PROBABILITY OF DECK WETNESS



$H_{1/3} = 5.5$ METRES. $T_0 = 12.4$ SECONDS

FIG.41 PREDICTED AND MEASURED
PROBABILITY OF DECK WETNESS



$H_{1/3} = 5.5$ METRES
 $T_0 = 12.4$ SECONDS

FIG. 42 PREDICTED AND MEASURED DECK
 WETNESS FREQUENCY

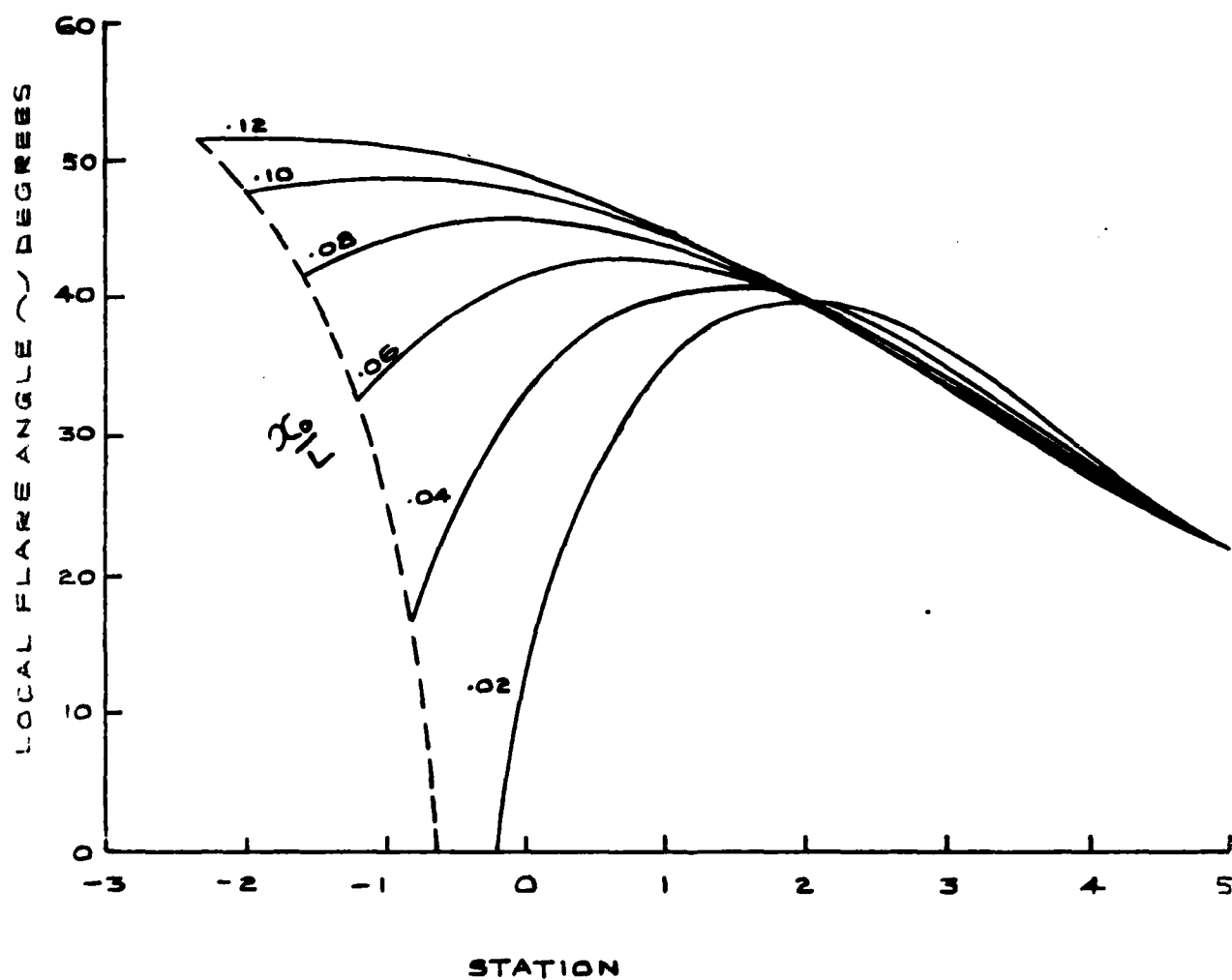


FIG.43 LOCAL FLARE ANGLE
NOMINAL FLARE ANGLE 40°

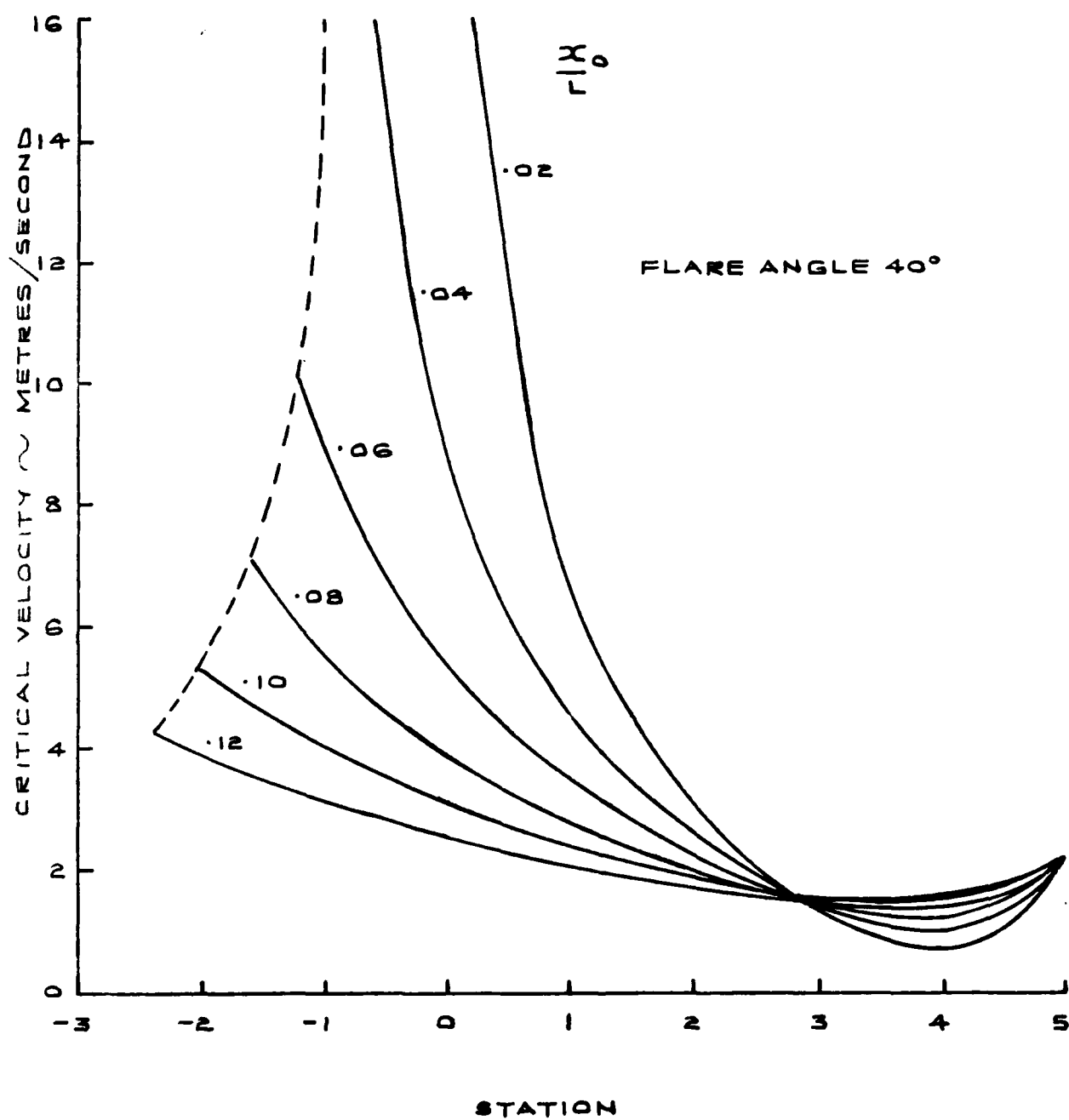


FIG.44 CRITICAL VELOCITY

$H_{1/3} = 5.5$ METRES

$T_0 = 12.4$ SECONDS

□ ~ STEM

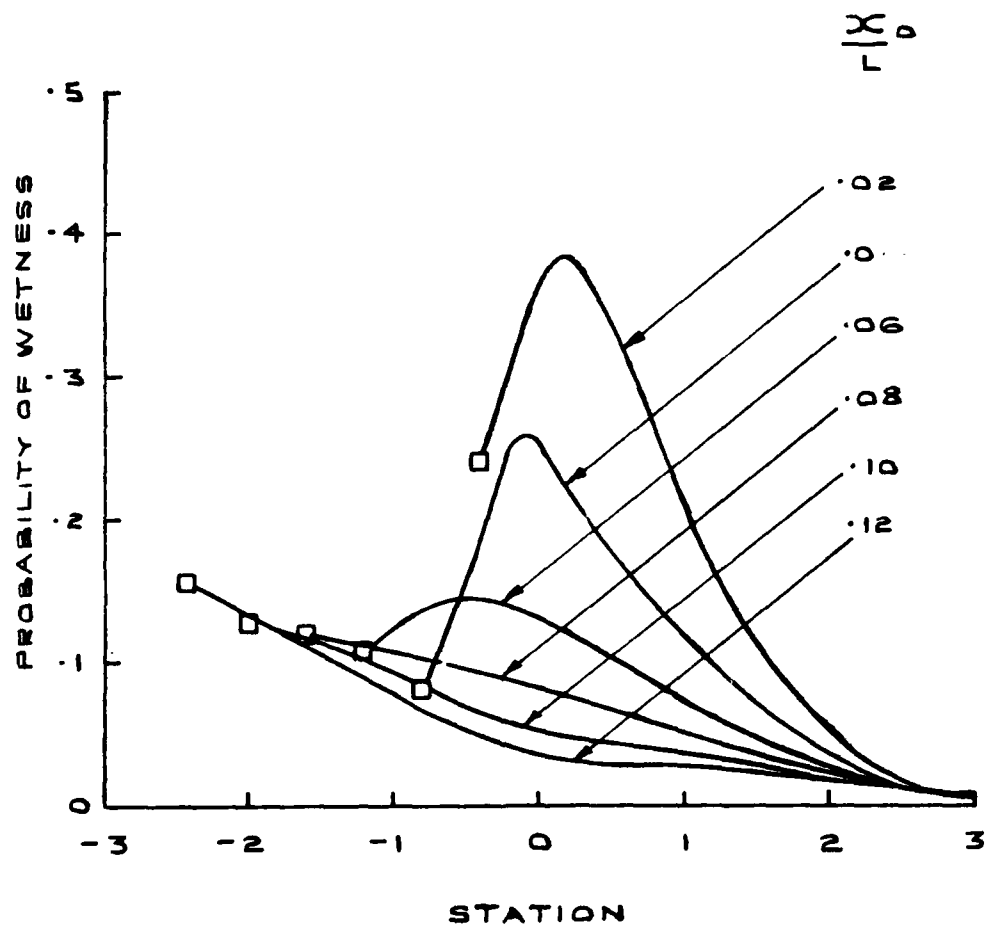


FIG.45 COMPUTED WETNESS PROBABILITIES
FOR 40° FLARE AND VARIOUS OVERHANGS

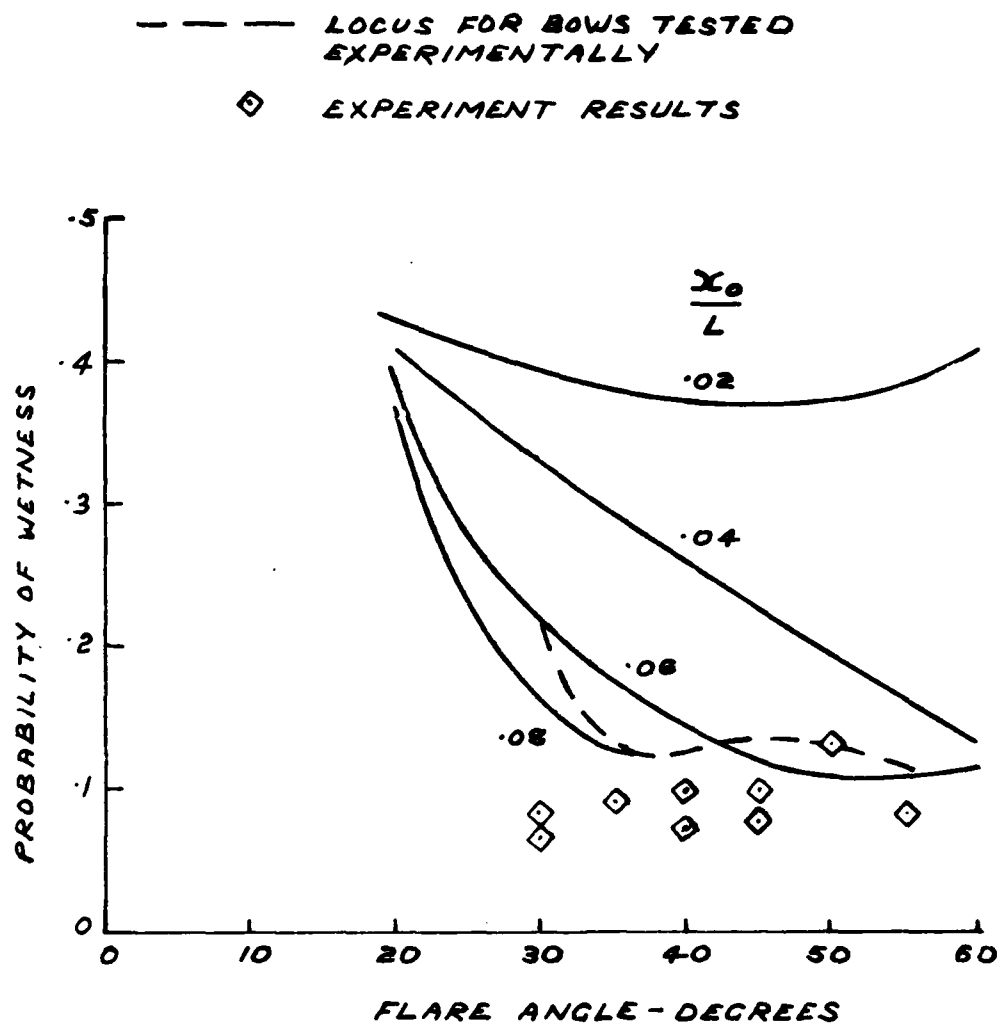
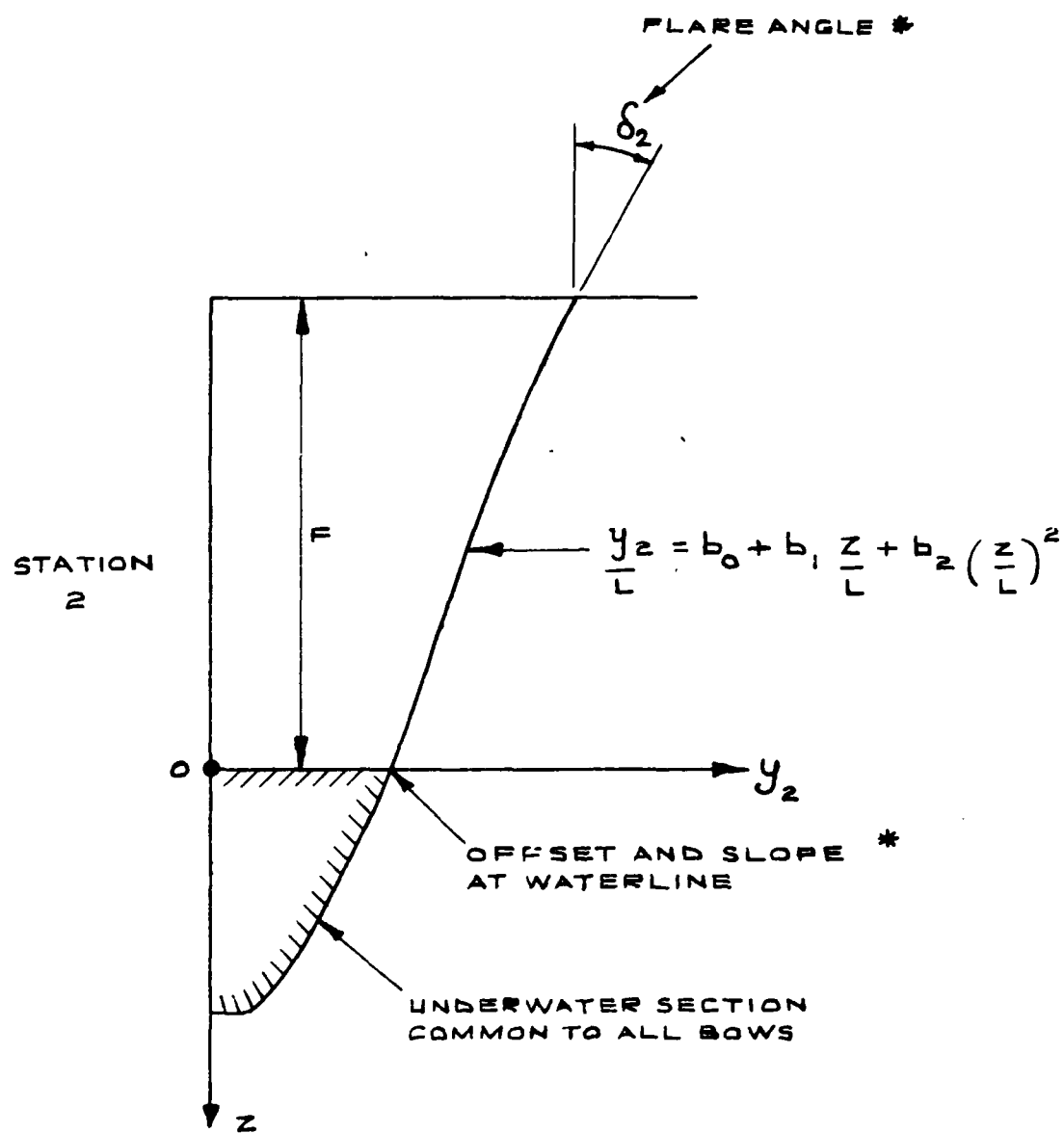
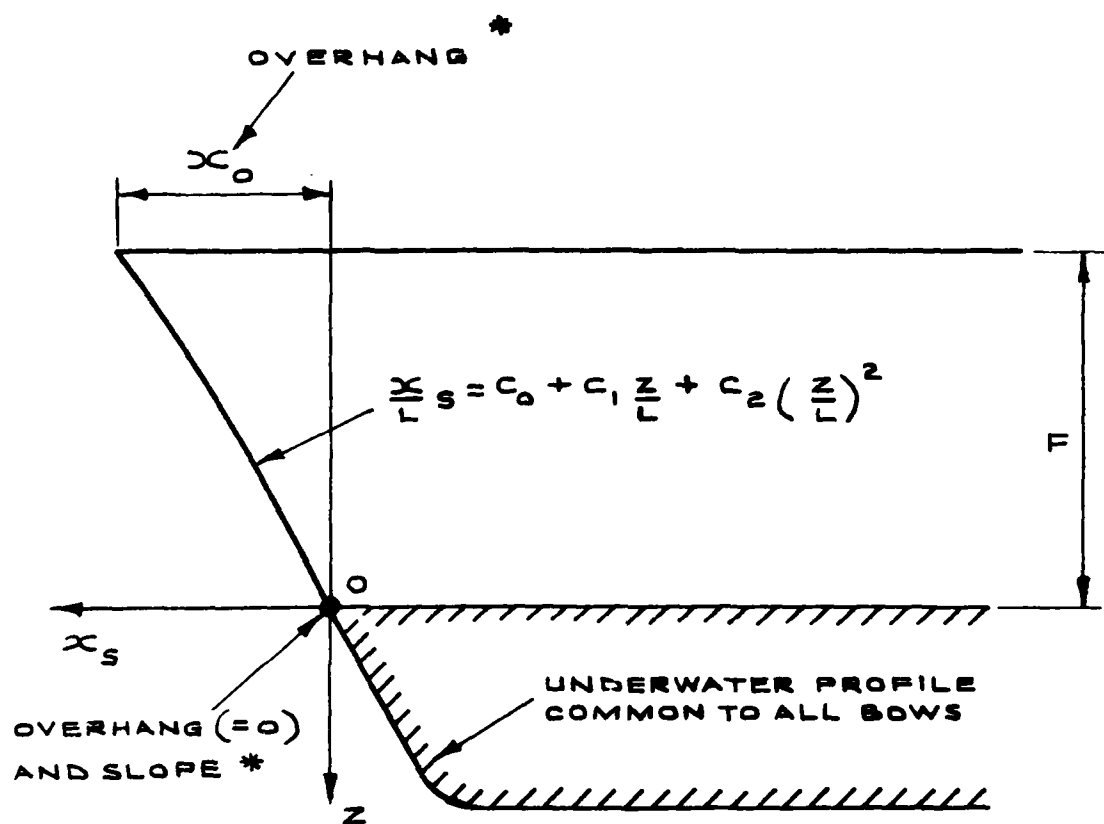


FIG. 46 PREDICTED BOW PERFORMANCE



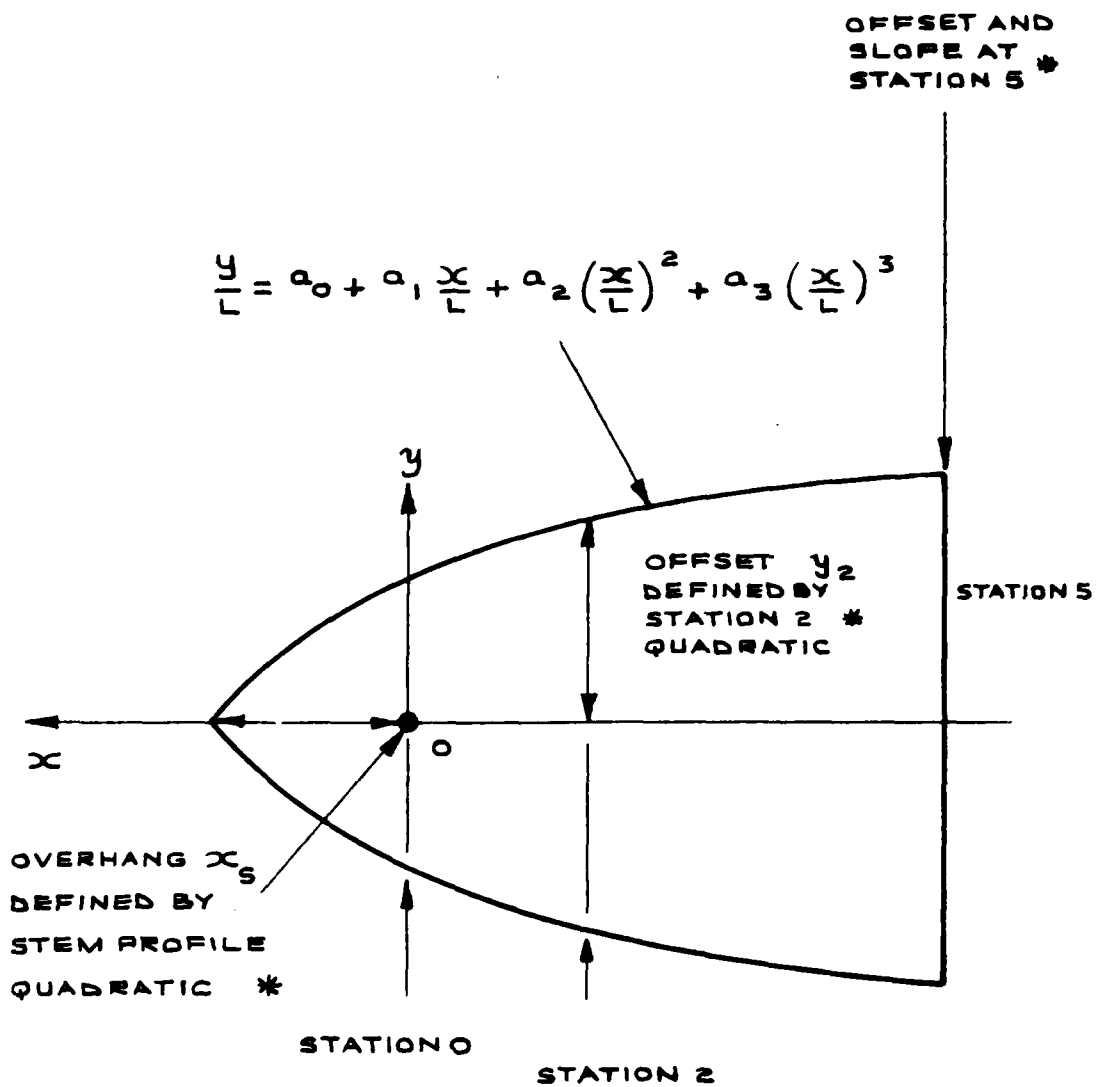
* BOUNDARY CONDITIONS FOR QUADRATIC

FIG. A1-1 DESIGN METHOD FOR SECTION SHAPE AT STATION 2



* BOUNDARY CONDITIONS FOR QUADRATIC

FIG. A1-2 DESIGN METHOD FOR STEM PROFILE



* BOUNDARY CONDITIONS FOR CUBIC

FIG. A1-3 DESIGN METHOD FOR WATERLINES

Distribution

Copy Numbers	1	DGRA/CS(RN)/DNA
	2-4	Deputy Controller (Warships) ADSS/NA 122
	5	Director ARE
	6	Managing Director Marine Technology and Deputy Director Admiralty Research Establishment
	7	Head of Hydrodynamics and Engineering Department ARE
	8	Staff Officer (C) BNS
	9-14	US Navy Technical Liaison Officer
	15	CS(R) 2E (Navy)
	16-18	DRIC

END

FILMED

11-84

DTIC